INFORMATION TO USERS

This material was produced from a microfilm copy of the original document. While the most advanced technological means to photograph and reproduce this document have been used, the quality is heavily dependent upon the quality of the original submitted.

The following explanation of techniques is provided to help you understand markings or patterns which may appear on this reproduction.

1. The sign or "target" for pages apparently lacking from the document photographed is "Missing Page(s)". If it was possible to obtain the missing page(s) or section, they are spliced into the film along with adjacent pages. This may have necessitated cutting thru an image and duplicating adjacent pages to insure you complete continuity.

2. When an image on the film is obliterated with a large round black mark, it is an indication that the photographer suspected that the copy may have moved during exposure and thus cause a blurred image. You will find a good image of the page in the adjacent frame.

3. When a map, drawing or chart, etc., was part of the material being photographed the photographer followed a definite method in "sectioning" the material. It is customary to begin photoing at the upper left hand corner of a large sheet and to continue photoing from left to right in equal sections with a small overlap. If necessary, sectioning is continued again — beginning below the first row and continuing on until complete.

4. The majority of users indicate that the textual content is of greatest value, however, a somewhat higher quality reproduction could be made from "photographs" if essential to the understanding of the dissertation. Silver prints of "photographs" may be ordered at additional charge by writing the Order Department, giving the catalog number, title, author and specific pages you wish reproduced.

5. PLEASE NOTE: Some pages may have indistinct print. Filmed as received.

Xerox University Microfilms

300 North Zeeb Road
Ann Arbor, Michigan 48106

Reproduced with permission of the copyright owner. Further reproduction prohibited without permission.

74-14,263

BLEVINS, Robert Dilworth, 1948-
FLOW INDUCED VIBRATION OF BLUFF STRUCTURES.

California Institute of Technology, Ph.D., 1974
Engineering Mechanics

University Microfilms, A XEROX Company, Ann Arbor, Michigan

THIS DISSERTATION HAS BEEN MICROFILMED EXACTLY AS RECEIVED.

Reproduced with permission of the copyright owner. Further reproduction prohibited without permission.

FLOW INDUCED VIBRATION OF BLUFF STRUCTURES

Thesis by

Robert Dilworth Blevins

In Partial Fulfillment of the Requirements

For the Degree of

Doctor of Philosophy

California Institute of Technology

Pasadena, California

1974

(Submitted on August 17, 1973)

Reproduced with permission of the copyright owner. Further reproduction prohibited without permission.

ACKNOWLEDGMENTS

The author wishes to express his gratitude to Dr. W. D. Iwan for his guidance and encouragement during the course of his graduate studies and in the preparation of this work. He is pleased to acknowledge the valuable suggestions of Dr. A. Roshko, Dr. T. K. Caughey and Dr. C. D. Babcock.

The author wishes to thank Mrs. Carol Timkovich for her skillful typing of the manuscript and Mrs. Janice Scott for her excellent drawings.

The author would like to express his appreciation to the John and Fannie Hertz Foundation for financial support during his years of graduate study. The partial support of this work under a grant from the National Science Foundation is also acknowledged.

Reproduced with permission of the copyright owner. Further reproduction prohibited without permission.

ABSTRACT

Models are developed for both multi-degree-of-freedom aerodynamic galloping and vortex induced oscillation of bluff structures. These models are useful in the analysis of elastic structures exposed to a steady fluid flow.

An asymptotic method, based on the approximation of Bogoliubov and Mitropolsky, is developed for the analysis of the autonomous, internally resonant, nonlinear differential equations produced by the models. It is shown that the solutions of these systems can be divided into two classes by the nature of the secular terms arising in the perturbation equations.

A model for multi-degree-of-freedom galloping is developed by modeling the aerodynamic forces on the structure as dependent only on the relative magnitude and velocity of the flow to the structure. A simple criterion for the stability of the zero solution is presented. Examples are made with a noninertially coupled system with the torsion and plunge degrees-of-freedom and a cubic curve fit to the aerodynamic coefficients. Examples show that the system is dominated by either a torsion or a plunge mode except when the natural frequencies of these modes are in certain integer multiples. In these cases the two modes interact strongly and they achieve first order limit cycles simultaneously.

A model for vortex induced vibration of elastic structures is produced from a control volume approach to the vortex shedding process. The model features both fluid and structural oscillators. The model

Reproduced with permission of the copyright owner. Further reproduction prohibited without permission.

parameters are determined from experimental data by matching the model response to experimental observation for the cases of fixed and forced cylinder motion. A frequency entrainment effect is produced by the model for an elastically mounted cylinder resonating with vortex shedding. The resonant amplitude of an elastically mounted cylinder predicted by the model is in good agreement with experimental data.

Reproduced with permission of the copyright owner. Further reproduction prohibited without permission.

TABLE OF CONTENTS

Chapter			Page
I	GENERAL INTRODUCTION		1
II	AN ASYMPTOTIC METHOD FOR INTERNALLY RESONANT AUTONOMOUS NONLINEAR SYSTEMS		5
	2.1	Introduction	5
	2.2	Uniqueness and Stability of the Zero Solution	6
	2.3	Formulation	8
	2.4	Perturbation and Variational Equations	10
	2.5	Resonance	11
	2.6	Solution of the Variational Equations	14
	2.7	Stability	18
	2.8	One and Two Degrees-of-Freedom	20
	2.9	Summary and Conclusions	23
	2.10	References	25
III	MULTI-DEGREE-OF-FREEDOM GALLOPING		26
	3.1	Introduction	26
	3.2	General Formulation	28
	3.3	Forces	33
	3.4	Stability of the Zero Solution	37
	3.5	An Estimate of the Maximum Amplitude of Galloping	38
	3.6	Simplifications Due to the Uncoupling of Lateral Displacement from Plunge and Torsion	41
	3.7	On Application of Asymptotic Nonlinear Analysis	44

Reproduced with permission of the copyright owner. Further reproduction prohibited without permission.

Chapter			Page
	3.8	Examples	45
		3.8.1 Example Formulation	49
		3.8.2 Combined Resonant Oscillation	53
		3.8.3 Harmonic Resonant Example I	60
		3.8.4 Harmonic Resonant Example II	68
	3.9	Summary and Conclusions	71
	3.10	References	73
IV		A MODEL FOR VORTEX INDUCED OSCILLATIONS	75
	4.1	Introduction	75
	4.2	Dimensional Analysis	78
	4.3	Spanwise Correlation and Amplitude Dependence of the Vortex Lift Force	79
	4.4	Derivation of the Model	85
	4.5	Analysis of the Model	96
		4.5.1 Stationary Cylinder	96
		4.5.2 Forced Cylinder Motion	98
		4.5.3 Elastically Mounted Cylinder	105
	4.6	Determination of the Model Parameters for a Circular Cylinder	109
	4.7	Nature of the Solution	114
		4.7.1 Frequency Entrainment	114
		4.7.2 Cylinder Amplitude at Resonance	122
	4.8	Effect of Varying Input Experimental Parameters on Model Response	125
	4.9	Pivoted Rod	129
	4.10	Summary and Conclusions	134
	4.11	References	135
V		GENERAL CONCLUSIONS	137

Reproduced with permission of the copyright owner. Further reproduction prohibited without permission.

I. GENERAL INTRODUCTION

Vortex shedding and aerodynamic galloping can cause large amplitude vibrations in an elastic structure exposed to a steady flow. If the structure periodically sheds vortices at a frequency near a harmonic of the natural frequency of the structure, vortex shedding may couple with structural vibration and generate a synchronous oscillating force on the structure [1]. Vortex shedding has produced destructive vibrations in stacks [2], marine cables [3] and launch vehicles [4]. If the vortex shedding frequency is much greater than the natural frequency of the structure the vortex shedding does not couple with structural oscillations, however, the structure may respond to aerodynamic forces generated by an oscillating relative flow field. If the structure vibrates slightly then the flow relative to the structure will oscillate. The aerodynamic forces produced by the oscillating relative flow can cause the amplitude of vibration to increase until limited by nonlinearities in the system. These flow induced vibrations are called galloping or flutter. Aerodynamic galloping has caused adjacent ice coated power lines to arc [5] and vibrated aircraft to failure [6].

The two mechanisms of flow induced vibration are illustrated in Figure 1. The amplitude of vibration of an elastically mounted rectangular section constrained to move normal to the free stream is expressed as a function of reduced velocity. The vortex shedding frequency for most bluff structures is given by $f_s = SU/D$ where f_s is the shedding frequency in Hertz, U is the free stream velocity, D is

Reproduced with permission of the copyright owner. Further reproduction prohibited without permission.

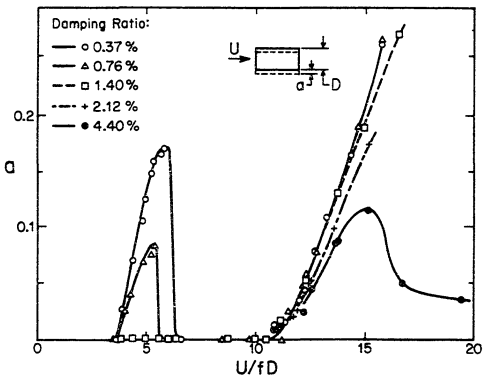

Fig. 1. Lateral Response of a Tall Building Model with Side Ratio of Two [7].

Reproduced with permission of the copyright owner. Further reproduction prohibited without permission.

the maximum width normal to the free stream and the proportionality constant S is ordinarily near .2. Hence resonance of a structure with vortex shedding is expected near $U/fD = 5$ where f is the natural frequency of the structure. This is the first peak in the amplitude in the figure. As the free stream velocity is increased beyond this point the vortex shedding frequency becomes greater than the natural frequency of the structure. The structure no longer resonates with vortex shedding and the amplitude drops sharply. The vibrations which arise near $U/fD = 11$ are due to aerodynamic galloping. These oscillations generally will persist with increasing flow velocity.

Both galloping and vortex induced oscillation are explored here. In Chapter III multi-degree-of-freedom galloping is investigated by modeling the aerodynamic forces on the structure as dependent only on the relative angle of attack of the fluid to the structure and allowing the structure to move both normal to the flow and in torsion. The aerodynamic forces couple the torsion and plunge modes of oscillation.

In Chapter IV a model for vortex induced oscillation of cylindrical structures is developed based on a control volume approach to the vortex shedding process. The model has both a fluid and structural degree of freedom. The model parameters are determined from experimental data for stationary and forced cylinders. The model predictions are compared with experimental data for an elastically mounted cylinder.

Since the flow induced oscillation of bluff structures is inherently nonlinear, asymptotic techniques are necessary to analyze both mathematical models. A method for the asymptotic analysis of autonomous,

Reproduced with permission of the copyright owner. Further reproduction prohibited without permission.

internally resonant oscillators is presented in Chapter II. The asymptotic method is applied to the multi-degree-of-freedom galloping in Chapter III and the vortex model in Chapter IV.

REFERENCES

1. Bishop, R. E. D., and Hassan, A. Y., "The Lift and Drag Forces on a Circular Cylinder in a Flowing Fluid," Proceedings of the Royal Society of London, Vol. 277, Series A, 1964, pp. 51-75.

2. Pagon, W. E., "Vibration Problem in Tall Stacks Solved by Aerodynamics," Engineering News Record, 12 July 1934.

3. Dale, J. R., and Holler, R. A., "Vortex Wakes from Flexible Circular Cylinders at Low Reynolds Numbers," NADC Report NADC-AE-7011, July 1970.

4. Goldman, R. L., "Karman Vortex Forces on theVanguard Rocket," Shock and Vibration Bulletin, Part II, Dec. 1958.

5. Cheers, F., "A Note on Galloping Conductors," National Research Council of Canada, Report No. MT-14, June 1950.

6. Garrick, I. E., editor, Aerodynamic Flutter, AIAA Selected Reprint Series, Vol. V., 1969.

7. Novak, M., "Galloping and Vortex Induced Oscillation of Structures," Proc. Conf. on Wind Effects on Buildings and Structures, Tokyo, 1971.

Reproduced with permission of the copyright owner. Further reproduction prohibited without permission.

II. AN ASYMPTOTIC TECHNIQUE FOR INTERNALLY RESONANT AUTONOMOUS NONLINEAR SYSTEMS

2.1 INTRODUCTION

An asymptotic method is here developed for the analysis of oscillations in a system of weakly nonlinear autonomous second order differential equations which are internally resonant. The asymptotic method is based on the approximation of Bogoliubov and Mitropolsky [1]. Order one solutions are assumed to be nearly harmonic at the natural frequency of the system but with slowly varying amplitude and phase.

Autonomous system herein are called internally resonant if secular terms arising in the asymptotic series expansions for the system response couple the response of two or more oscillators. Internally resonant systems can be divided into two classes by the nature of the secular coupling terms. First, if the frequency of any secular terms generated in the series expansions for the response of one oscillator are functions of the frequency of the order one response of any other oscillator, the system is called harmonically internally resonant. Small changes in the natural frequencies can greatly change the response of harmonically resonant oscillators. Second, if the frequency of all secular coupling terms arising in the series expansions for the response of each oscillator are independent of the frequencies of the order one response of the remaining oscillators then the system is called combined internally resonant.

A first order approximation to the amplitude and frequency of oscillation is developed for both harmonically internally resonant

Reproduced with permission of the copyright owner. Further reproduction prohibited without permission.

systems and combined internally resonant systems. Examples are given for one and two degree-of-freedom systems. The asymptotic method is then applied to problems of flow induced vibration in Chapters III and IV.

2.2 UNIQUENESS AND STABILITY OF THE ZERO SOLUTION

A wide variety of dynamic structural systems including galloping systems may be placed in the principal coordinate form [2]:

$$\ddot{p}_i + \omega_i^2 p_i = \epsilon f_i(p_1, p_2, \cdots p_N, \dot{p}_1, \dot{p}_2, \cdots \dot{p}_N) \qquad (2.2.1)$$

$$i = 1, N$$

where p_i is a generalized displacement, ϵ is a small parameter and the functions f_i consist of linear and nonlinear terms. The vector $\underline{f}$ is defined as the vector whose components are f_i. From the theory of differential equations it is known that if $\underline{f}$ is Lipschitzian, that is if there exists a constant m such that

$$|\underline{f}(\underline{x}) - \underline{f}(\underline{y})| \leq m|\underline{x} - \underline{y}| \qquad (2.2.2)$$

for each $\underline{x}$ and $\underline{y}$, then Equation (2.2.1) possesses a unique solution for a given set of initial conditions. $\underline{f}$ is separated into linear and nonlinear components $\underline{f} = \underline{f}_L + \underline{f}_{NL}$. If the nonlinear component satisfies the condition

$$\lim_{|\underline{y}| \to 0} \frac{|\underline{f}_{NL}(\underline{y})|}{|\underline{y}|} = 0 \qquad (2.2.3)$$

and if the linear terms in Equation (2.2.1) have stable zero solution,

Reproduced with permission of the copyright owner. Further reproduction prohibited without permission.

the zero solution of Equation (2.2.1) is stable. Conditions (2.2.2) and (2.2.3) are always satisfied if $\underline{f}$ is globally analytic as is the case when $\underline{f}$ is a polynomial.

A simple stability criteria can be developed for the zero solution of the system (2.2.1) if $\underline{f}$ satisfies the nonlinearity condition of Equation (2.2.3) and the natural frequencies of the oscillators are well separated. The set of principal coordinate oscillators are linearized for small oscillations by expanding f_i in a power series about zero and retaining only linear terms. The linearized analog of (2.2.1) then becomes

$$\ddot{p}_i+\omega_i^2 p_i = \varepsilon \sum_{j=1}^{N} \left(\frac{\partial f_i}{\partial p_j}\bigg|_{\underline{p}=\dot{\underline{p}}=0} p_j + \frac{\partial f_i}{\partial \dot{p}_j}\bigg|_{\underline{p}=\dot{\underline{p}}=0} \dot{p}_j \right) \tag{2.2.4}$$

The linear system (2.2.4) possesses the solution

$$p_i = \bar{p}_i e^{\lambda t} \tag{2.2.5}$$

where $\bar{p}_i$ and λ are constants. Substituting this solution form into the linearized oscillator set yields the following eigenvalue problem:

$$\begin{bmatrix} \lambda^2+\omega_1^2-\varepsilon\lambda\frac{\partial f_1}{\partial \dot{p}_1}-\varepsilon\frac{\partial f_1}{\partial p_1} & \cdots & -\varepsilon\lambda\frac{\partial f_1}{\partial \dot{p}_N}-\varepsilon\frac{\partial f_1}{\partial p_N} \\ \vdots & & \vdots \\ -\varepsilon\lambda\frac{\partial f_N}{\partial \dot{p}_1}-\varepsilon\frac{\partial f_N}{\partial p_1} & \cdots & \lambda^2+\omega_N^2-\varepsilon\lambda\frac{\partial f_N}{\partial \dot{p}_N}-\varepsilon\frac{\partial f_N}{\partial p_N} \end{bmatrix} \begin{bmatrix} \bar{p}_1 \\ \vdots \\ \bar{p}_N \end{bmatrix} = 0 \tag{2.2.6}$$

Reproduced with permission of the copyright owner. Further reproduction prohibited without permission.

Only the diagonal terms contain order one components. Thus if the natural frequencies are well separated so that $\omega_i \neq \omega_j + O(\epsilon)$ for all $i \neq j$ then the values of λ are determined from

$$\left[O(1) \text{ terms}\right]\left[\lambda^2 - \epsilon\lambda \frac{\partial f_i}{\partial \dot{p}_i}\bigg|_{\substack{p=\dot{p}=0}} - \epsilon \frac{\partial f_i}{\partial p_i}\bigg|_{\substack{p=\dot{p}=0}} + \omega_i^2\right] = O(\epsilon^2) \qquad (2.2.7)$$

The zero solution is stable only if the real part of λ is negative. Hence, the system will have a stable zero solution only if

$$\frac{\partial f}{\partial \dot{p}_i}\bigg|_{\substack{p=\dot{p}=0}} + O(\epsilon) < 0 \qquad (2.2.8)$$

for each i. Thus if each oscillator in the system has a distinct natural frequency well separated from other natural frequencies then the zero solution of the system will be stable only if each oscillator possesses sufficient damping so that Equation (2.2.8) holds. However, if the natural frequencies are close, $\omega_i = \omega_j + O(\epsilon)$ for some $i \neq j$ then the zero solution stability criteria is more complex. Each root of the polynomial generated by setting the determinant (2.2.6) to zero must be generally explored.

2.3 FORMULATION

Oscillatory solutions to the system

$$\ddot{p}_i + \omega_i^2 p_i = \epsilon f_i(p_1, p_2, \cdots p_N, \dot{p}_1, \dot{p}_2, \cdots \dot{p}_N) \qquad (2.2.1)$$

$i = 1, N$

Reproduced with permission of the copyright owner. Further reproduction prohibited without permission.

are sought of the form

$$p_i(t) = A_i(t)\cos\theta_i(t) + \varepsilon u_i^1(A_1, A_2, \cdots A_N, \theta_1, \theta_2, \cdots \theta_N)$$
$$+ \varepsilon^2 u_i^2(A_1, A_2, \cdots A_N, \theta_1, \theta_2, \cdots \theta_N) + \cdots$$
$$+ \varepsilon^m u_i^m(A_1, A_2, \cdots A_N, \theta_1, \theta_2, \cdots \theta_N) \qquad (2.3.1)$$

where

$$\theta_i = \underline{\omega}_i\left[t - \Psi_1(t) - \Psi_2(t) - \cdots - \Psi_i(t)\right] \qquad (2.3.2)$$

$$\underline{\omega}_i = \omega_i + O(\varepsilon)$$

The form of (2.3.2) using time shifts, Ψ_i, instead of the ordinary phase angles was chosen, since it allows any θ_i to be represented as a linear combination of any other θ_j and all time shifts except Ψ_1. This form greatly simplifies the manipulations required in the solution of the variational equations. The absence of terms explicitly dependent on time form the right side of Equation (2.2.1) reflects the fact that the system is autonomous. Clearly, the solution is a function of the relative phase between oscillators.

The fundamental assumption of the asymptotic analysis is that for a sufficiently small value of the parameter ε the solution of Equation (2.2.1) is nearly harmonic but with amplitude and phase which vary slowly over one cycle of oscillation. $\dot{A}_i$ and $\dot{\Psi}_i$ are assumed to be order ε functions of $A_i(t)$ and $\Psi_i(t$ Thus $\ddot{A}_i$ and $\ddot{\Psi}_i$ are order ε^2 [3].

Reproduced with permission of the copyright owner. Further reproduction prohibited without permission.

2.4 PERTURBATION AND VARIATIONAL EQUATIONS

The first derivative of p_i with respect to time is taken to be

$$\dot{p}_i = -\underline{\omega}_i A_i \sin\theta_i + \epsilon\dot{u}_i^1 + \cdots + \epsilon^m \dot{u}_i^m \qquad (2.4.1)$$

Equation (2.4.1) requires that the following terms have been set to zero forming the first set of variational equations [4].

$$0 = \dot{A}_i \cos\theta_i + A_i\underline{\omega}_i(\dot{\Psi}_1 + \dot{\Psi}_2 + \cdots + \dot{\Psi}_i)\sin\theta_i \qquad (2.4.2)$$

If the nonlinear functions f_i are expanded in a power series in ϵ,

$$f_i = f_i\Big|_{\epsilon=0} + \epsilon\sum_{j=1}^{N}\left(\frac{\partial f_i}{\partial p_j}\frac{\partial p_j}{\partial \epsilon}\Big|_{\epsilon=0} + \frac{\partial f_i}{\partial \dot{p}_j}\frac{\partial \dot{p}_j}{\partial \epsilon}\Big|_{\epsilon=0}\right) + \cdots \qquad (2.4.3)$$

then Equations (2.4.1) and (2.4.3) may be substituted into the system differential Equation (2.2.1) and powers of ϵ equated to generate the perturbation equations. The first set of perturbation equations are:

$$\begin{aligned}\epsilon(\ddot{u}_i^1 + \omega_i^2 u_i^1) = {} & \epsilon f_i(A_1, A_2, \cdots A_N, \theta_1, \theta_2, \cdots \theta_N) \\ & + (\underline{\omega}_i^2 - \omega_i^2) A_i \cos\theta_i \\ & + \underline{\omega}_i \dot{A}_i \sin\theta_i - \underline{\omega}_i^2 A_i(\dot{\Psi}_1 + \dot{\Psi}_2 + \cdots + \dot{\Psi}_i)\cos\theta_i \end{aligned} \qquad (2.4.4)$$

where $\underline{\omega}_i = \omega_i + O(\epsilon)$. Secular terms in the right side of Equation (2.4.4) have frequencies near the natural frequency ω_i. These secular terms will cause resonance of the perturbation equation and produce a solution of order $1/\epsilon$. This solution is greater than order one and so not a proper member of the series expansion (2.3.1). These secular

Reproduced with permission of the copyright owner. Further reproduction prohibited without permission.

terms are removed from the perturbation equation and form the second set of variational equations:

$$-\underline{\omega}_i \dot{A}_i \sin\theta_i + A_i \underline{\omega}_i^2 (\dot{\psi}_1 + \dot{\psi}_2 + \cdots \dot{\psi}_N)\cos\theta_i = (\underline{\omega}_i^2 - \omega_i^2) A_i \cos\theta_i + \epsilon H_i^1 \quad (2.4.5)$$

where $H_i^1(A_1, A_2, \cdots A_N, \theta_1, \theta_2, \cdots \theta_N)$ represents the secular terms which arise from $f_i\big|_{\epsilon=0}$. The perturbation equation (2.4.5) is now free of secular terms and may be solved for $u_i^1(A_1, A_2, \cdots A_N, \theta_1, \theta_2, \cdots \theta_N)$.

The solution process may be continued with the second set of perturbation equations. The secular terms are cast into the variational equation (2.4.5) to generate a higher order approximation and investigate higher order effects. Or the investigation may stop with the first set of perturbation equation. This limits the accuracy of the solution but it does avoid the necessity of defining a suitable parameter ϵ. In any case, the order one amplitude and phase must be found from the variational equations.

2.5 RESONANCE

The resonance character of the differential equation system (2.2.1) is determined by the nature of the secular terms arising in the perturbation equations. If these secular terms couple two or more oscillators then the system is said to be internally resonant. If the frequency of secular coupling terms is a function of the detuning ($\underline{\omega}_i/\underline{\omega}_j$ for $i \neq j$) between oscillators then the system is termed harmonically internally resonant. If the frequency of secular coupling terms is independent of the detuning between oscillators then the system is said to be combined resonant.

Reproduced with permission of the copyright owner. Further reproduction prohibited without permission.

An example will clarify the difference between a harmonically internally resonant system and a combined resonant system. Consider the following special form of oscillator from the system (2. 2. 1):

$$\ddot{p}_1+\omega_1^2 p_1 = \epsilon p_1 p_2^2$$

where

$$p_1 = A_1 \cos\theta_1+\epsilon u_1^1+\cdots \qquad \theta_1 = \underline{\omega}_1(t-\Psi_1)$$

$$p_2 = A_2 \cos\theta_2+\epsilon u_2^1+\cdots \qquad \theta_2 = \underline{\omega}_2(t-\Psi_1-\Psi_2)$$

The first member of the family of perturbation equations which are generated from the oscillator equation is:

$$\ddot{u}_1^1+\omega_1^2 u_1^1 = -\frac{A_1^2 A_2^2}{2}\cos\theta_1+\frac{A_1 A_2^2}{4}\cos(2\theta_2+\theta_1)$$

$$+\frac{A_1 A_2^2}{4}\cos(2\theta_2-\theta_1)+(\underline{\omega}_1^2-\omega_1^2)A_1\cos\theta_1$$

$$+\underline{\omega}_1\dot{A}_1\sin\theta_1-\underline{\omega}_1^2 A_1\dot{\Psi}_1\cos\theta_1$$

If

$$2\omega_2\pm\omega_1\neq\omega_1+O(\epsilon)$$

then the first term on the right side of the perturbation equation is secular. The amplitude of this term is a function of both A_1 and A_2 so the order one response of the system is coupled and the system is internally resonant. The frequency of this term is independent of the frequency ratio ω_2/ω_1 so the secular term does not produce harmonic resonance.

Reproduced with permission of the copyright owner. Further reproduction prohibited without permission.

When

$$2\omega_2 - \omega_1 = \omega_1 + O(\varepsilon)$$

the third term on the right side of the perturbation equation is secular. The amplitude of this term is a function of A_1 and A_2 and the frequency of this term is a function of ω_1 and ω_2 so the system is harmonically internally resonant.

Small shifts in the frequency ratio ω_2/ω_1 can change the third and fourth terms, on the right side of the perturbation equation, from secular to nonsecular. Small shifts in the natural frequencies of harmonically resonant systems can alter the resonance of the perturbation equations and so greatly change the response of the system.

A necessary condition for harmonic resonance is

$$i\omega_1 + j\omega_2 + \cdots + q\omega_N = O(\varepsilon) \qquad (2.5.1)$$

where i, j, $\cdots$q are integers. This is shown by expanding each term in the power series expansion for f_i (Eqn. (2.4.3)) in a harmonic series. The harmonic series can only contain terms whose frequencies are integer linear combinations of the frequencies $\underline{\omega}_1, \cdots \underline{\omega}_N$. Since $\underline{\omega}_i = \omega_i + O(\varepsilon)$ secular coupling terms which produce harmonic resonance can only arise if the natural frequencies of one oscillator is nearly an integer linear combination of the natural frequencies of two or more of the oscillators. This implies Equation (2.5.1).

Reproduced with permission of the copyright owner. Further reproduction prohibited without permission.

The frequency of secular terms is defined independently of order ϵ changes in detuning using the order ϵ arbitrariness in the definition of $\underline{\omega}_i$ so that all secular terms arising in each family of perturbation equations (those perturbation equations which determine the higher order solutions to an oscillator) have the same frequency. This allows the variational equations to be solved by averaging them over one cycle of the secular terms. Since the natural frequencies of harmonically resonant systems satisfy Equation (2.5.1) one or more $\underline{\omega}_k$ are defined as

$$i\omega_1 + \cdots + j\omega_{k-1} + \underline{k}\underline{\omega}_k + m\omega_{k+1} + \cdots + q\omega_N = 0 \tag{2.5.2}$$

$$\underline{\omega}_j = \omega_j \qquad j = 1, \cdots k-1, k+1, \cdots N$$

so that all secular terms arising in each family of perturbation equations have the same frequency. If the system is not harmonically resonant then all secular terms arising in each family of perturbation equations have the same frequency independently of detuning so the $\underline{\omega}_i$ may be defined as

$$\underline{\omega}_i = \omega_i \tag{2.5.3}$$

2.6 SOLUTION OF THE VARIATIONAL EQUATIONS

Once the secular terms have been cast into the variational equations, the variational equations become

$$\dot{A}_i \cos\theta_i + \underline{\omega}_i A_i (\dot{\Psi}_1 + \dot{\Psi}_2 + \cdots + \dot{\Psi}_i) \sin\theta_i = 0 \tag{2.6.1}$$

$$-\underline{\omega}_i \dot{A}_i \sin\theta_i + A_i \underline{\omega}_i^2 (\dot{\Psi}_1 + \dot{\Psi}_2 + \cdots + \dot{\Psi}_i) \cos\theta_i = \left(\underline{\omega}_i^2 - \omega_i^2\right) A_i \cos\theta_i + \sum_{k=1}^{m} \epsilon^k H_i^k \tag{2.6.2}$$

Reproduced with permission of the copyright owner. Further reproduction prohibited without permission.

If the rate of change of the amplitudes, A_i, and time shifts, Ψ_i, with time are sufficiently small then they can be considered constant over one cycle of vibration. The variational equation is solved by averaging the equation over one cycle of vibration while holding $\dot{A}_i$ and $\dot{\Psi}_i$ fixed.

The ith equation from the set (2.6.1) is multiplied by $-\underline{\omega}_i \cos\theta_i$ and the ith equation from the set (2.6.2) is multiplied by $\sin\theta_i$. These equations are summed to give:

$$-\underline{\omega}_i \dot{A}_i = \sum_{k=1}^{m} \epsilon^k H_i^k \sin\theta_i + (\underline{\omega}_i^2 - \omega_i^2) A_i \sin\theta_i \cos\theta_i \qquad (2.6.3)$$

Averaging Equation (2.6.3) over one cycle of the secular terms gives

$$\dot{A}_i = -S_i / \underline{\omega}_i \qquad (2.6.4)$$

where

$$S_i(A_1, \cdots A_N, \Psi_2, \cdots \Psi_N) = \sum_{k=1}^{m} \frac{\epsilon^k}{T_i} \int_0^{T_i} H_i^k \sin\theta_i \, d\theta_i \qquad (2.6.5)$$

and T_i is the period of the secular terms. The ith equation from (2.6.1) is multiplied by $\underline{\omega}_i \sin\theta_i$ and the ith Equation from (2.6.2) is multiplied by $\cos\theta_i$. The equations are added and averaged over one cycle of the secular terms to give

$$\dot{\Psi}_1 + \dot{\Psi}_2 + \cdots \dot{\Psi}_i = C_i / A_i \underline{\omega}_i^2 + (\underline{\omega}_i - \omega_i) / \underline{\omega}_i \qquad (2.6.6)$$

where

$$C_i(A_1, \cdots A_N, \Psi_2, \cdots \Psi_N) = \sum_{k=1}^{m} \frac{\epsilon^k}{T_i} \int_0^{T_i} H_i^k \cos\theta_i \, d\theta_i \qquad (2.6.7)$$

Reproduced with permission of the copyright owner. Further reproduction prohibited without permission.

C_i and S_i are independent of the time shift Ψ_1 since any θ_i may be expressed as a linear combination of any other θ_j and the time shifts Ψ_2 through Ψ_N. Moreover if the system is not harmonically internally resonant then the integration eliminates all time shift dependence from the right sides of Equations (2.6.4) and (2.6.6).

By successively subtracting the jth equation from the j+1st equation of the set (2.6.6) a set of 2N-1 equations are formed in the variables $A_1, \cdots A_N, \Psi_2, \cdots, \Psi_N$ plus an auxiliary equation which determines Ψ_1. These averaged variational equations are:

$$\dot{A}_i = S_i/\underline{\omega}_i \qquad i=1,N \tag{2.6.7}$$

$$\dot{\Psi}_i = C_i/A_i\underline{\omega}_i^2 + (\underline{\omega}_i - \omega_i)/\underline{\omega}_i - \sum_{k=1}^{i-1}\left[C_j/A_j\underline{\omega}_j^2 + (\underline{\omega}_j - \omega_j)/\underline{\omega}_j\right] \quad i=2,N \tag{2.6.8}$$

$$\dot{\Psi}_1 = C_1/\underline{\omega}_1^2 A_1 + (\underline{\omega}_1 - \omega_1)/\underline{\omega}_1 \tag{2.6.9}$$

$A_1, \cdots A_N, \Psi_2, \cdots \Psi_N$ can be found by simultaneous integration of Equations (2.6.7) and (2.6.8) with appropriate initial conditions. If the system is not harmonically resonant the right sides of Equations (2.6.7), (2.6.8) and (2.6.9) are independent of all time shifts and equation sets (2.6.7) and (2.6.8) uncouple.

The frequency of the order one displacement of the ith oscillator correct to order ε is:

$$\frac{d\theta_i}{dt} = \underline{\omega}_i(1 - \dot{\Psi}_1 - \dot{\Psi}_2 - \cdots - \dot{\Psi}_i) \tag{2.6.10}$$

Let

$$\Delta_i = -\underline{\omega}_i(\dot{\Psi}_1 - \dot{\Psi}_2 - \cdots - \dot{\Psi}_i) \tag{2.6.11}$$

Reproduced with permission of the copyright owner. Further reproduction prohibited without permission.

Δ_i is the frequency correction to the order one approximation of the frequency of oscillation, $\underline{\omega}_i$. Greater accuracy may then be achieved in the order one solution by incorporating the frequency correct to order ε in the approximate solution.

Simple harmonic solutions are sought by setting $\dot{A}_1$ through $\dot{A}_N$ and $\dot{\Psi}_2$ through $\dot{\Psi}_N$ to zero and seeking solutions of Equations (2.6.7) and (2.6.8). If $\dot{\Psi}_2$ through $\dot{\Psi}_N$ are set to zero, Equation (2.6.11) implies the frequency corrections are in the same ratio as the order one approximation to the frequencies of oscillation. That is,

$$\frac{\Delta_i}{\Delta_j} = \frac{\underline{\omega}_i}{\underline{\omega}_j} \tag{2.6.11}$$

Equations (2.5.2) and (2.6.10) imply

$$i\frac{d\theta_1}{dt} + j\frac{d\theta_2}{dt} + \cdots + \ell\frac{d\theta_N}{dt} = 0 \tag{2.6.12}$$

for some integers i, j, $\cdots \ell$. That is if two or more oscillators are harmonically internally resonant then for simple harmonic solutions the first order solutions must oscillate at the same frequency or harmonics of some frequency.

It is not always possible to find simple harmonic solutions for resonant oscillators. Gilchrist [5] in experiments with multiple pendulums in free vibration found that internal harmonic resonance was characterized by a beating response.

Reproduced with permission of the copyright owner. Further reproduction prohibited without permission.

2.7 STABILITY

The stability of periodic solutions is determined by Equations (2.6.7) and (2.6.8). The periodic amplitudes and time shifts are perturbed by small quantities ξ_i and η_i. Let

$$A_i(t) = \overline{A}_i(t) + \xi_i(t) \qquad i = 1, N \qquad (2.7.1)$$

$$\Psi_i(t) = \overline{\Psi}_i(t) + \eta_i \qquad i = 2, N \qquad (2.7.2)$$

where $\overline{A}_i(t)$ and $\overline{\Psi}_i(t)$ are periodic solutions to Equations (2.6.7) and (2.6.8). The system is considered stable if all possible perturbations ξ_i and η_i diminish in time. Substituting Equations (2.7.1) and (2.7.2) into Equations (2.6.7) and (2.6.8) and retaining only first order terms in ξ_i and η_i gives

$$\dot{\xi}_i = \sum_{j=1}^{N} \frac{\partial \dot{A}_i}{\partial \xi_j}\bigg|_{\substack{\Psi=\overline{\Psi} \\ A=\overline{A}}} \xi_j + \sum_{j=2}^{N} \frac{\partial \dot{A}_i}{\partial \eta_j}\bigg|_{\substack{\Psi=\overline{\Psi} \\ A=\overline{A}}} \eta_j \qquad i = 1, N \qquad (2.7.3)$$

$$\dot{\eta}_i = \sum_{j=1}^{N} \frac{\partial \dot{\Psi}_i}{\partial \xi_j}\bigg|_{\substack{\Psi=\overline{\Psi} \\ A=\overline{A}}} \xi_j + \sum_{j=2}^{N} \frac{\partial \dot{\Psi}_i}{\partial \eta_j}\bigg|_{\substack{\Psi=\overline{\Psi} \\ A=\overline{A}}} \eta_j \qquad i = 2, N \qquad (2.7.4)$$

In the case of simple harmonic motion $\dot{A}_i = 0$ for each i and $\dot{\Psi}_j = 0$ for j = 2, ··N and Equations (2.7.3) and (2.7.4) have solutions of the form

$$\xi_i = \overline{\xi}_i e^{\lambda t} \qquad (2.7.5)$$

$$\eta_i = \overline{\eta}_i e^{\lambda t} \qquad (2.7.6)$$

Reproduced with permission of the copyright owner. Further reproduction prohibited without permission.

where $\bar{\xi}_i$ and $\bar{\eta}_i$ are constant. Substituting Equations (2. 7. 5) and (2. 7. 6) into Equations (2. 7. 3) and (2. 7. 4) produces an eigenvalue problem. For nontrivial solutions the determinant of the coefficient matrix must be zero. Hence,

$$\begin{vmatrix} \frac{\partial \dot{A}_1}{\partial \xi_1} - \lambda & \frac{\partial \dot{A}_1}{\partial \xi_2} & \cdots & \frac{\partial \dot{A}_1}{\partial \xi_N} & \frac{\partial \dot{A}_1}{\partial \eta_2} & \cdots & \frac{\partial \dot{A}_1}{\partial \eta_N} \\ \frac{\partial \dot{A}_2}{\partial \xi_1} & \frac{\partial \dot{A}_2}{\partial \xi_2} - \lambda & & & & & \\ \vdots & & \ddots & & & & \\ \frac{\partial \dot{\Psi}_2}{\partial \xi_1} & & & \frac{\partial \dot{\Psi}_2}{\partial \eta_2} - \lambda & & & \\ \vdots & & & & \ddots & & \\ \frac{\partial \dot{\Psi}_N}{\partial \xi_1} & \cdots & \cdots & \cdots & \cdots & \cdots & \frac{\partial \dot{\Psi}_N}{\partial \eta_N} - \lambda \end{vmatrix} = 0 \qquad (2.7.7)$$

evaluating the determinant produces a polynomial of the form

$$\lambda^{2N-1} + a_1 \lambda^{2N-2} + \cdots + a_{2N-2} \lambda + a_{2N-1} = 0 \qquad (2.7.8)$$

If the polynomial has only negative or zero real parts the perturbations will remain constant or die with time. The criterion of Hurwitz gives necessary and sufficient conditions that Equation (2. 7. 8) have roots with only negative real parts [6].

Consider the finite array associated with Equation (2. 7. 8)

$$\left.\begin{matrix} a_1 & 1 & 0 & 0 & 0 \cdots \\ a_3 & a_2 & a_1 & 1 & 0 \cdots \\ a_5 & a_4 & a_3 & a_2 & 1 \cdots \\ a_7 & a_6 & a_5 & a_4 & a_3 \cdots \end{matrix}\right\} \qquad (2/7/9)$$

Reproduced with permission of the copyright owner. Further reproduction prohibited without permission.

where a_k is taken to be zero for $k > 2N-1$. Then a necessary and sufficient condition that all the roots of (2.7.7) have negative real parts is that the sequence

$$\left.\begin{vmatrix} a_1 \end{vmatrix}, \quad \begin{vmatrix} a_1 & 1 \\ a_3 & a_2 \end{vmatrix}, \quad \begin{vmatrix} a_1 & 1 & 0 \\ a_3 & a_2 & a_1 \\ a_5 & a_4 & a_3 \end{vmatrix} \right\} \tag{2.7.10}$$

formed from the array (2.7.9) be positive.

2.8 ONE AND TWO DEGREES OF FREEDOM

For a single degree of freedom the Equations (2.6.7), (2.6.8) and (2.6.9) reduce to

$$\dot{A} = -S(A)/\omega \tag{2.8.1}$$

$$\dot{\Psi} = C(A)/\omega^2 \tag{2.8.2}$$

where A is the order one amplitude of the oscillator and Ψ is the associated time shift. Equation (2.8.1) may be integrated directly from time $t = t_o$

$$\int_{t_o}^{t} \frac{dA}{S(A)} = \frac{t_o - t}{\omega} \tag{2.8.3}$$

with the initial value of A at $t = t_o$. Equation (2.8.3) is integrated using the resultant A(t). The amplitude of the solution is independent of the

Reproduced with permission of the copyright owner. Further reproduction prohibited without permission.

time shift Ψ since the system is autonomous. Simple harmonic solutions to Equation (2.8.1) may be found graphically by plotting $\dot{A}$ against A and seeking roots $\dot{A} = 0$. If the slope of this curve is negative at a root $\dot{A} = 0$ then perturbations will diminish in time and the root is stable.

For two degrees of freedom, Equations (2.6.7), (2.6.8) and (2.6.9) become

$$\dot{A}_1 = -S_1/\underline{\omega}_1 \tag{2.8.5}$$

$$\dot{A}_2 = -S_2/\underline{\omega}_2 \tag{2.8.6}$$

$$\dot{\Psi}_2 = C_2/A_2\underline{\omega}_2^2 - C_1/A_1\underline{\omega}_1^2 + (\underline{\omega}_2 - \omega_2)/\underline{\omega}_2 - (\underline{\omega}_1 - \omega_1)/\underline{\omega}_1 \tag{2.8.7}$$

$$\dot{\Psi}_1 = C_1/A_1\underline{\omega}_1^2 + (\underline{\omega}_1 - \omega_1)/\underline{\omega}_1 \tag{2.8.8}$$

If the system is not harmonically resonant S_1, S_2, C_1 and C_2 are independent of both time shifts Ψ_1 and Ψ_2 so Equations (2.8.5) and (2.8.6) are decoupled from Equations (2.8.7) and (2.8.8).

If the system is harmonically resonant then Equation (2.5.2) implies

$$i\omega_1 + j\omega_2 = O(\varepsilon) \tag{2.8.9}$$

where i and j are some integers. $\underline{\omega}_1$ and $\underline{\omega}_2$ can be defined by

$$\left.\begin{aligned} \underline{\omega}_1 &= \frac{j}{i}\omega_2 \\ \underline{\omega}_2 &= \omega_2 \end{aligned}\right\} \tag{2.8.10}$$

so that the period of secular terms are independent of small shifts in the natural frequencies ω_1 and ω_2. S_1, S_2, C_1 and C_2 are function of A_1, A_2 and Ψ_2 so Equations (2.8.5), (2.8.6) and (2.8.7) may be solved

Reproduced with permission of the copyright owner. Further reproduction prohibited without permission.

independently of Equation (2. 8. 8) by simultaneous integration with appropriate initial conditions.

Setting $\dot{A}_1 = \dot{A}_2 = \dot{\Psi}_2 = 0$ and seeking roots of Equations (2. 8. 5), (2. 8. 6) and (2. 8. 7) may yield simple harmonic solutions. The stability of simple harmonic solutions is determined by perturbing the steady values of A_1, A_2 and Ψ_2 by the small quantities ξ_1, ξ_2 and η_2 respectively and linearizing equations (2. 8. 5), (2. 8. 6) and (2. 8. 7) for small perturbations. Solutions of the form

$$\left.\begin{aligned} \xi_1 &= \overline{\xi}_1 e^{\lambda t} \\ \xi_2 &= \overline{\xi}_2 e^{\lambda t} \\ \eta_2 &= \overline{\eta}_2 e^{\lambda t} \end{aligned}\right\} \qquad (2.8.11)$$

are sought by substituting the set (2. 8. 11) into Equations (2. 8. 5), (2. 8. 6) and (2. 8. 7). Expressing the result in matrix form yields,

$$\begin{bmatrix} \frac{\partial \dot{A}_1}{\partial \xi_1} & \frac{\partial \dot{A}_1}{\partial \xi_2} & \frac{\partial \dot{A}_1}{\partial \eta_2} \\ \frac{\partial \dot{A}_2}{\partial \xi_1} & \frac{\partial \dot{A}_2}{\partial \xi_2} & \frac{\partial \dot{A}_2}{\partial \eta_2} \\ \frac{\partial \dot{\Psi}_2}{\partial \xi_1} & \frac{\partial \dot{\Psi}_2}{\partial \xi_2} & \frac{\partial \dot{\Psi}_2}{\partial \eta_2} \end{bmatrix} \begin{bmatrix} \overline{\xi}_1 \\ \overline{\xi}_2 \\ \overline{\eta}_2 \end{bmatrix} - \lambda \begin{bmatrix} \overline{\xi}_1 \\ \overline{\xi}_2 \\ \overline{\eta}_2 \end{bmatrix} = 0 \qquad (2.8.12)$$

This eigenvalue problem will have stable nontrivial solutions only if the polynomial formed by setting the determinant of the matrix on the left hand side of Equation (2. 8. 12) to zero has only roots with negative real parts. Setting the determinant of this matrix to zero gives

Reproduced with permission of the copyright owner. Further reproduction prohibited without permission.

$$-\lambda^3+I_1\lambda^2-I_2\lambda+I_3=0 \qquad (2.8.13)$$

where I_1, I_2 and I_3 are the first, second and third invariants of the first matrix on the left hand side of (2.8.12). For negative roots of the polynomial (2.8.13) the Hurwitz criterion requires

$$\begin{aligned} -I_1 &> 0 \\ -I_3 &> 0 \\ -I_1 I_2 &> I_3 \end{aligned} \qquad (2.8.14)$$

2.9 SUMMARY AND DISCUSSION

An asymptotic method has been developed for weakly nonlinear, autonomous, internally resonant oscillator systems. The method is based on the approximation of Bogoliubov and Mitropolsky. Two classes of solutions have been developed for internally resonant systems. One class is valid for harmonic resonance. A necessary condition for harmonic resonance is that two or more natural frequencies of the oscillators be integer multiples of a third frequency. The second class of solution, called combined resonance, is valid only outside the bands of natural frequencies which produce harmonic resonance. The two classes of solution may not match as the system approaches harmonic resonance. Indeed secular terms in the perturbation equations may cause the higher order members of the combined resonant solution to become infinite as the system approaches harmonic resonance. The harmonic resonant solution may not produce a useful approximation outside the harmonic resonance frequency bands since the amplitude and

Reproduced with permission of the copyright owner. Further reproduction prohibited without permission.

phase of the first order solution may not be slowly varying in time. A stability analysis is developed using standard linearization techniques to generate a eigenvalue problem whose eigenvalues determine if small perturbations will grow in time. The criterion of Hurwitz gives conditions that the eigenvalues have only negative real parts and perturbations will die with time.

The asymptotic method is useful in the analysis of multi-degree-of-freedom systems which arise in flow induced vibration. For many structures the nonlinear aerodynamic forces are small. Unfortunately in aerodynamic galloping the model for the aerodynamic coefficients can generate a large number of nonlinear terms so that no closed form simple harmonic solutions exist. Any simple harmonic solutions are sought by either numerically searching for roots to the averaged variation equations or by directly integrating these variational equations until a steady solution is found. The principal advantage of the later technique over direct numerical integration of the system differential equations is that it is more efficient. Numerical integration over one period of oscillation of the system differential equations may require as many as 50 time steps for an accurate approximation. The variational equations with slowly varying amplitude and phase have been averaged over one cycle of the associated secular terms. These equations can be integrated with time steps of at least one period of the secular terms. Thus numerically integrating the variational equation can be one or two orders of magnitude more efficient than direct numerical integration of the system differential equations.

Reproduced with permission of the copyright owner. Further reproduction prohibited without permission.

2.10 REFERENCES

1. Bogoliubov, N.M., Mitropolsky, Y.A. "Asymptotic Methods in the Theory of Nonlinear Oscillations," Translated from the second Russian edition, Hindustan Publishing Corporation, Delhi, 1961.

2. Meirovitch, L., Analytical Methods in Vibrations, Macmillian, New York, 1967.

3. Minorsky, N., Nonlinear Oscillations, D. van Nostrand, New York, 1962.

4. Struble, R.A. "Nonlinear Differential Equations," McGraw-Hill, New York, 1962.

5. Gilchrist, A.O., "The Free Oscillations of Conservative Quasi Linear Systems with Two Degrees of Freedom," Int. J. Mech. Sci., 1961.

6. Bellman, R., Introduction to Matrix Analysis, McGraw-Hill, New York, 1970.

Reproduced with permission of the copyright owner. Further reproduction prohibited without permission.

III. MULTI-DEGREE-OF-FREEDOM GALLOPING

3.1 INTRODUCTION

If an elastic structure oscillates in steady flow the flow field relative to the structure also oscillates. The oscillating relative flow field produces a fluctuating component of aerodynamic force on the structure that may tend to increase the amplitude of vibration. The limiting amplitude, if any, is determined by energy dissipation in the structure and the nature of the aerodynamic force. For sufficiently small amplitudes the aerodynamic force can be modeled as a linear function of angle of attack. The linear model has proven very useful with airfoil type cross sections where the flow induced vibrations are called flutter. A linear structure susceptible to linear flutter will have either a stable zero solution or divergent vibrations. If the flow separates from the cross section of the structure the aerodynamic force is nonlinear in angle of attack and the structure is termed bluff. The flow induced vibrations of bluff structures are commonly called stall flutter or galloping. Galloping vibrations normally have stable finite limit cycles. The multi-degree-of-freedom galloping of bluff structures is the subject of this section.

The classic example of galloping is the vibration of ice coated power lines in Canada [1]. Ice solidifying on power lines tends to form aerodynamically unstable cross sections. The low structural damping of the power lines and moderate wind velocities can produce very large amplitude vibrations perpendicular to the flow causing

Reproduced with permission of the copyright owner. Further reproduction prohibited without permission.

adjacent power lines to arc. The stall flutter of turbine blades has also been shown to produce large steady amplitude vibrations both in plunge and in torsion [2]. New steel frame structures have become progressively lighter and more slender, so that aerodynamic vibration has become a design factor. Marine structures such as oil rigs and terminals are also susceptable to galloping. The high density of water can produce a large fluid force even at the flow velocities comparable to those of marine currents.

At the heart of the analysis of galloping is the quasi-static assumption. It is assumed that the aerodynamic force on the cross section in a flow at any time is identical with the force on the same cross section in a steady flow at the same relative angle of attack and flow velocity. Essentially the fluid is assumed to have no memory of structural motion. The assumption has been found to be a useful approximation as long as the vortex shedding frequency is much higher than the frequency of vibration.

Analysis of galloping in the literature has generally been limited to single-degree-of-freedom systems. A variety of cross sections including square, rectangle, stalled airfoil and angle section are known to be susceptible to galloping [3], [4], [5]. In every case elastically mounted sections have been found to achieve a stable harmonic limit cycle for flow velocities above a threshold velocity. Multiple limit cycles are possible. While the one-degree-of-freedom models have shown good agreement with experimental evidence, they are inadequate for multi-degree-of-freedom structures of practical importance.

Reproduced with permission of the copyright owner. Further reproduction prohibited without permission.

In the following discussion a model for multi-degree-of-freedom galloping system is developed. The model is analyzed by the asymptotic technique discussed in Chapter II. Simple criteria for the stability of the zero solution and the threshold velocity are determined as well as an estimate of the maximum galloping amplitude. Examples using a cubic approximation for the nonlinear aerodynamic terms and a two-degree-of-freedom noninertially coupled system show the asymptotic analysis provides a good approximation for the system response. When the system is not harmonically resonant examples show that the system response is generally dominated by either a plunge or a torsion mode. As the system approaches harmonic resonance the plunge and torsional modes interact strongly, small changes in frequency may greatly change the amplitude of the system and the two modes lock into a single frequency with simple harmonic vibration.

3.2 GENERAL FORMULATION

It will be assumed in the following analysis that bending-torsion galloping may be represented by a three dimensional model in which the structural resistance to vertical and lateral bending and torsion is represented by springs and dampers as shown in Figure 1. Two dimensional flow is assumed to hold. This is strictly applicable to large aspect ratio structures but may hold for relatively short aspect ratios if the end effects are minimal.

The absolute displacement of each point of the cross section is, for small θ,

Reproduced with permission of the copyright owner. Further reproduction prohibited without permission.

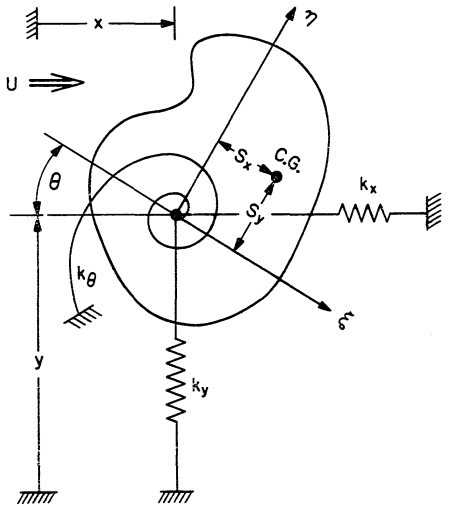

Fig. 1. Structural Model (dampers parallel to springs not shown).

Reproduced with permission of the copyright owner. Further reproduction prohibited without permission.

$$\left.\begin{aligned} X &= x + \eta\theta + \xi \\ Y &= y - \xi\theta + \eta \end{aligned}\right\} \tag{3.2.1}$$

The corresponding velocities are

$$\left.\begin{aligned} \dot{X} &= \dot{x} + \eta\dot{\theta} \\ \dot{Y} &= \dot{y} - \xi\dot{\theta} \end{aligned}\right\} \tag{3.2.2}$$

X and Y are the absolute displacements. The displacement of the shear center is given by x and y. θ is the rotation about the shear center. The ξ, η coordinate system is fixed in the body (Figure 1).

The kinetic energy of the section is

$$T = \frac{1}{2}\int_A (\dot{X}^2+\dot{Y}^2)\,\sigma d\xi d\eta = \frac{1}{2}\,m(\dot{x}^2+\dot{y}^2) + \frac{1}{2}\,I\dot{\theta}^2 + S_y\dot{\theta}\dot{x} - S_x\dot{\theta}\dot{y} \tag{3.2.3}$$

where

$$\left.\begin{aligned} I &= \int_A (\xi^2+\eta^2)\sigma d\xi d\eta \\ m &= \int_A \sigma d\xi d\eta \\ S_y &= \int_A \eta\sigma d\xi d\eta \\ S_x &= \int_A \xi\sigma d\xi d\eta \end{aligned}\right\} \tag{3.2.4}$$

σ is the density per unit length over the cross section A. The potential energy of the structure per unit length is

$$V = \frac{1}{2}k_x x^2 + \frac{1}{2}k_y y^2 + \frac{1}{2}k_\theta \theta^2 \tag{3.2.5}$$

Reproduced with permission of the copyright owner. Further reproduction prohibited without permission.

k_x, k_y and k_θ are the spring constants per unit length. The equations of motion are derived by Lagrange's equations:

$$L = T - V \tag{3.2.6}$$

$$\frac{d}{dt}\left(\frac{\partial L}{\partial \dot{q}_i}\right) - \frac{\partial L}{\partial q_i} = Q_i \tag{3.2.7}$$

Q_i is the generalized forces with respect to the generalized coordinate q_i and is obtained from virtual work considerations.

$$\delta W = \sum_{n=1}^{N} Q_i \delta q_i \tag{3.2.8}$$

thus

$$\left.\begin{aligned} Q_x &= F_x \\ Q_y &= F_y \\ Q_\theta &= F_M \end{aligned}\right\} \tag{3.2.9}$$

F_x, F_y, and M are the sum of aerodynamic and damping forces along x and y axes and in torsion respectively. Applying Lagrange's equations to Equations (3.2.3) and (3.2.5) gives:

$$m\ddot{x} + S_y\ddot{\theta} + k_x x = F_x \tag{3.2.10}$$

$$m\ddot{y} - S_x\ddot{\theta} + k_y y = F_y \tag{3.2.11}$$

$$I\ddot{\theta} + S_y\ddot{x} - S_x\ddot{y} + k_\theta \theta = F_M \tag{3.2.12}$$

It is convenient to place these equations in matrix form.

$$[M]\{\ddot{x}\} + [K]\{x\} = \{F\} \tag{3.2.13}$$

Reproduced with permission of the copyright owner. Further reproduction prohibited without permission.

where

$$[M] = \begin{bmatrix} m & 0 & +S_y \\ 0 & m & -S_x \\ +S_y & -S_x & I \end{bmatrix} \qquad [K] = \begin{bmatrix} k_x & 0 & 0 \\ 0 & k_y & 0 \\ 0 & 0 & k_\theta \end{bmatrix} \tag{3.2.14}$$

$$\{\underline{x}\} = \begin{Bmatrix} x \\ y \\ \theta \end{Bmatrix} \qquad \{\underline{F}\} = \begin{Bmatrix} F_x \\ F_y \\ F_M \end{Bmatrix}$$

$[M]$ and $[K]$ are the mass and stiffness matricies respectively.

Principal coordinates are sought such that

$$\{\underline{x}\} = \{\underline{P}^j\} \cos \omega_j t \tag{3.2.15}$$

by formulating the eigenvalue problem

$$\left[-\omega_j^2 [M] + [K]\right] \underline{P}^j = 0 \tag{3.2.16}$$

Nontrivial solutions exist only if the determinate of the coefficient matrix is zero. This gives

$$\omega^6 (1 - S_x^2/Im - S_y^2/Im) - \omega^4 (\omega_x^2 + \omega_y^2 + \omega_\theta^2 - \omega_y^2 S_y^2/Im - \omega_x^2 S_x^2/Im) + \omega^2 (\omega_x^2 \omega_y^2 + \omega_x^2 \omega_\theta^2 + \omega_y^2 \omega_\theta^2) - \omega_x^2 \omega_y^2 \omega_\theta^2 = 0 \tag{3.2.17}$$

where the natural frequencies ω_x, ω_y and ω_θ are

$$\omega_x^2 = k_x/m \qquad \omega_y^2 = k_y/m \qquad \omega_\theta^2 = k_\theta/I \tag{3.2.18}$$

Since the mass and stiffness matricies are symmetric, the characteristic equation (3.2.17) has three real eigenvalues ω_j corresponding to three vectors $\underline{P}^j$ of (3.2.16). For a given geometry ω_j and $\underline{P}^j$ are found numerically.

Reproduced with permission of the copyright owner. Further reproduction prohibited without permission.

The set of coordinates

$$\{\underline{x}\} = \left[\underline{P}^1\underline{P}^2\underline{P}^3\right]\begin{Bmatrix} p_1 \\ p_2 \\ p_3 \end{Bmatrix} \tag{3.2.19}$$

will diagonalize the mass and stiffness matrices producing the system

$$\ddot{p}_i + \omega_i^2 p_i = f_i \tag{3.2.20}$$

where

$$f_i = \left(\left[\underline{P}^1\underline{P}^2\underline{P}^3\right]^T\left[M\right]\left[\underline{P}^1\underline{P}^2\underline{P}^3\right]\right)^{-1}\left[\underline{P}^1\underline{P}^2\underline{P}^3\right]^T\{\underline{F}\}$$

The proceeding analysis can be directly applied to a continuous system by assuming a single spanwise mode for each degree of freedom. The kinetic and potential energies are found by integrating along the span to produce the total energies of each mode. If the generalized forces are summed along the span and Lagrange's equations are applied, thena system with the same form as equation set (3.2.20) is generated. If multiple spanwise modes are used in the structural model then additional oscillator equations will be produced of the same form as Equation (3.2.20) provided the mode shapes are orthogonal over the span.

3.3 FORCES

The generalized forces are the sum of the structural damping and the aerodynamic forces on the structure. The aerodynamic forces are assumed to depend only on the magnitude and angle of attack of the relative wind. The steady values of the aerodynamic force may be found from wind tunnel measurements. This assumption breaks down

Reproduced with permission of the copyright owner. Further reproduction prohibited without permission.

if the periodicity of the near wake associated with vortex shedding approaches the frequency of vibration. An approximate condition for the vortex shedding frequency to be well above the natural frequency of the structure is [6]:

$$\frac{U}{\omega d} > \frac{5}{\pi} \qquad (3.3.1)$$

U is the free stream velocity, d is a characteristic dimension, normally the maximum width of the cross section normal to the free stream and ω is the natural frequency of vibration.

The relative angle of attack and the magnitude of the relative flow are required to compute the aerodynamic forces on the cross section. For a cross section in plunge the components of relative velocity depend only on $\dot{y}$ and U and are pictured in Figure 2a. For a cross section in torsion the relative velocity depends on both θ and $\dot{\theta}$ and the relative velocity varies over the surface of the cross section (Figure 2b). Choosing a single characteristic radius R and angle γ defines a characteristic relative velocity for the cross section which may approximate the net flow field. This approximation has proven useful in one dimensional galloping [2]. The alternative is to perform a full range of dynamic tests to characterize the forces on the rotating cross section. The relative velocity and angle of attack for a cross section in plunge and torsion, using a characteristic radius, are shown in Figure 2c. For a section in plunge and torsion the square of the relative velocity and relative angle of attack are:

$$U_{rel}^2 = U^2+\dot{x}^2+\dot{y}^2+R\dot{\theta}^2+2R\dot{\theta}\dot{y}\sin\gamma-2\dot{x}\dot{\theta}R\cos\gamma+2\dot{\theta}UR\cos\gamma \qquad (3.3.2)$$

Reproduced with permission of the copyright owner. Further reproduction prohibited without permission.

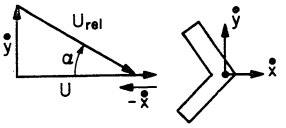

Fig. 2A. Translation.

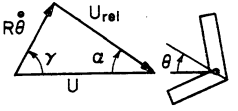

Fig. 2B. Rotation.

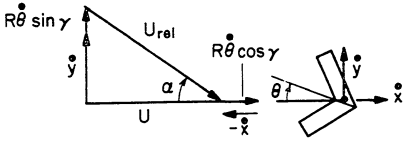

Fig. 2C. Translation and Rotation.

Reproduced with permission of the copyright owner. Further reproduction prohibited without permission.

$$\alpha = \theta - \tan^{-1} \frac{\dot{\theta} R \sin \gamma + \dot{y}}{U - \dot{x} + R\dot{\theta} \cos \gamma} \tag{3.3.3}$$

Certain small amplitude assumptions are useful in simplifying U_{rel} and α. The condition for the validity of the quasi-static assumption (Eqn. 3.3.1) implies $\omega d < .2U$ so that the maximum velocity of the surface of the structure is much less than the free stream velocity for vibration amplitudes less than the characteristic dimension, d. If the translational and rotational surface velocities of the cross section are small compared to the free stream velocity, in particular if

$$\left.\begin{aligned} |\dot{y}/U| &< .3 \\ |\dot{x}/U| &< .02 \\ |R\dot{\theta}/U| &< .02 \end{aligned}\right\} \tag{3.3.4}$$

as is consistent with both experimental evidence [3], [4] and the quasi-static assumption then the linearizing approximations

$$U_{rel} = U \tag{3.3.5}$$

$$\alpha = \theta - R_1/U - \dot{y}/U \tag{3.3.6}$$

$$R_1 = R \sin \gamma$$

are useful. These approximations involve a maximum error of less than 15% and a maximum error averaged over one cycle of oscillation of less than 8% of the peak values of angle of attack and relative velocity.

With the above assumptions, the aerodynamic and damping forces per unit length are

Reproduced with permission of the copyright owner. Further reproduction prohibited without permission.

$$F_x = \frac{1}{2}\rho U^2 d C_x(\alpha) - c_x \dot{x} \tag{3.3.7}$$

$$F_y = \frac{1}{2}\rho U^2 d C_y(\alpha) - c_y \dot{y} \tag{3.3.8}$$

$$F_M = \frac{1}{2}\rho U^2 d^2 C_M(\alpha) - c_\theta \dot{\theta} \tag{3.3.9}$$

ρ is the fluid density. c_x, c_y and c_θ are the viscous damping coefficients. The aerodynamic coefficients C_x, C_y and C_M determine the net aerodynamic forces on the cross section parallel to the x, y axes and the torsional moment respectively. These coefficients are defined by

$$C_x = C_D + \alpha C_L$$

$$C_y = C_L - \alpha C_D$$

$$C_M = C_M$$

C_L, C_D, and C_M are the aerodynamic coefficients defined in the customary airfoil sense and are the coefficients of force perpendicular and parallel to the free stream and in torsion respectively. C_x, C_y and C_M are ordinarily expressed as polynomials in the angle of attack.

3.4 STABILITY OF THE ZERO SOLUTION

Since the aerodynamic pressure on the cross section increases with the square of free stream velocity and the structural damping is independent of free stream velocity, a threshold velocity may exist below which the damping exceeds the destabilizing aerodynamic force and the zero solution is stable. The determination of the threshold velocity is a linear problem analogous to finding the flutter speed in classical aerodynamic theory.

Reproduced with permission of the copyright owner. Further reproduction prohibited without permission.

The aerodynamic forces are ordinarily analytic in angle of attack so the stability of the zero solution is determined by the linear terms in Eqn. (3.2.20). The single-degree-of-freedom case was analyzed by Den Hartog [4] who produced a simple single stability criteria. The analysis is considerably more complex for multi-degree-of-freedom systems. The Routh-Hurwitz criteria may be directly applied to the eigenvalue problem produced by considering the linear terms in Eqn. (3.2.20) to determine conditions for small oscillations to grow. This approach has the advantage of directness but generally requires exploring the roots of a six-order polynomial so physical interpretation is difficult [5]. A second approach is to place the oscillator equations in normal coordinates and then apply the Routh-Hurwitz criteria. If the natural frequencies of the normal modes are well separated and the sum of the damping and aerodynamic forces is small then this procedure produces a simple approximate stability criterion which is outlined in Section 2.2. This criterion can be expressed simply in closed form if the system is limited to two-degrees-of-freedom as will be shown in Section 3.6.

3.5 AN ESTIMATE OF THE MAXIMUM AMPLITUDE OF GALLOPING

If (1) the system response can be well approximated as simple harmonic, (2) the velocity at the surface of the cross section remains small in comparison to the free stream velocity, (3) the system possesses some damping, then a simple estimate of the maximum amplitude of galloping is easily produced. The aerodynamic lift, drag and moment coefficients of bluff structures are bounded, while the

Reproduced with permission of the copyright owner. Further reproduction prohibited without permission.

viscous damping force increase with amplitude. Hence for fixed free stream velocity there exists some amplitude above which the energy input to each oscillator per cycle by the aerodynamic force is less than the energy dissipated in damping. The oscillator cannot maintain oscillations above this amplitude. An estimate of the maximum amplitude is found by equating the energy expended in damping to the maximum energy that may be input to an oscillator by the aerodynamic force.

The principal part of the displacement of the normal coordinated is assumed to be simple harmonic:

$$P_i = A_i \cos(\omega_i t - \varphi_i) \tag{3.5.1}$$

A_i is the amplitude of the normal mode and ω_i is the frequency of that mode. The damping force is:

$$F_d = -c_i \omega_i A_i \sin(\omega_i t - \varphi_i) \tag{3.5.2}$$

c_i is the viscous damping coefficient of the ith normal mode. The energy extracted from the oscillator by viscous damping per cycle is:

$$E_d = \int_0^{2\pi/\omega_i} F_d \dot{p}_i dt = \pi c_i \omega_i A_i^2 \tag{3.5.3}$$

The maximum energy input to the system by the aerodynamic force is:

$$E_a = \frac{1}{2}\rho U^2 d \int_0^{2\pi/\omega_i} \left(C_i\right)_{max} \dot{p}_i dt \leq \rho U^2 dA_i \left(C_i\right)_{max} \tag{3.5.4}$$

where $\left(C_i\right)_{max}$ is the maximum of the aerodynamic force coefficient for the mode of interest. For energy balance

$$E_d = E_a \tag{3.5.5}$$

Reproduced with permission of the copyright owner. Further reproduction prohibited without permission.

Thus

$$\left(A_i\right)_{max} = \frac{\rho U^2 d \left(C_i\right)_{max}}{\pi c_i \omega_i} \tag{3.5.6}$$

If the oscillator is limited to the plunge then:

$$\overline{A}_y / D = U_y^2 n_y \left(C_y\right)_{max} / \pi \beta_y \tag{3.5.7}$$

If the oscillator is limited to torsion then:

$$A_\theta = U_\theta^2 n_\theta \left(C_\theta\right)_{max} / \pi \beta_\theta \tag{3.5.8}$$

Equations (3.5.7) and (3.5.8) have been nondimensionalized in terms of the following dimensionless variables which have proven useful in flow induced vibration:

$$U_y = \frac{U}{\omega_y d} \qquad U_\theta = \frac{U}{\omega_\theta d} \qquad \beta_y = \frac{c_y}{2m\omega_y} \qquad \beta_\theta = \frac{c_\theta}{2I\omega_\theta}$$

$$n_y = \frac{\rho d^2}{2m} \qquad n_\theta = \frac{\rho d^4}{2I} \qquad r_1 = \frac{R_1}{d} \qquad r_2 = \frac{R_1 \omega_\theta}{d \omega_y} \qquad \overline{A}_y = \frac{A_y}{d}$$

β_θ and β_y are the fractions of critical damping of plunge and torsion and are called damping factors. U_y and U_θ are reduced velocities. n_y and n_θ are mass and inertia ratios.

The estimate for the maximum amplitude increases as the square of the free stream velocity and decreases with damping and frequency. If the damping goes to zero, the estimate goes to infinity. However, investigations of single degree-of-freedom systems have found the solution is bounded regardless of the presence or absence of damping due to the nonlinearity of the aerodynamic forces at large angles of attack.

Reproduced with permission of the copyright owner. Further reproduction prohibited without permission.

3.6 SIMPLIFICATIONS DUE TO UNCOUPLING OF LATERAL DISPLACEMENT FROM PLUNGE AND TORSION

Vibrations parallel to the free stream flow are decoupled from torsion and vibration normal to the free stream flow if the lateral position of the center of mass of the section coincides with the shear center so $S_y = 0$ (Fig. 1). Setting $S_y = 0$ the torsional and plunge oscillator equations become

$$m\ddot{y} - S_x\ddot{\theta} + k_y y = \frac{1}{2}\rho U^2 d C_y - c_y \dot{y} \tag{3.6.1}$$

$$-S_x\ddot{y} + I\ddot{\theta} + k_\theta \theta = \frac{1}{2}\rho U^2 d^2 C_m - c_\theta \dot{\theta} \tag{3.6.2}$$

In order to place the left sides of these equations in principal coordinates the associated eigenvalue problem must be solved:

$$\begin{bmatrix} k_y - m\omega^2 & +S_x\omega^2 \\ +S_x\omega^2 & k_\theta - I\omega^2 \end{bmatrix} \left\{\underline{n}\right\} = 0 \tag{3.6.3}$$

The characteristic frequencies are:

$$\omega_{1,2}^2 = \frac{\omega_y^2 + \omega_\theta^2 \pm \left\{(\omega_y^2 + \omega_\theta^2)^2 - 4\omega_y^2\omega_\theta^2(1 - S_x^2/Im)\right\}^{1/2}}{2(1 - S_x^2/Im)} \tag{3.6.4}$$

The characteristic vectors are:

$$\underline{n}_1 = \begin{Bmatrix} K_1 \\ 1 \end{Bmatrix} \qquad \underline{n}_2 = \begin{Bmatrix} 1 \\ K_2 \end{Bmatrix} \tag{3.6.5}$$

where

$$K_1 = \frac{-S_x}{m}\frac{\omega_1^2}{\omega_y^2 - \omega_1^2} \qquad K_2 = \frac{-S_x}{I}\frac{\omega_2^2}{\omega_\theta^2 - \omega_2^2} \tag{3.6.6}$$

Reproduced with permission of the copyright owner. Further reproduction prohibited without permission.

The principal coordinates are defined by

$$\begin{Bmatrix} y \\ \theta \end{Bmatrix} = p_1 \begin{Bmatrix} K_1 \\ 1 \end{Bmatrix} + p_2 \begin{Bmatrix} 1 \\ K_2 \end{Bmatrix} \tag{3.6.7}$$

The oscillator equations transformed to principal coordinates are

$$\ddot{p}_1 + \omega_1^2 p_1 = \frac{K_1\left[.5\rho U^2 dC_y - c_y(K_1\dot{p}_1 + \dot{p}_2)\right] + \left[.5\rho U^2 d^2 C_m - c_\theta(\dot{p}_1 + K_2\dot{p}_2)\right]}{mK_1^2 - 2S_x K_1 + I} \tag{3.6.8}$$

$$\ddot{p}_2 + \omega_2^2 p_2 = \frac{.5\rho U^2 dC_y - c_y(K\dot{p}_1 + \dot{p}_2) + K_2\left[.5\rho U^2 d^2 C_m - c_\theta(\dot{p}_1 + K_2\dot{p}_2)\right]}{m - 2S_x K_2 + IK_2^2} \tag{3.6.9}$$

The net angle of attack is

$$\alpha = p_1 + K_2 p_2 - R_1(\dot{p}_1 + K_2\dot{p}_2)/U - (K_1\dot{p}_1 + \dot{p}_2)/U \tag{3.6.10}$$

For small oscillations about the equilibrium position $\alpha = y = \theta = 0$, the aerodynamic forces are linearized in terms of the local tangent at $\alpha = 0$.

$$\left.\begin{aligned} C_y &= \frac{\partial C_y}{\partial \alpha}\Big|_{\alpha=0} \alpha \\ C_M &= \frac{\partial C_M}{\partial \alpha}\Big|_{\alpha=0} \alpha \end{aligned}\right\} \tag{3.6.11}$$

Substituting these into Equations (3.6.9) and (3.6.10) produces a linear problem which determines the stability of the zero solution. This problem was treated in Section 2.2. If the natural frequencies of the normal modes are well separated, the zero solution is stable as long

Reproduced with permission of the copyright owner. Further reproduction prohibited without permission.

as the net damping coefficient of each oscillator is sufficiently positive. Assuming $\omega_1 \neq \omega_2 + O(\epsilon)$, where ϵ is a small parameter discussed in the following section, then the threshold velocity is determined to order ϵ by requiring that the sum of all coefficients of $\dot{p}_1$ in Equation (3.6.8) and the sum of all coefficients of $\dot{p}_2$ on the right hand side of Equation (3.6.9) be zero. This gives two criteria. The threshold velocity for the onset of galloping is the minimum of the individual thresholds. The threshold velocity is the minimum of:

$$U_{threshold} = \min \left\{ \begin{array}{l} \dfrac{-2c_y - 2K_2^2 c_\theta}{\left(\rho d R_1 K_2 + 1\right)\left(dK_2 \dfrac{\partial C_M}{\partial \alpha}\Big|_{\alpha=0} + \dfrac{\partial C_y}{\partial \alpha}\Big|_{\alpha=0}\right)} \\ \\ \dfrac{-2K_1^2 c_y - 2c_\theta}{\rho d\left(R_1 + K_1\right)\left(K_1 \dfrac{\partial C_y}{\partial \alpha}\Big|_{\alpha=0} + d \dfrac{\partial C_M}{\partial \alpha}\Big|_{\alpha=0}\right)} \end{array} \right. \tag{3.6.12}$$

If the center of mass coincides with the shear center then $S_x = S_y = 0$ and the stability criteria reduce to the den Hartog relation. The threshold velocity is the minimum of

$$U_{threshold} = \min \left\{ \begin{array}{l} \dfrac{-2c_y}{\rho d} \dfrac{\partial \alpha}{\partial C_y}\Big|_{\alpha=0} \\ \\ \dfrac{-2c_\theta}{\rho d^2 R_1} \dfrac{\partial \alpha}{\partial C_M}\Big|_{\alpha=0} \end{array} \right. \tag{3.6.13}$$

Reproduced with permission of the copyright owner. Further reproduction prohibited without permission.

3.7 ON APPLICATION OF ASYMPTOTIC NONLINEAR ANALYSIS

The accuracy of the asymptotic analysis is a function of the sum of the magnitude of the aerodynamic and damping forces compared to the linear inertia and spring force terms in the oscillator equation. While it is not necessary to define a small parameter ϵ if solutions are limited to first order, nevertheless such a definition is useful.

The linear terms in the sum of the structural damping and aerodynamic forces are proportional to both the slope of the aerodynamic coefficients and the damping factor. If the small parameter ϵ is defined as the minimum damping factor required to produce onset of galloping then ϵ is proportional to the linear terms in the aerodynamic force. This definition of ϵ is useful in stability analysis and in estimating the bandwidth of frequencies containing the harmonic resonant frequency band. If the shear center coincides with the center of mass then

$$\epsilon = \min \begin{cases} n_y U_y \dfrac{\partial C_y}{\partial \alpha}\Big|_{\alpha=0} \\ \\ n_\theta U_\theta r_1 \dfrac{\partial C_M}{\partial \alpha}\Big|_{\alpha=0} \end{cases} \tag{3.7.1}$$

ϵ increases with the ratio of the mass of the fluid displaced by the structure to the mass of the structure and with increasing reduced velocity. The density ratios and ϵ are apt to be small for most bluff civil engineering type structures oscillating in air. However, if

Reproduced with permission of the copyright owner. Further reproduction prohibited without permission.

the construction is sufficiently light as is the case with aircraft or the fluid sufficiently dense as may be the case with marine structures, then ϵ can become large and the asymptotic method may not provide a useful approximation.

3.8 EXAMPLES

The nonlinearity in the system and hence the complexity of solution comes from the curve fits of the nonlinear aerodynamic coefficients. Polynomials as high as 25th order in angle of attack have been used to approximate the aerodynamic coefficients [8]. The complexities introduced by the many nonlinear terms in a high order polynomial curve fit forces numerical solution with a necessary loss in physical understanding for the effect of various parameters on the system. A low order (cubic) curve fit has been used in the examples which allow some closed form approximate solutions. It is felt that this simple approximation will predict the gross phenomena that could be observed with higher order curve fits.

The prototype system used for the examples is the right angle section shown in Figure 3. The aerodynamic properties of this section have been determined by Slater [8], and are shown in Figures 4 and 5 along with the cubic approximations. The shear center of the section is located at the center of gravity so there is no inertial coupling.

The section is symmetric about $\vartheta = 0$. A cubic polynomial curvefit composed of odd powers of the angle of attack was obtained by the least squares technique. The polynomial fit is a good approximation to the data points for angles of attack less

Reproduced with permission of the copyright owner. Further reproduction prohibited without permission.

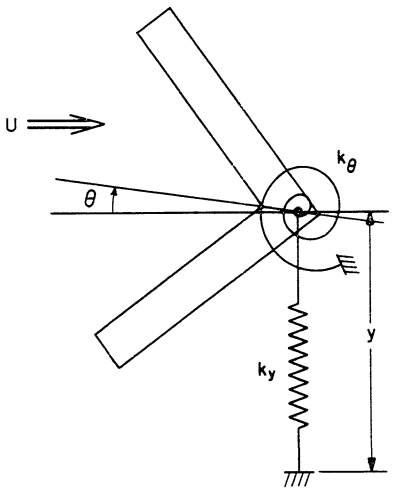

Fig. 3. Right Angle Section Model (dampers parallel to springs not shown).

Reproduced with permission of the copyright owner. Further reproduction prohibited without permission.

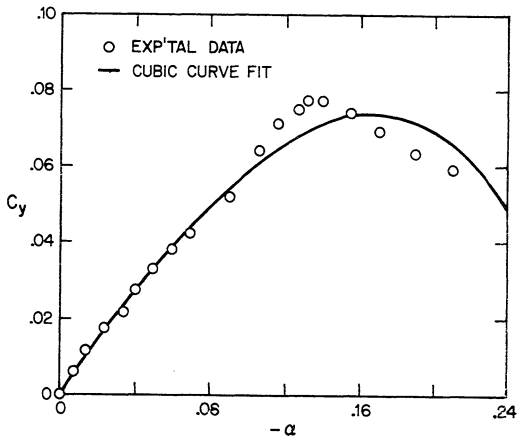

Fig. 4. Cubic Curve Fit to Vertical Force Coefficient of Right Angle Section.

Reproduced with permission of the copyright owner. Further reproduction prohibited without permission.

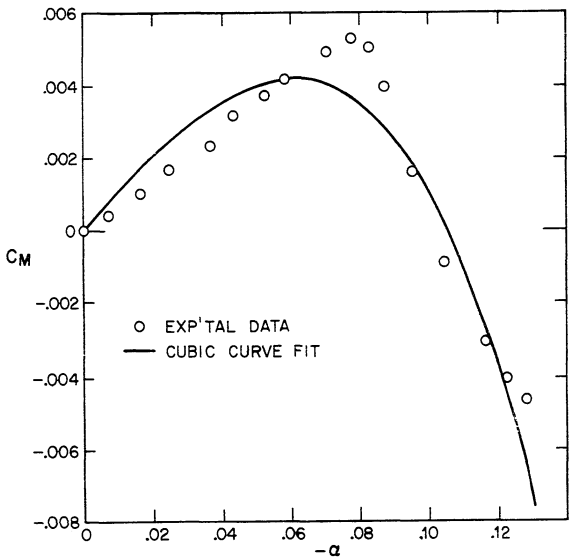

Fig. 5. Cubic Curve Fit to Moment Coefficient of Right Angle Section.

Reproduced with permission of the copyright owner. Further reproduction prohibited without permission.

than .15 radians. The characteristic dimension, R sin γ, used to approximate the effect of torsion on the flow field is taken to be one half the width of the section normal to the free stream. A more precise estimate would require dynamic tests. It can be shown that the limiting amplitude of a one-degree-of-freedom torsion oscillator with increasing flow velocity and a cubic fit of the aerodynamic coefficients is independent of the characteristic radius. This indicates that the imprecision of the estimate of this parameter should not greatly effect the results.

The asymptotic technique outlined in the first section was used in the solution of the simultaneous oscillator equations. The solution is limited to first order. Examples are limited to two-degrees-of-freedom with torsion and displacement normal to the free stream velocity.

3.8.1 Example Formulation

Since the system is not inertially coupled the differential oscillator equations are immediately in principal coordinates:

$$\ddot{y}+\omega_y^2 y = -c_y\dot{y}/m+\rho U^2\left(-a_1\alpha+b_1\alpha^3\right)/2m \tag{3.8.1}$$

$$\ddot{\theta}+\omega_\theta^2\theta = c_\theta\dot{\theta}/I+\rho U^2\left(-a_2\alpha+b_2\alpha^3\right)/2I \tag{3.8.2}$$

a_1, a_2, b_1 and b_2 are the aerodynamic coefficient curve fit parameters. c_y and c_θ are the viscous damping coefficients. y and θ are expressed by asymptotic expansions to order ϵ.

$$y = A_y \cos \Phi_y + \epsilon y_1 \tag{3.8.3}$$

Reproduced with permission of the copyright owner. Further reproduction prohibited without permission.

$$\theta = A_\theta \cos \bar{\theta}_\theta + \varepsilon\theta_1 \tag{3.8.4}$$

where

$$\bar{\theta}_y = \underline{w}_y(t-\Psi_1) \tag{3.8.5}$$

$$\bar{\theta}_\theta = \underline{w}_\theta(t-\Psi_1-\Psi_2) \tag{3.8.6}$$

The angle of attack to first order is

$$\alpha = \theta - R_1\dot{\theta}/U - \dot{y}/U = A_\theta \cos \bar{\theta}_\theta + R_1\underline{w}_\theta A_\theta \sin \bar{\theta}_\theta/U + \underline{w}_y A_y \sin \bar{\theta}_y/U \tag{3.8.7}$$

A_y, A_θ, Ψ_1 and Ψ_2 are slowly varying parameters. The perturbation equations are generated by the technique outlined in Section III. The perturbation equations are:

$$\begin{aligned}\varepsilon\ddot{y}_1 + \varepsilon\underline{w}_y^2 y_1 = \underline{w}_y^2 d\Big[& m_1 \sin \bar{\theta}_y + m_2 \cos \bar{\theta}_y + m_3 \sin \bar{\theta}_\theta + m_4 \cos \bar{\theta}_\theta \\ & + m_5 \sin 3\bar{\theta}_y + m_6 \sin 3\bar{\theta}_\theta + m_7 \cos 3\bar{\theta}_\theta \\ & + m_8 \sin (2\bar{\theta}_\theta - \bar{\theta}_y) + m_9 \cos (2\bar{\theta}_\theta - \bar{\theta}_y) + m_{10} \sin (2\bar{\theta}_\theta + \bar{\theta}_y) \\ & + m_{11} \cos (2\bar{\theta}_\theta + \bar{\theta}_y) + m_{12} \sin (2\bar{\theta}_y - \bar{\theta}_\theta) + m_{13} \cos (2\bar{\theta}_y - \bar{\theta}_\theta) \\ & + m_{14} \sin (2\bar{\theta}_y + \bar{\theta}_\theta) + m_{15} \cos (2\bar{\theta}_y + \bar{\theta}_\theta)\Big]\end{aligned} \tag{3.8.8}$$

$$\begin{aligned}\varepsilon\ddot{\theta}_1 + \varepsilon\underline{w}_\theta^2 \theta_1 = \underline{w}_y^2\Big[& n_1 \sin \bar{\theta}_y + n_2 \cos \bar{\theta}_y + n_3 \sin \bar{\theta}_\theta + n_4 \cos \bar{\theta}_\theta \\ & + n_5 \sin 3\bar{\theta}_y + n_6 \sin 3\bar{\theta}_\theta + n_7 \cos 3\bar{\theta}_\theta + n_8 \sin (2\bar{\theta}_\theta - \bar{\theta}_y) \\ & + n_9 \cos (2\bar{\theta}_\theta - \bar{\theta}_y) + n_{10} \sin (2\bar{\theta}_\theta + \bar{\theta}_y) + n_{11} \cos (2\bar{\theta}_\theta + \bar{\theta}_y) \\ & + n_{12} \sin (2\bar{\theta}_y - \bar{\theta}_\theta) + n_{13} \cos (2\bar{\theta}_y - \bar{\theta}_\theta) + n_{14} \sin (2\bar{\theta}_y + \bar{\theta}_\theta) \\ & + n_{15} \cos (2\bar{\theta}_y + \bar{\theta}_\theta)\Big]\end{aligned} \tag{3.8.9}$$

Reproduced with permission of the copyright owner. Further reproduction prohibited without permission.

where

$$m_1 = 2\beta_y \overline{A}_y + n_y U_y \left[-a_1 \overline{A}_y + b_1 \left(3\overline{A}_y^3/4U_y^2 + 3\overline{A}_y A_\theta^2/2 + 3r_2^2 \overline{A}_y A_\theta^2/U_y^2 \right) \right] + \dot{A}_y/\underline{\omega}_y$$

$$m_2 = \overline{A}_y \left(\underline{\omega}_y^2 - \omega_y^2 \right)/\omega_y^2 - A_y \dot{\psi}_1$$

$$m_3 = n_y U_y \left[-a_1 r_2 A_\theta + b_1 \left(3r_2^3 A_\theta^3/4U_y^2 + 3r_2 A_\theta^2/4 + 3r_2 \overline{A}_y^2 A_\theta/2U_y^2 \right) \right]$$

$$m_4 = n_y U_y^2 \left[-a_1 A_\theta + b_1 \left(3A_\theta^3/4 + 3r_2^2 A_\theta^3/4U_y^2 + 3\overline{A}_y^2/2U_y^2 \right) \right]$$

$$m_5 = -n_y b_1 \overline{A}_y^3/4U_y$$

$$m_6 = -n_y b_1 U_y \left(r_2^3 A_\theta^3/4U_y^2 + 3r_2 A_\theta^3/4 \right)$$

$$m_7 = -n_y U_y^2 b_1 \left(A_\theta^3/4 + r_2^2 A_\theta^3/4U_y^2 \right)$$

$$m_8 = -n_y U_y b_1 \left(-3\overline{A}_y A_\theta^2/4 + 3r_2^2 A_y A_\theta^2/4U_y^2 \right)$$

$$m_9 = 3n_y b_1 r_2 \overline{A}_y A_\theta^2/2$$

$$m_{10} = n_y U_y b_1 \left(3\overline{A}_y A_\theta^2/4 - 3r_2^2 \overline{A}_y A_\theta^2/4U_y^2 \right)$$

$$m_{11} = -3n_y b_1 r_2 \overline{A}_y A_\theta^2/2$$

$$m_{12} = -3n_y b_1 r_2 \overline{A}_y^2 A_\theta/4U_y$$

$$m_{13} = -3n_y b_1 \overline{A}_y^2 A_\theta/4$$

$$m_{14} = 3n_y b_1 r_2 \overline{A}_y^2 A_\theta/4$$

$$m_{15} = -3n_y b_1 \overline{A}_y^2 A_\theta/4$$

(3. 8. 10)

Reproduced with permission of the copyright owner. Further reproduction prohibited without permission.

and

$$
\begin{aligned}
n_1 &= n_\theta U_y\left[-a_2\overline{A}_y+b_2\left(3\overline{A}_y^3/4U_y^2+3\overline{A}_yA_\theta^2/2+3n_2^2\overline{A}_yA_\theta^2/2U_y^2\right)\right]\\
n_2 &= 0\\
n_3 &= 2\beta_\theta\underline{w}_\theta^2A_\theta/\underline{w}_y^2+n_\theta U_y\left[-a_2r_1A_\theta+b_2\left(3r_2^3A_\theta^3/4U_y^2+3r_2A_\theta^3/4\right.\right.\\
&\quad\left.\left.+3r_2\overline{A}_y^2A_\theta/2U_y^2\right)\right]+\underline{w}_\theta\dot{A}_\theta/\underline{w}_y^2\\
n_4 &= n_\theta U_y^2\left[-a_2A_\theta+b_2\left(3A_\theta^3/4+3r_2^2A_\theta^3/4U_y^2+3\overline{A}_y^2A_\theta/2U_y^2\right)\right]\\
&\quad+A_\theta\left(\underline{w}_\theta^2-w_\theta^2\right)/\underline{w}_y^2-\underline{w}_\theta^2A_\theta(\ddot{\psi}_1+\ddot{\psi}_2)/\underline{w}_y^2\\
n_5 &= -n_\theta b_2A_y^3/4U_y\\
n_6 &= -n_\theta U_yb_2\left(r_2^3A_\theta^3/4\ {}^2_y+3r_2A_\theta^3/4U_y\right)\\
n_7 &= -n_\theta U_y^2b_2\left(A_\theta^3/4+r_2^2A_\theta^3/4U_y^2\right)\\
n_8 &= n_\theta U_yb_2\left(-3\overline{A}_yA_\theta^2/4+3r_2^2\overline{A}_yA_\theta^2/4U_y^2\right)\\
n_9 &= 3n_\theta b_2r_2\overline{A}_y^2A_\theta/2\\
n_{10} &= n_\theta U_yb_2\left(3\overline{A}_yA_\theta^2/4-3r_2^2\overline{A}_yA_\theta^2/U_y^2\right)\\
n_{11} &= -3n_\theta b_2r_2\overline{A}_yA_\theta^2/2\\
n_{12} &= 3n_\theta b_2r_2\overline{A}_y^2A_\theta/4U_y\\
n_{13} &= -3n_\theta b_2\overline{A}_y^2/4\\
n_{14} &= 3n_\theta b_2r_2^2\overline{A}_y^2A_\theta/4\\
n_{15} &= -3n_\theta b_2\overline{A}_y^2A_\theta/4
\end{aligned}
\qquad (3.8.11)
$$

Reproduced with permission of the copyright owner. Further reproduction prohibited without permission.

The secular terms whose amplitudes are m_1 and m_2 and n_3 and n_4 will cause resonance of the perturbation equations in y_1 and θ_1 respectively regardless of the detuning between the oscillators. These secular terms are functions of the amplitudes of both oscillators so the system is always combined resonant. In addition the system will be harmonically internally resonant if

$$\omega_y \pm O(\varepsilon) = \begin{cases} \omega_\theta \\ 3\omega_\theta \\ 2\omega_y \pm \omega_\theta \\ 2\omega_\theta \pm \omega_y \end{cases} \qquad (3.8.12)$$

or

$$\omega_\theta \pm O(\varepsilon) = \begin{cases} \omega_y \\ 3\omega_y \\ 2\omega_y \pm \omega_\theta \\ 2\omega_\theta \pm \omega_y \end{cases} \qquad (3.8.13)$$

so that secular terms whose frequency depends on the detuning between parameters arise in the perturbation equations. Two classes of asymptotic solution may be developed. One class is valid only for cases of harmonic resonance and the other class is valid outside the harmonic resonance band of frequencies.

3.8.2 Combined Resonant Oscillations

In the absence of harmonic resonance $\underline{\omega}_y = \omega_y$ and $\underline{\omega}_\theta = \omega_\theta$. Those terms in the perturbation equations whose amplitudes

Reproduced with permission of the copyright owner. Further reproduction prohibited without permission.

are m_1, m_2, n_3 and n_4 are cast into the variational equations. Averaging the variational equations as outlined in the second section produces the following system of first order differential equations:

$$2\dot{\bar{A}}_y/\underline{\omega}_y A_y = -2\beta_y + n_y a_1 U_y - n_y b_1 \left(3\bar{A}_y^2/4\, U_y + 3A_\theta^2 U_y/2 + 3r_2^2 A_\theta^2/2U_y\right) \tag{3.8.14}$$

$$2\underline{\omega}_\theta \dot{A}_\theta/A_\theta \underline{\omega}_y^2 = -2\beta_\theta \underline{\omega}_\theta^2/\underline{\omega}_y^2 + n_\theta a_2 r_2 U_y - n_\theta b_2 U_y \left(3r_2^3 A_\theta^2/4U_y^2 + 3r_2 A_\theta^2/4 + 3r_2 \bar{A}_y^2/2U_y^2\right) \tag{3.8.15}$$

$$2\underline{\omega}_\theta^2 \dot{\Psi}_2/\underline{\omega}_y^2 = -n_\theta a_2 U_y^2 A_\theta + n_\theta b_2 \left(3A_\theta^3 U_y^2/4 + 3r_2^2 A_\theta^3/4 + 3\bar{A}_y^2 A_\theta/2\right) \tag{3.8.16}$$

$$\dot{\Psi}_1 = 0 \tag{3.8.17}$$

The right sides of Equations (3.8.14) through (3.8.17) are independent of the time shift Ψ_2 since the system is not harmonically resonant and independent of Ψ_1 as the system is autonomous. Equations (3.8.14) and (3.8.15) alone determine the amplitude of the solutions. Simple harmonic solutions are sought by setting $\dot{A}_y = \dot{A}_\theta = 0$ and seeking roots of Equations (3.8.14) and (3.8.15). There are four possible sets of simple harmonic solutions which are listed in Table I with the corresponding stability criteria found by requiring small perturbations to diminish in time.

If

$$\left.\begin{aligned} b_1 &> 0 \\ r_1 b_2 &> 0 \end{aligned}\right\} \tag{3.8.18}$$

Reproduced with permission of the copyright owner. Further reproduction prohibited without permission.

as is required for bounded solutions then solution #4 where both plunge and torsion participate to first order is never stable. Moreover at least one of the first three solutions must be stable. The solutions will either be zero or dominated by plunge or torsion to first order. The stability criteria of these solutions can be specified in terms of the two variables U_y^* and U_θ^*.

$$\left.\begin{aligned} U_y^* &= n_y U_y a_1 / 2\beta_y \\ U_\theta^* &= n_\theta U_\theta a_2 r_1 / 2\beta_\theta \end{aligned}\right\} \qquad (3.8.19)$$

A two dimensional stability map is constructed in these variables using the aerodynamic coefficients determined by the cubic fit of the right angle section (Figs. 4 and 5) shown in Figure 6. There exists a range of parameters where both the plunge dominated solution #2 and the torsion dominated solution #3 are stable. Both solutions cannot simultaneously exist. The solution obtained in this region depends on the initial conditions.

The order ε terms in the asymptotic series for y and θ are found by substituting the order one solutions listed in Table 1 into the remaining terms on the right hand sides of the perturbation equations and solving for εy_1 and $\varepsilon\theta_1$. Solution #2, correct to order ε terms, is

$$\left.\begin{aligned} y/d &= \overline{A}_y \cos\bar{\tau}_y - m_5 \sin 3\bar{\tau}_y/8 \\ \theta &= n_1 \sin\bar{\tau}_y \Big/ \left(\omega_\theta^2/\omega_y^2 - 1\right) + n_5 \sin 3\bar{\tau}_y \Big/ \left(\omega_\theta^2/\omega_y^2 - 9\right) \end{aligned}\right\} \qquad (3.8.20)$$

where n_1, n_5 and m_5 are given by equations sets (3.8.10) and (3.8.11) and are evaluated at the amplitudes A_y and A_θ given by solution #2 of

Reproduced with permission of the copyright owner. Further reproduction prohibited without permission.

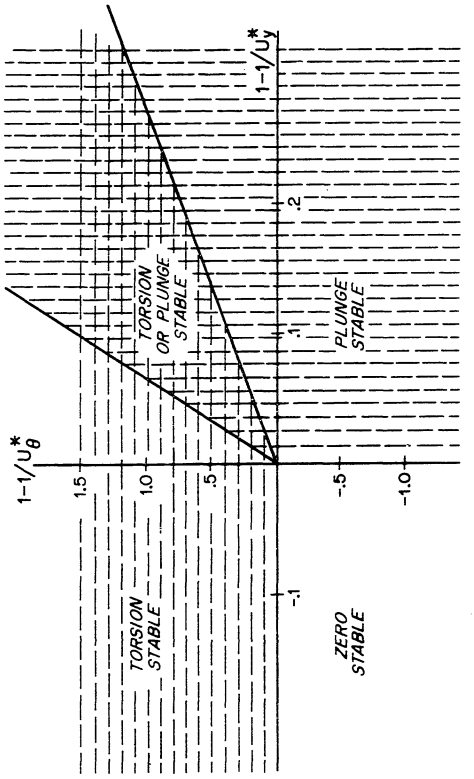

Fig. 6, Stability Map for Combined Resonance.

Reproduced with permission of the copyright owner. Further reproduction prohibited without permission.

Table 1. Solution #3, correct to order ϵ terms, is:

$$\left.\begin{aligned} y/d &= \left(m_3 \sin \bar{\xi}_\theta + m_4 \cos \bar{\xi}_\theta\right) \Big/ \left(1 - \omega_\theta^2/\omega_y^2\right) + \left(m_6 \sin 3\bar{\xi}_\theta \right. \\ &\quad \left. + m_7 \cos 3\bar{\xi}_\theta\right) \omega_y^2/\omega_\theta^2 \left(1 - 9\omega_\theta^2/\omega_y^2\right) \\ \theta &= A_\theta \cos \bar{\xi}_\theta - \left(n_6 \sin 3\bar{\xi}_\theta + n_7 \cos 3\bar{\xi}_\theta\right)/8 \end{aligned}\right\} \quad (3.8.21)$$

where m_3, m_4, m_6, m_7, n_6 and n_7 are evaluated with the order one amplitudes given by solution #3 in Table 1. The order ϵ terms will remain small only if the system is not harmonically resonant so that neither $\omega_y \approx \omega_\theta$ nor $\omega_y \approx 3\omega_\theta$ nor $\omega_\theta \approx 3\omega_y$. As the system approaches harmonic resonance these terms become large and the combined resonant solution is no longer applicable.

Parkinson [3] has shown that the order one amplitude of a viscously damped plunge oscillator may be expressed in terms of a single variable as the angle of attack of a plunge oscillator only depends on the single parameter $\dot{y}/U$. The order one amplitude of a viscously damped torsion galloping oscillator is determined by two variables as the angle of attack of a torsion oscillator depends both on θ and $\dot{\theta}$. Four variables are required to specify the first order behavior of combined resonant torsion and plunge galloping oscillations since the system angle of attack depends on $\dot{y}/U$, θ, $\dot{\theta}/U$ and the frequency ratio ω_y/ω_θ.

Bounds for the plunge dominated and torsion dominated, order one, combined resonant solutions are obtained by taking the limit as damping approaches zero. This gives

Reproduced with permission of the copyright owner. Further reproduction prohibited without permission.

$$\left(\overline{A}_y\right)_{max} = U_y\left(4a_1/3b_1\right)^{1/2}$$

$$\left(A_\theta\right)_{max} = \left[4U_\theta^2 a_2 r_1/3b_2\left(r_1^3 + r_1 U_\theta^2\right)\right]^{1/2}$$

As the flow velocity becomes large the angle of attack of the flow to the structure approaches maximum limiting values. The increase with $\left(\overline{A}_y\right)_{max}$ with U_y reflects the fact that the maximum angle of attack of the plunge oscillator is proportional to A_y/U. The maximum order one torsion amplitude becomes independent of flow velocity and characteristic radius if $U_\theta^2 \gg r_1$.

Reproduced with permission of the copyright owner. Further reproduction prohibited without permission.

#	SOLUTION	STABILITY CRITERIA
1	$\overline{A}_y = 0$	$1 - \frac{1}{U_y^*} < 0$
	$A_\theta = 0$	$1 - \frac{1}{U_\theta^*} < 0$
2	$\overline{A}_y = \left[\frac{4U_y}{3b_1}\left(a_1 U_y - \frac{2\beta_y}{n_y}\right)\right]^{1/2}$	$1 - \frac{1}{U_y^*} > 0$
	$A_\theta = 0$	$2\frac{b_2 a_1}{a_2 b_1}\left(1 - \frac{1}{U_y^*}\right) > 1 - \frac{1}{U_\theta^*}$
3	$\overline{A}_y = 0$	$1 - \frac{1}{U_\theta^*} > 0$
	$A_\theta = \left[\frac{4U_\theta}{3b_2}\left(\frac{a_2 r_1 U_\theta - 2\beta_\theta / n_\theta}{r_1^3 + r_1 U_\theta^2}\right)\right]^{1/2}$	$2\frac{b_1 a_2}{b_2 a_1}\left(1 - \frac{1}{U_\theta^*}\right) > 1 - \frac{1}{U_y^*}$
4	$\overline{A}_y = \left[\frac{S_1 S_6 - S_3 S_4}{S_5 S_3 - S_6 S_2}\right]^{1/2}$	$S_3 A_\theta^2 + S_5 A_y^2 / \omega_y < 0$
	$A_\theta = \left[\frac{S_2 S_4 - S_1 S_5}{S_5 S_3 - S_6 S_2}\right]^{1/2}$	$-b_1 b_2 r_1 > 0$
	$S_1 = -2\beta_\theta \omega_\theta^2 / \omega_y^2 + a_2 n_\theta r_2 U_y$	
	$S_2 = -3b_2 r_2 n_\theta / 2U_y$	
	$S_3 = -3b_2 r_2^3 n_\theta / 4U_y - 3b_2 r_2 n_\theta U_y / 4$	
	$S_4 = -2\beta_y + a_1 n_y U_y$	
	$S_5 = -3b_1 n_y / 4U_y$	
	$S_6 = -3b_1 n_y U_y / 2 - 3r_2^2 n_y b_1 / 2U_y$	

TABLE 1 - COMBINED RESONANT SOLUTIONS

Reproduced with permission of the copyright owner. Further reproduction prohibited without permission.

3.8.3 Harmonically Resonant Example I

Consider the right angle section with the ratio of natural frequencies near unity, $\omega_y/\omega_\theta = 1 + O(\epsilon)$. With this frequency ratio the terms in the perturbation equations whose amplitudes are $n_3, n_4, n_8, n_9, n_{12}$, n_{13} and $m_1, m_2, m_8, m_9, m_{12}, m_{13}$ are now secular. The amplitude and frequency of some of these secular terms are dependent on $\overline{A}_y$, A_θ and ω_y/ω_θ respectively so the system is harmonically resonant. It is convenient to define

$$\underline{\omega}_y = \omega_y \tag{3.8.23}$$

$$\underline{\omega}_\theta = \omega_y \tag{3.8.24}$$

The secular terms are cast into the variational equation and these equations are averaged. The following set of equations is produced by the technique of Chapter II.

$$-2\dot{\overline{A}}_y/n_y\omega_y U_y^2 = 2\beta_y A_y/n_y U_y^2 - a_1\left(A_\theta \sin(\omega_y\Psi_2) + A_\theta r\cos(\omega_y\Psi_2)/U_y + \overline{A}_y/U_y\right) + b_1\left(d_{11}\overline{A}_y^3 + d_{12}\overline{A}_y^2 + d_{13}\overline{A}_y A_\theta^2 + d_{14}A_\theta^3\right) \tag{3.8.25}$$

$$-2\dot{A}_\theta/n_\theta U_y^2\omega_y = 2\beta_\theta A_\theta/n_\theta U_y^2 - a_2\left(r_1 A_\theta/U_y + \overline{A}_y\cos(\omega_y\Psi_2)/U_y\right) + b_2\left(d_{21}\overline{A}_y^3 + d_{22}\overline{A}_y^2 A_\theta + d_{23}\overline{A}_y A_\theta^2 + d_{24}A_\theta^3\right) \tag{3.8.26}$$

$$2\dot{\Psi}_2/n_y U_y^2 = 2\left(\omega_y - \omega_\theta\right)/n_y^2 U_y^2\omega_y + n_\theta\Big[-a_2\left(A_\theta + \overline{A}_y\sin(\omega_y\Psi_2)/U_y\right) + b_2\left(d_{31}\overline{A}_y^3 + d_{32}\overline{A}_y^2 A_\theta + d_{33}\overline{A}_y A_\theta^2 + d_{34}A_\theta^3\right)\Big]/n_y A_\theta - \Big[-a_1\left(A_\theta\cos(\omega_y\Psi_2) - A_\theta r\sin(\omega_y\Psi_2)/U_y\right) + b_1\left(d_{41}\overline{A}_y^3 + d_{42}\overline{A}_y^2 A_\theta + d_{43}\overline{A}_y A_\theta^2 + d_{44}A_\theta^3\right)\Big] \tag{3.8.27}$$

Reproduced with permission of the copyright owner. Further reproduction prohibited without permission.

where

$$d_{11} = 3/4U_y^3$$

$$d_{12} = 9\sin(\omega_y \Psi_2)/4U_y^2 + 9r_1\cos(\omega_y \Psi_2)/4U_y^3$$

$$d_{13} = 3\left(1-\cos(2\omega_y \Psi_2)/2\right)/2U_y + 3r_1^3\left(1+\cos(2\omega_y \Psi_2)/2\right)/2U_y^3 + 3r_1\sin(2\omega_y \Psi_2)/2U_y^2$$

$$d_{14} = 3\sin(\omega_y \Psi_2)/4 + 3r_1^3\cos(\omega_y \Psi_2)/4U_y^3 + 3r\cos(\omega_y \Psi_2)/4U_y + 3r_1^2\sin(\omega_y \Psi_2)/4U_y^2$$

$$d_{21} = 3\cos(\omega_y \Psi_2)/4U_y^3$$

$$d_{22} = 3\sin(2\omega_y \Psi_2)/4U_y^2 + 3r_1\left(1+\cos(2\omega_y \Psi_2)/2\right)/2U_y^3$$

$$d_{23} = 3\cos(\omega_y \Psi_2)/4U_y + 9r_1^2\cos(\omega_y \Psi_2)/4U_y^3 + 3r_1\sin(\omega_y \Psi_2)/2U_y^2$$

$$d_{24} = 3r_1^3/4U_y^3 + 3r_1/4U_y$$

$$d_{31} = 3\sin(\omega_y \Psi_2)/4U_y^3$$

$$d_{32} = 3\left(1-\cos(2\omega_y \Psi_2)/2\right)/2U_y^2 + 3r_1\sin(2\omega_y \Psi_2)/4U_y^3$$

$$d_{33} = 9\sin(\omega_y \Psi_2)/4U_y + 3r_1^2\sin(\omega_y \Psi_2)/4U_y^3 + 3r_1\cos(\omega_y \Psi_2)/2U_y^2$$

$$d_{34} = 3/4 + 3r_1^2/4U_y^2$$

$$d_{41} = 0$$

$$d_{42} = 3\cos(\omega_y \Psi_2)/4U_y^2 - 3r_1\sin(\omega_y \Psi_2)/4U_y^3$$

(3.8.28)

Reproduced with permission of the copyright owner. Further reproduction prohibited without permission.

$$d_{43} = 3 \sin (2\omega_y \Psi_2)/4U_y - 3r_1^2 \sin (2\omega_y \Psi_2)/4U_y^3 + 3r_1 \cos (2\omega_y \Psi_2)/2U_y^2$$

$$d_{44} = 3 \cos (\omega_y \Psi_2)/4 - 3r_1^2 \sin (\omega_y \Psi_2)/4U_y^3 - 3r_1 \sin (\omega_y \Psi_2)/4U_y + 3r_1^2 \cos (\omega_y \Psi_2)/4U_y^2$$

As noted earlier four parameters are required to specify the steady first order solution if the system is not harmonically resonant. If the system is harmonically resonant two additional parameters are required to scale the small shifts in frequency produced by each oscillator. A total of six parameters such as β_y/n_y, β_θ/n_θ, ω_y/ω_θ, U_y, n_θ and n_y are required to specify the steady response of harmonically resonant two-degree-of-freedom galloping systems.

Equations (3.8.25) through (3.8.27) are independent of the time shift Ψ_1 so these equations form an independent set which determine the amplitude and relative phase of the two oscillators. Even though a simple cubic curve fit was employed there are a total of 16 nonlinear terms in these three equations. No closed for solutions are known for this set even in the case of simple harmonic motion. The large number of parameters and the necessity of numerical solutions makes it difficult to fully catalog the response of the system. For a limited range of parameters some insight may be gained into the behavior of the solution. Indeed the form of the averaged variational equations makes two observations immediately apparent:

1. No steady solutions corresponding to $A_y = 0$, A_θ finite or $A_\theta = 0$, A_y finite are possible. Any steady solutions will be characterized by both oscillators participating

Reproduced with permission of the copyright owner. Further reproduction prohibited without permission.

with order one solutions.

2. Small shifts in the ratio of natural frequencies, ω_y/ω_θ, may strongly affect the result.

Solutions to Equations (3.8.25), (3.8.26) and (3.8.27) were obtained by directly integrating these equations numerically using a Runge-Kutta scheme on an IBM 370/75 computer until a steady response was obtained. In every case a simple harmonic limit cycle was obtained corresponding to $\dot{\bar{A}}_y = \dot{A}_\theta = \dot{\psi}_2 = 0$, although several hundred cycles were generally required. In none of the cases was a first order beating solution of the type observed in certain conservative systems [9] found.

In Figure 7 the harmonic resonant solution amplitudes as a function of the detuning are compared with the combined resonant solution and data points obtained by direct integration of the nonlinear differential equations. The harmonic resonant solution and the data points obtained by direct integration are in good agreement for small values of detuning (specifically $|\omega_y/\omega_\theta - 1| < 10\varepsilon$ where ε is defined by Equation (3.7.1)). For small detuning the changes in angle of attack produced by the torsion and plunging oscillations are of the same order. The combined resonant solution provides a good approximation outside the frequency band that contains the harmonic resonant effects, but the combined resonant solution is not capable of predicting the complex interaction of the two degrees of freedom that occurs at harmonic resonance.

Outside the harmonic resonant frequency band only one of the oscillators will have a stable first order limit cycle. The remaining

Reproduced with permission of the copyright owner. Further reproduction prohibited without permission.

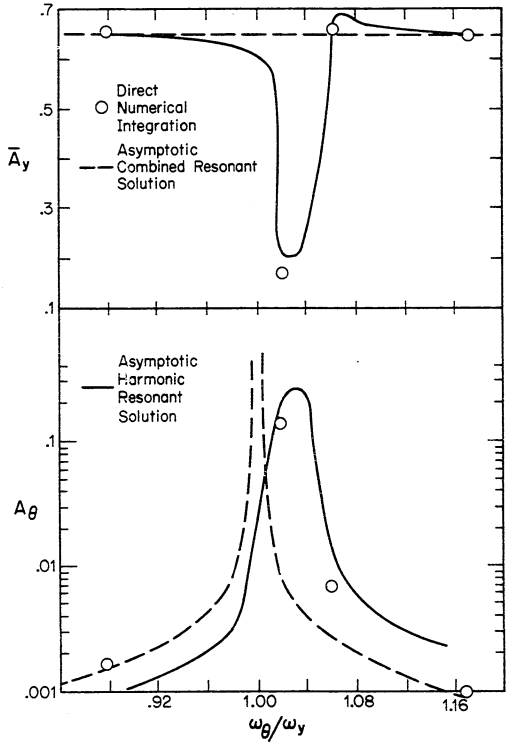

Fig. 7. Comparison of Solutions for Harmonic Resonance, $U_y = 5$, $n_\theta = .01952$, $n_y = .002975$, $\beta_y = .004125$, $\beta_\theta = .00513$.

Reproduced with permission of the copyright owner. Further reproduction prohibited without permission.

oscillator has an order ε limit cycle. As the two oscillators approach harmonic resonance one oscillator will contribute forcing terms through the aerodynamic coupling to the other oscillator which produce internal resonance. The oscillators interact strongly. Both oscillators achieve order one limit cycles. The resultant motion depends on the details of each oscillator and the aerodynamic coupling.

In Figure 8 the density of the cross section is varied through a range corresponding roughly to a hollowed out plastic shell, solid aluminum and solid steel composition. The maximum amplitudes of plunge and torsion are unchanged by varying the density since the ratio of the maximum aerodynamic forces in phase with velocity to damping was held constant. Decreasing the density of the cross section does increase the width of the harmonic resonance frequency band.

Figure 9 shows the effect of increasing the free stream velocity on a system which has an order one torsion limit cycle and order ε plunge oscillation outside the harmonic resonance band of frequencies. Increasing the free stream velocity has negligible effect on the torsion amplitude outside the harmonic resonant frequency band since, as noted earlier, the maximum amplitude of a purely torsional oscillator is independent of free stream velocity. The plunge amplitude and torsion amplitude within the harmonic resonant frequency band both increase with increasing free stream velocity. All the order one harmonic resonance effects are contained in the frequency band $|1-\omega_y/\omega_\theta| < 10\varepsilon$ where ε defined from Equation (3.7.1) is $n_y U_y^2 \partial C_y/\partial\alpha$. The width of the harmonic resonant band increases with free stream velocity as the dynamic pressure increases.

Reproduced with permission of the copyright owner. Further reproduction prohibited without permission.

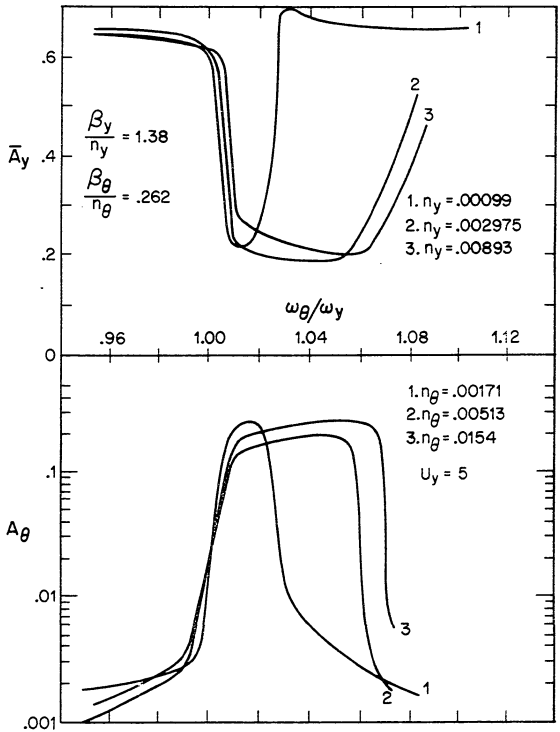

Fig. 8. Effect of Varying Structural Density on Harmonic Resonance.

Reproduced with permission of the copyright owner. Further reproduction prohibited without permission.

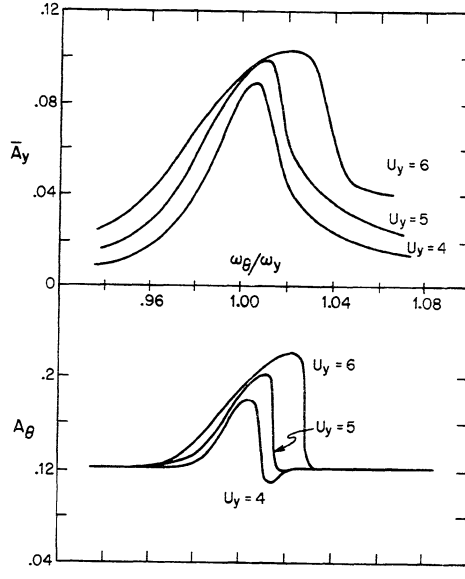

Fig. 9. Effect of Varying Free Stream Velocity on Harmonic Resonance, $n_y = .002975$, $n_\theta = .01952$, $\beta_y = .0075$, $\beta_\theta = 0$.

Reproduced with permission of the copyright owner. Further reproduction prohibited without permission.

Figure 10 shows the amplitude of plunge as a function of detuning while increasing plunge damping and decreasing torsion damping. The damping parameters were chosen from each of the three quadrants of Figure 6 corresponding to nontrivial combined resonant solutions. As the damping of plunge is progressively increased and the damping of torsion is decreased, the system changes from plunge dominated response to torsion dominated response. The small changes in damping, less than 1% of critical damping, greatly change the response of the system.

3.8.4 Harmonic Resonant Example II

If $\omega_\theta = 3\omega_y + O(\varepsilon)$ the system is harmonically resonant. The secular terms in the perturbations are cast into the variational equations and these equations are averaged. This produces a system of the same form as Equations (3.8.25) through (3.8.27). Figure 11 shows the results of integrating the averaged variational equations until a steady solution is reached. The plunge amplitude predicted by the harmonically resonant solution is compared with the combined resonant solution and data points obtained by direct numerical integration of the differential oscillator equations. Although the harmonic resonant solution does predict a stable solution for a broad frequency band, the numerical data points show it is a good approximation only in the narrow band where the combined resonant solution becomes order one. Outside this narrow frequency band the combined resonant solution provides a good approximation.

Reproduced with permission of the copyright owner. Further reproduction prohibited without permission.

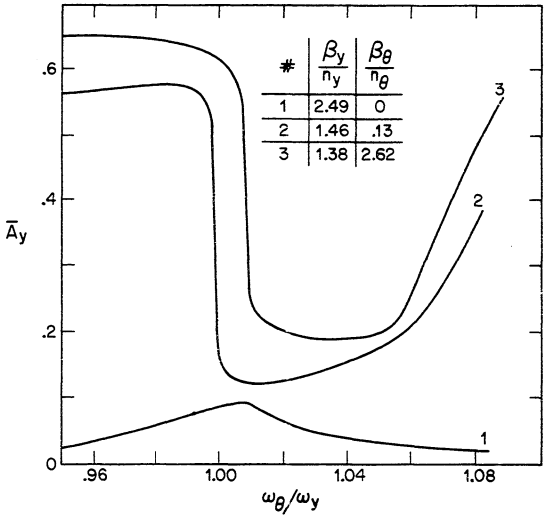

Fig. 10. Effect of Varying Damping on Plunge Amplitude, $n_y = .002975$, $n_\theta = .01952$, $U_y = 5$.

Reproduced with permission of the copyright owner. Further reproduction prohibited without permission.

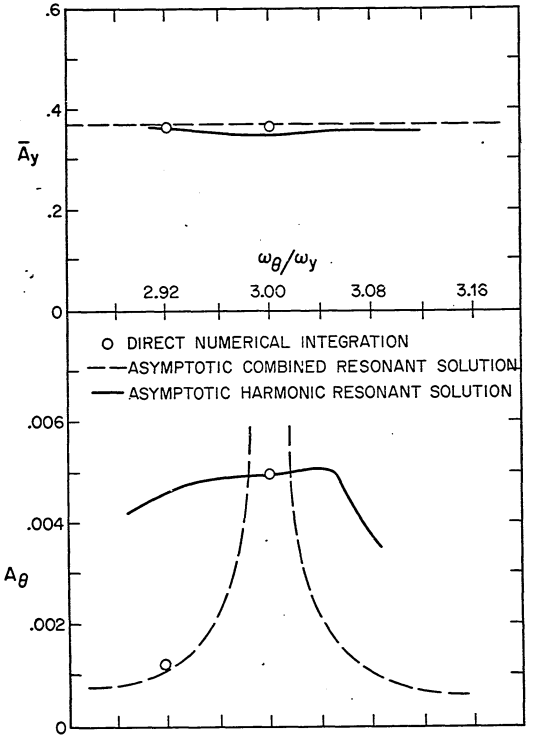

Fig. 11. Solutions at Harmonic Resonance for $\omega_\theta/\omega_y \approx 3$, $n_y = .002975$, $n_\theta = .01952$, $U_y = 4.5$, $\beta_y = .004125$, $\beta_\theta = .00513$.

Reproduced with permission of the copyright owner. Further reproduction prohibited without permission.

Experiments at the frequency ratio $\omega_\theta/\omega_y = 2.92$ with the right angle section and no inertial coupling were performed by Slater [8]. Comparison of predicted plunge amplitude and the experimental data points (Fig. 12) show there is substantial agreement with the combined resonant solution. A higher order curve fit of the aerodynamic force coefficients should produce the hysteristic jump contained in the experimental data. The amplitude of torsion, not shown, is order ε and contains much scatter due to vortex shedding effects. The reduced velocity of torsion corresponding to $U_y = 4$ is $U_\theta = 1.4$. U_θ is well below the minimum reduced velocity required for validity of the quasi-static assumption.

3.9 SUMMARY AND CONCLUSIONS

A model has been presented for multi dimensional galloping. The aerodynamic forces on the cross section are assumed to be dependent only on the relative flow velocity and angle of attack. The angle of attack is approximated as a linear function of torsion and displacement. A simple stability criteria for the zero solution and an estimate of the maximum galloping amplitude are developed.

Two-degree-of-freedom examples are made using a cubic curve fit to the aerodynamic coefficients for the right angle section. The example system has plunge and torsion degrees-of-freedom and is not inertially coupled. The system is analyzed using asymptotic techniques. Numerical solution is required in some cases due to the large number of nonlinear terms. Two regimes of solution are shown to exist. One solution regime, called combined resonance, is

Reproduced with permission of the copyright owner. Further reproduction prohibited without permission.

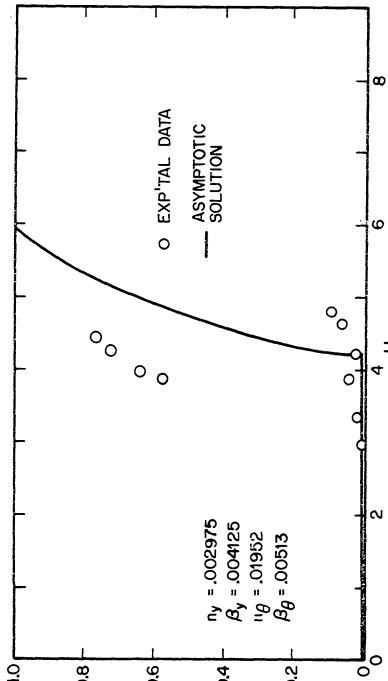

Fig. 12. Comparison of Experimental Data [8] with Combined Resonant Solution for Plunge.

Reproduced with permission of the copyright owner. Further reproduction prohibited without permission.

characterized by dominance of either the torsion or the plunge degree-of-freedom. The second solution regime, called harmonic resonance, can occur only if the natural frequencies of the principal modes are nearly integer multiples. Harmonic resonance is characterized by the exchange of large amounts of energy between the torsion and plunge degrees-of-freedom. Order one amplitudes arise both in torsion and plunge degrees-of-freedom. The harmonic resonance solution amplitudes are very sensitive to small changes in the natural frequency. In both solution regimes the order one solutions were simple harmonic.

Examples show the width of the band of natural frequencies containing the harmonic resonance increases with free stream flow velocity and decreases with the ratio of structure density to fluid density. The amplitude of solution increased or remained constant with increasing free stream velocity. The asymptotic solution is found to be in good agreement with the available experimental data.

3.10 REFERENCES

1. Cheers, F., "A Note on Galloping Conductors," National Research Council of Canada, Report No. MT-14, June 1950.

2. Sisto, F., "Stall-Flutter in Cascades," J. Aeronautical Sciences, Vol. 20, No. 9, 1953, pp. 598-604.

3. Parkinson, G. V. and Smith, J. D., "The Square Prism as an Aeroelastic Non-Linear Oscillator," Quart. J. Mech. and Appl. Math., Vol. 17, Part 2, May 1964, pp. 225-239.

4. Den Hartog, J. P., Mechanical Vibrations, McGraw-Hill, New York, 4th ed., 1956.

5. Richardson, A. S., Martucelli, J. R. and Price, W. S., "Research Study on Galloping of Electric Power Transmission Lines," Proc. First Int. Conf. on Wind Effects on Bldgs. and Structures, NPL, Teddington, Vol. II, 1965, pp. 612-686.

Reproduced with permission of the copyright owner. Further reproduction prohibited without permission.

6. Personal communication, A. G. Davenport, April 1972.

7. Hogg, A. D., Edwards, A. T., "The Status of the Conductor Galloping Problem in Canada," Proc. First Int. Conf. on Wind Effects on Bldgs. and Structures, NPL, Teddington, Vol. II, 1965.

8. Slater, J. E., "Aeroelastic Instability of a Structural Angle Section," Ph. D. Thesis, University of British Columbia, March 1969.

9. Gilchrist, A. O., "The Free Oscillation of Conservative Quasi-linear Systems with Two Degrees of Freedom," Int. J. Mech. Sci., 1961, Vol. 3, pp. 286-311.

Reproduced with permission of the copyright owner. Further reproduction prohibited without permission.

IV. A MODEL FOR VORTEX INDUCED VIBRATION OF CIRCULAR CYLINDERS

4.1 INTRODUCTION

A circular cylinder in a subsonic flow experiences oscillating lift and drag forces at Reynolds numbers greater than 100. These forces are the result of fluctuating fluid pressure on the cylinder surface generated by vortices shed alternately from each side of the cylinder. The oscillating vortex forces arise both with stationary and vibrating cylinders and they can cause an elastically mounted cylinder to vibrate and emit aeolian tones. The large amplitude oscillation induced in elastic structures by vortex shedding are of great practical importance because of the potentially destructive effect on bridges, antennas, cables and launch vehicles. The objective of this section is to develop a model for the interaction between a structure and the vortex shedding which will be useful in the analysis of the response of structural systems.

In 1878 Strouhal [1] found, with experiments on a taut wire in an air stream, that aeolian tones generated by the vibrating wire were dependent only on the air stream velocity and the wire diameter. He also observed that the sound greatly increased when the natural tones of the wire coincided with the aeolian tones. That is, when the shedding frequency coincided with the natural frequency of an elastic system the system resonated. In 1879, Lord Rayleigh [2] discovered that a violin string vibrating in the wind oscillated in the plane perpendicular to the wind indicating that the oscillating force component

Reproduced with permission of the copyright owner. Further reproduction prohibited without permission.

normal to the wind was far greater than the component parallel to the wind. Landweber [3] noted that at certain speeds, the submarine periscope undergoes such violent vibration that it becomes utterly useless. Since the periscope may be considered a circular cylinder clamped at one end and free at the other, Landweber suspected that the vibration might be due to a resonance between the eddy (vortex) frequency and the natural frequency of the periscope in its fundamental mode. No oscillations were observed outside of the resonant condition. This suggests that there is a strong coupling between the vortex shedding and the structural response.

Given a structural system which incorporates circular cylinders exposed to fluid flow, one would like to calculate the amplitude and frequency of structural vibration as a function of the structural and flow parameters. Unfortunately, the theory of vortex shedding, especially the near wake region, is very complex with turbulent oscillating boundary layer separation. An exact solution to the fluid elastic problem is not feasible. Therefore a model will be developed which approximates the gross two dimensional behavior of the fluid. The self excited vortex shedding and resonance behavior suggests the fluid oscillations may be modeled by a nonlinear oscillator as was first noted by Bishop and Hassan [4]. Hartlen, Baines, and Currie [5] have arbitrarily constructed a nonlinear representation which shows some of this behavior. Skop and Griffin [6] have refined the Hartlen, Baines and Currie model. The Skop and Griffin model predictions for the response of an elastically mounted cylinder are in quantitative agreement with experimental data. Skop and Griffin

Reproduced with permission of the copyright owner. Further reproduction prohibited without permission.

provide a means for determining the model parameters as a function of physical parameters. Unfortunately this model is not applied to the case of forced cylinder motion.

These models for vortex induced vibration have several weaknesses, among them:

(1) The models for the fluid behavior are arbitrarily derived. No systematic attempt is made to base the components of the model on known fluid dynamic behavior. The model behavior cannot be generally interpreted in terms of fluid phenomena. The models are not useful for identifying the relevant nondimensional variables.

(2) The model parameters are chosen to back fit the same experimental data that the models are used to predict. It is not surprising that the Skop and Griffin model shows good quantitative agreement with experimental data since the model parameters were chosen to produce this.

(3) Evidently no attempt has been made to apply these models to continuous systems of practical importance.

Here a two-degree-of-freedom oscillator model will be developed by considering a control volume approach to the vortex shedding process which allows the model response to be interpreted in terms of physical behavior. The model parameters are fixed by back fitting experimental results for stationary and forced cylinder motion. The model is then compared with experimental results for the elastically mounted cylinder. The model is applied to a pivoted rod which approximates the fixed-free bending cantilever in its first mode.

Reproduced with permission of the copyright owner. Further reproduction prohibited without permission.

4.2 DIMENSIONAL ANALYSIS

The following nondimensional parameters have proven useful in describing the vortex force on a cylinder in simple harmonic motion:

UD/ν - Reynolds number

U/fD - Reduced velocity

A_y/D - Amplitude

L/D - Aspect ratio

where U is the free stream velocity, D is the cylinder diameter, ν is the kinematic viscosity, f is the frequency of vibration, A_y is the cylinder amplitude and L is the spanwise length. For elastically mounted cylinders the following additional parameters have proven useful in analysis:

$\rho D^2/m$ - Mass ratio

δ - Logrithmic decrement of damping

where ρ is the fluid density and m is the mass per unit length of the cylinder.

The Reynolds number of the flow governs the gross laminar or turbulent flow behavior. Attention will be limited to the Reynolds number range where there exists a well formed vortex street. The reduced velocity is useful in describing the natural frequency of vortex shedding relative to the frequency of structural motion. Changes in the amplitude of the cylinder can produce large changes in

Reproduced with permission of the copyright owner. Further reproduction prohibited without permission.

the amplitude of the vortex force. The aspect ratio of the cylinder can have a large effect on the vortex force due to end effects and the spanwise correlation of vortex shedding which is discussed in the following section.

4.3 SPANWISE CORRELATION AND AMPLITUDE DEPENDENCE OF THE VORTEX LIFT FORCE

A two dimensional flow model for the vortex shedding process cannot approximate spanwise flow effects known to arise at low vibration amplitudes. For example, Figure 1 shows the spanwise flow correlation of a cylinder vibrating at resonance with vortex shedding as a function of cylinder amplitude. The low spanwise flow correlation for a stationary cylinder may contribute to the relatively large scatter in experimental measurements of the amplitude of the vortex lift force on a stationary cylinder shown in Figure 2. When a long cylinder is stationary, vortices shed along the span with no apparent fixed phase relationship so the fluctuating lift force generated by a vortex shed at one location maybe nearly canceled by the force generated by another vortex at a different spanwise location. However as vibration amplitude increases the flow becomes correlated along the span and the vortices shed in nearly two dimensional sheets. The oscillating vortex forces generated at different spanwise locations are in phase and the forces sum along the span to produce a large oscillating force on the cylinder.

The vortex force on the cylinder may be dependent on the amplitude of vibration. In order to investigate quantatively the manner in

Reproduced with permission of the copyright owner. Further reproduction prohibited without permission.

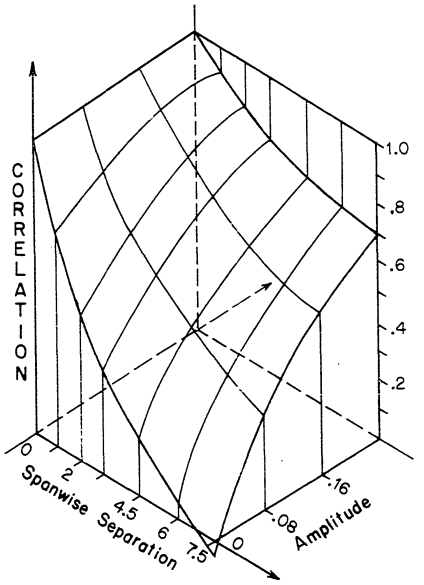

Fig. 1. Spanwise correlation as a function of Double Amplitude and Spanwise Separation for Vortex Shedding from Stationary Cylinder [7].

Reproduced with permission of the copyright owner. Further reproduction prohibited without permission.

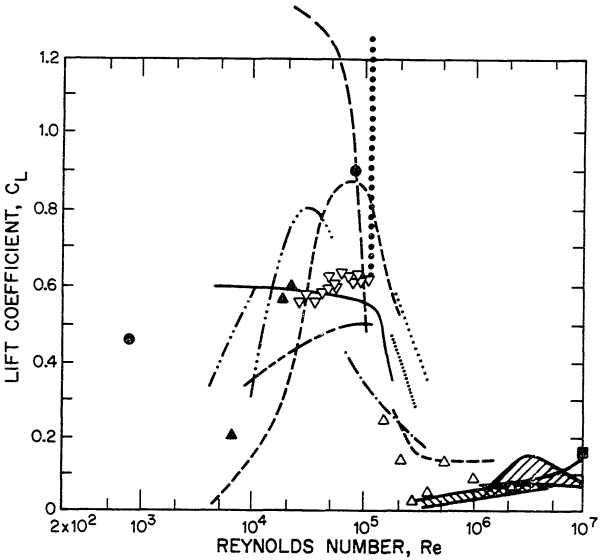

Fig. 2. Lift Coefficient for a Stationary Cylinder [8][9][10].

Reproduced with permission of the copyright owner. Further reproduction prohibited without permission.

which the vortex force varies with amplitude the vortex force is modeled as harmonic,

$$F_y = F_y^o \sin \omega t \tag{4.3.1}$$

Applying this vortex force to a viscously damped spring supported cylinder constrained free stream (Fig. 3) gives

$$\ddot{y} + 2\xi\dot{y} + \omega_y^2 y = \frac{F_y^o}{m} \sin \omega t$$

$$\ddot{y} + 2\xi\dot{y} + \omega_y^2 y = \frac{F_y}{m} \sin \omega t \tag{4.3.2}$$

m is the mass per unit length of the cylinder, ξ is the damping factor and ω_y is the natural frequency of the cylinder structure. For the near resonant condition $\omega_y \cong \omega$ and

$$F_y^o = 2m\xi\omega^2 \tilde{A}_y \tag{4.3.3}$$

where $\tilde{A}_y$ is the resonant cylinder amplitude. An empirical least squares curve fit to the experimental data of damping for each value of amplitude of resonant cylinder vibration (Fig. 4) may be used to express the resonant amplitude of the vortex force as a function of cylinder amplitude. Figure 4 implies

$$\xi = .15 \frac{\rho D^2}{m} \left(\frac{D}{\tilde{A}_y} \right)^{.65} \tag{4.3.4}$$

δ, the logarithmic decrement due to damping, is approximated by $2\pi\xi$ for the small values of damping used in this analysis. Equation (4.3.4) is substituted into Equation (4.3.3) to express the amplitude of the vortex force on a cylinder vibrating at resonance with vortex shedding as a function of cylinder amplitude. This gives

Reproduced with permission of the copyright owner. Further reproduction prohibited without permission.

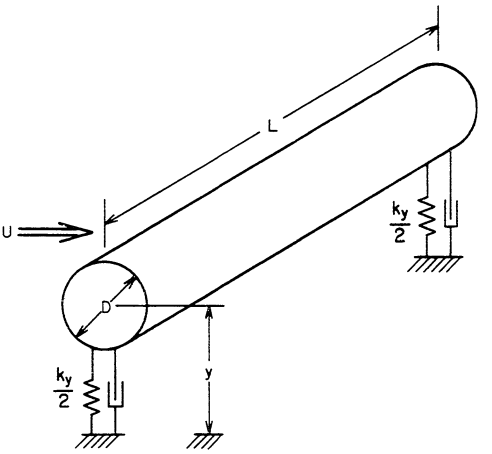

Fig. 3. Cylinder Support.

Reproduced with permission of the copyright owner. Further reproduction prohibited without permission.

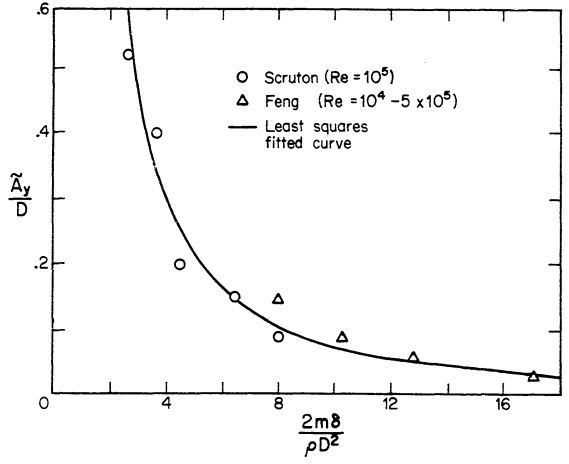

Fig. 4. Resonant Cylinder Amplitude as a Function of Damping [11] [12].

Reproduced with permission of the copyright owner. Further reproduction prohibited without permission.

$$F_y^o = .47\left(\frac{\tilde{A}_y}{D}\right)^{.35} \rho U^2 D \qquad (4.3.5)$$

The Strouhal relationship, $\omega = 2\pi S\frac{U}{D}$, where $S = .2$ has been incorporated into Equation (4.3.5). Equation (4.3.5) predicts that the magnitude of the vortex force approaches zero as the amplitude of vibration approaches zero even though it is known that vortex shedding persists. While this is in agreement with force measurements made directly on long vibrating cylinders at high Reynolds numbers [13] it is in conflict with the two dimensional forces measured by integrated pressure tap measurements. The discrepency is most likely explained by the reduced spanwide correlation at low vibration amplitudes.

These results indicate that the vortex force on long cylinders cannot well be approximated by a two dimensional flow model at small vibration amplitudes. The correlated flow model will over predict the result. But the two dimensional model should prove useful for examining the effect of varying structural parameters at moderate amplitudes where the flow is nearly two dimensional.

4.4 DERIVATION OF THE MODEL

A model will be developed for vortex induced transverse vibration of an elastically mounted circular cylinder by incorporating the essential features of the gross flow behavior and relating these to the dynamic motion of an oscillating cylinder. The resultant model can only approximate the complex structure-flow interaction but is nevertheless useful for identifying relevant system parameters, correlating

Reproduced with permission of the copyright owner. Further reproduction prohibited without permission.

one dimensional test data, and predicting the response of untested systems.

The basic fluid mechanic assumptions of the model are

1. Inviscid flow provides a good approximation for the flow field outside the near wake.
2. Vorticity is generated only in the near wake of the cylinder. The vortices grow uniformly to a maximum strength and move down stream.
3. Two dimensional flow.
4. Force exerted on the cylinder by the flow depends only on the velocity and acceleration of an averaged flow relative to the cylinder.

The forces on the cylinder are evaluated from the momentum equation in the y direction for the control volume shown in Figure 5,

$$P_y = \frac{dJ_y}{dt} + S_y + F_y \qquad (4.4.1)$$

where F_y is the fluid force on the cylinder. P_y is the pressure force on the control surface parallel to the y axis

$$P_y = -\int_s P dx \cos(n, y) = -\int_{AB} P dx + \int_{DC} P dx \qquad (4.4.3)$$

and S_y is the momentum flow through the control surface. Hence

$$S_y = \int_s \rho v u ds \qquad (4.4.3)$$

where v and u are the vertical and horizontal components of fluid velocity respectively. ρ is the fluid density. J_y is the momentum

Reproduced with permission of the copyright owner. Further reproduction prohibited without permission.

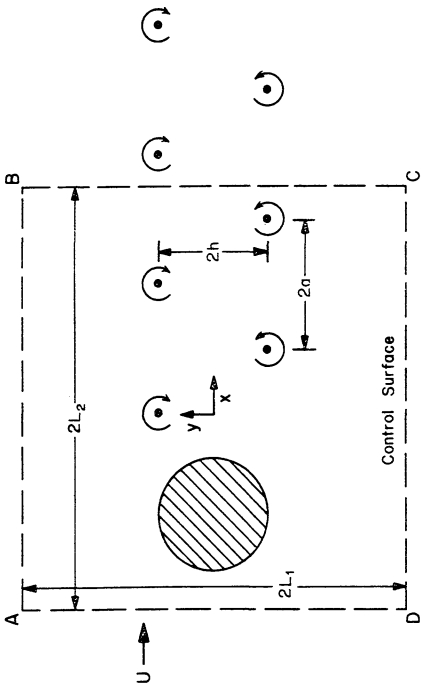

Fig. 5. Control Volume.

Reproduced with permission of the copyright owner. Further reproduction prohibited without permission.

within the control volume given by

$$J_y = \int\int_A \rho v dx dy \tag{4.4.4}$$

The variable z is defined as

$$J_y = a_o \rho \dot{z} D^2 \tag{4.4.5}$$

so that $\dot{z}$ is a weighted average of the transverse component of the flow within the control volume. D is the cylinder diameter and a_o is a proportionality constant.

The fluctuating component of the momentum within the control volume was neglected by Chen [15] in order to relate the force on the cylinder directly to the properties of the vortex street. Unfortunately this assumption neglects the fluctuating components of the near wake which determine the forces on the section. Indeed neglecting J_y implies the lift force on the section is independent of the cross section which produces the vortex street.

The potential for the vortex street viewed from a reference frame moving with the shed vortices is

$$\bar{\Phi} = ik \sum_{n=1}^{\infty} \ln\left(x-2na+i(y-h)\right) - \ln\left(x-2(n-1)a+i(y+h)\right) \tag{4.4.6}$$

where k is the vortex strength [15]. The velocity induced by this flow is

$$u' + iv' = \nabla \bar{\Phi} \tag{4.4.7}$$

$$u' + iv' = ik \sum_{n=1}^{\infty} \left(\frac{1}{x-2na+i(y-h)} - \frac{1}{x-(2n-1)a+i(y+h)} \right) \tag{4.4.8}$$

Reproduced with permission of the copyright owner. Further reproduction prohibited without permission.

the flow induced by the vortex street diminishes as

$$u' + iv' = O(1/r) \tag{4.4.9}$$

where r is the length of a vector from the vortex street to one of the control surfaces AB or CD or AD. Application of the Bernoulli equation to Equation (4.4.8) and integration of the fluid pressure along the boundaries BC and CD in the limit as L_1 approaches infinity while holding L_2 finite gives

$$P_y = 0 \tag{4.4.10}$$

S_y evaluated by the line integral on the sides BC and AD. Chen [14] has shown that for a line integral bisecting an infinite vortex street $|S_y| = \rho u_t \Gamma$ where Γ is the circulation of a vortex and u_t is the translational velocity of the vortex street. For the present model transverse components of flow forward of the cylinder are assumed to be small. S_y is taken to be:

$$|S_y| = \rho u_t \Gamma + \text{correction terms} \tag{4.4.11}$$

where k_1 is a dimensionless proportionality constant.

As a result of Equation (4.4.9) the circulation contained within the control volume for infinite L_1 and finite L_2 is

$$\Gamma_{cv} = \int_s \vec{v} \cdot d\vec{s} = \int_{\substack{AD \\ BC}} v dy \tag{4.4.12}$$

The circulation is a function only of the induced transverse component of velocity on the surfaces BC and AD. In light of this it is reasonable to expect the circulation of a vortex to be nearly proportional to the amplitude of the average transverse component of velcoity in the

Reproduced with permission of the copyright owner. Further reproduction prohibited without permission.

control volume. That is, it is assumed that

$$\Gamma = K |\dot{z}| D \qquad (4.4.13)$$

where K is the proportionality constant.

Since the vortex shedding process is cyclic, S_y and $\dot{z}$ are cyclic. Equations (4.4.11) and (4.4.13) relate the amplitude of these variables. By postulating a model for the near wake behavior it is possible to determine the phase angle between S_y and $\dot{z}$. Figure 6 shows a postulated model for the development of the vortex street as related to the near wake boundary surface B'C'. It is convenient to momentarily consider B'C' as the aft boundary of the control volume. In the first diagram one fully developed vortex is forward of the control surface. The up wash and down wash fore and aft of this vortex approximately cancel when averaged over the control volume so there is no net vertical component of flow within the control volume and $\dot{z} = 0$ but there is a strong momentum flow across B'C' directed downward since B'C' separates two fully developed vortices of opposite sign. One quarter of a cycle later a new vortex is beginning to form at the bottom of the cylinder while the fully formed vortex has moved down stream so that its center intersects B'C'. At this time a fully

Reproduced with permission of the copyright owner. Further reproduction prohibited without permission.

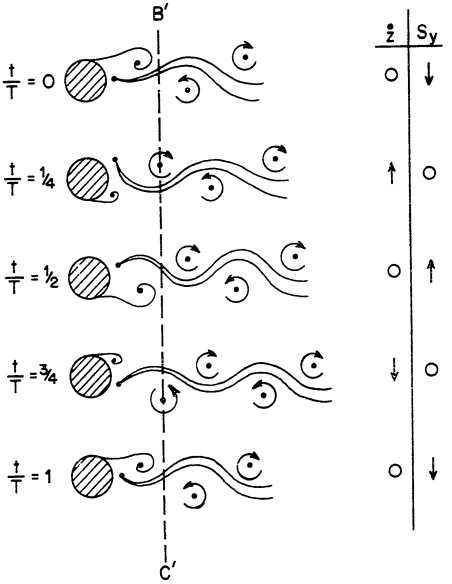

Fig. 6. Cyclic Momentum Flow in Control Volume.

Reproduced with permission of the copyright owner. Further reproduction prohibited without permission.

formed vortex produces a net upward flow in the control volume while the net momentum flow across B'C' is near zero. Following this development through a full cycle it is evident that S_y lags $\dot{z}$ by a quarter cycle. Shifting B'C' down stream does not change this result as the flow of each vortex pair sums to zero over the control volume. Equations (4.4.11) and (4.4.13) and Figure 6 imply that

$$S_y = K\rho u_t \dot{z}(t-T/4)D + \text{correction terms} \qquad (4.4.14)$$

T is the period of vortex shedding. Since S_y is analytic and periodic at the shedding frequency [15] it is reasonable to assume the correction terms can be expressed in a power series of odd powers of z and $\dot{z}$ which also oscillate at the shedding frequency. For simplicity only linear and cubic terms in $\dot{z}$ and a linear term in z are retained in S_y. S_y is assumed to have the form

$$S_y = K\rho u_t \omega_z^o z D - a_1 \rho U D \dot{z} + a_2 \rho \dot{z}^3 D/U \qquad (4.4.15)$$

where a_1, a_2 and K are dimensionless constants and a_1 and a_2 are assumed to be small compared to K. ω_z^o is the circular vortex shedding frequency.

The force exerted between the cylinder and the fluid is modeled consistent with the following assumptions:

1. The force depends only on a weighted relative average relative velocity and acceleration of the fluid to the flow.
2. The spectrum of frequencies known to be produced in the vortex shedding process can be approximated by a single frequency component.

Reproduced with permission of the copyright owner. Further reproduction prohibited without permission.

Implicit in these assumptions is that there is no fundamental fluid mechanic distinction between forced cylinder motion and elastically mounted cylinder motion. The vortex shedding may produce a multitude of frequencies intertwined with the basic shedding frequency, only one of these frequencies can be represented by the present model.

The force on the cylinder which is dependent on the relative acceleration of the fluid to the cylinder is assumed to be linear and is represented as

$$F_y^{(1)} = a_3 \rho D^2 (\ddot{z} - \ddot{y}) \tag{4.4.16}$$

where a_3 is a dimensionless proportionality constant.

The force exerted on the cylinder by the relative fluid velocity may be written in the form of a lift coefficient whose magnitude is proportional to the relative angle between the free stream and the normal component of the incoming flow to the cylinder. For small displacements this angle is $(\dot{z}-\dot{y})/U$ and the lift force takes the form

$$F_y^{(2)} = a_4 \rho DU (\dot{z} - \dot{y}) \tag{4.4.17}$$

where a_4 is a dimensionless constant. The net force exerted on the cylinder is the sum of $F_y^{(1)}$ and $F_y^{(2)}$ or

$$F_y = a_3 \rho D^2 (\ddot{z} - \ddot{y}) + a_4 \rho DU (\dot{z} - \dot{y}) \tag{4.4.18}$$

The fluid oscillator is assembled by substituting the component expressions, Equations (4.4.5), (4.4.10), (4.4.15) and (4.4.18) into the momentum Equation (4.4.1). This gives

Reproduced with permission of the copyright owner. Further reproduction prohibited without permission.

$$a_o \rho D^2 \ddot{z} + K\rho u_t \omega^o_z z = a_1 \rho UD\dot{z} - a_2 \rho \dot{z}^3 D/U - a_3 \rho D^2(\ddot{z}-\ddot{y}) - a_4 \rho DU(\dot{z}-\dot{y}) \tag{4.4.19}$$

or

$$\ddot{z} + K' \frac{u_t}{U} \frac{U^o}{D} \omega^o_z z = (a'_1 - a'_4) \frac{U}{D} \dot{z} - a'_2 \frac{\dot{z}^3}{UD} + a'_3 \ddot{y} + a'_4 \frac{U}{D} \dot{y}$$

where

$$K' = K/(a_0+a_3) \quad a'_i = a_i/(a_0+a_3) \tag{4.4.20}$$

If the cylinder in the flow is elastically mounted it will respond to the fluid forces on it. The motion of an elastically mounted viscously damped cylinder (Fig. 3) is described by

$$m\ddot{y} + 2\xi_s \omega_y m\dot{y} + k_y y = F_y = a_3 \rho D^2(\ddot{z}-\ddot{y}) + a_4 \rho DU(\dot{z}-\dot{y}) \tag{4.4.21}$$

or

$$\ddot{y} + 2\xi_T \omega_y \dot{y} + \omega_y^2 y = a''_3 \ddot{z} + a''_4 \dot{z}$$

where

$$a''_i = \rho D^2 a_i/(m+a_3\rho D^2) \tag{4.4.22}$$

$$\xi_T = \xi_s + \xi_f$$

$$\xi_f = a''_4 \frac{\rho D^2}{2} \frac{\omega^o_z}{\omega_y} \frac{1}{2\pi S}$$

m is the mass of the cylinder per unit length and ω_y is the circular natural frequency of the spring-cylinder system in vacuum. ξ_T is the total damping coefficient. It is composed of a component due to structural viscous damping, ξ_s, and a component due to viscous

Reproduced with permission of the copyright owner. Further reproduction prohibited without permission.

fluid damping, ξ_f, which arise from the fluid forces that dissipate energy of the cylinder.

The form of the fluid oscillator Equation (4.4.19) and the structural oscillator Equation (4.4.21) suggests the following:

1. The fluid and structural system has the form of two coupled autonomous oscillators.
2. The natural frequency of the fluid oscillator is given by

$$\omega_z^o = K' \frac{u_t}{U} \frac{U}{D} \tag{4.4.23}$$

Since u_t/U is approximately constant for a large range of Reynolds numbers [8] the model predicts the natural frequency of the fluid oscillator is proportional to the ratio of free stream velocity to cylinder diameter,

$$\omega_z^o = 2\pi S \frac{U}{D} \tag{4.4.24}$$

where S is the dimensionless Strouhal number. This is a well known experimental fact. Experimental values of the Strouhal number, which like u_t/U is a function of Reynolds number, determine the parameter K.

3. The spring constant like term in the fluid oscillator arises from vortex feedback in the near wake. For the fluid oscillator to have bounded amplitude the feedback must be self limiting. That is, the feedback must be nonlinear.
4. Large amplitude structural oscillations are expected only if the shedding frequency is equal to or a multiple of the

Reproduced with permission of the copyright owner. Further reproduction prohibited without permission.

the natural frequency of the structure so that the two oscillators are internally resonant.

To this point no restriction has been placed on the cross section which produces the vortex street. The model parameters are fixed by matching experimental data for a given cross section with the model response as predicted by analysis.

4.5 ANALYSIS OF THE MODEL

Steady response for three cases will be analyzed:

1. Fixed Cylinder
2. Forced Cylinder Motion
3. Elastically Mounted Cylinder

The goal will be to determine the model parameter from experimental data for the first two cases for comparison with experimental data of elastically mounted cylinders.

4.5.1 Stationary Cylinder

If $y = 0$ the fluid oscillator Equation (4.4.19) is:

$$\ddot{z} + \omega_z^{o2} z = (a_1' - a_4') U\dot{z}/D - a_2' \dot{z}^3/UD \qquad (4.5.1)$$

A solution of the form

$$z = A_z^o(t) \cos\left(\omega_z^o t - \varphi(t)\right) \qquad (4.5.2)$$

is assumed where $A_z^o(t)$ and $\varphi(t)$ are slowly varying in time. A straight forward application of asymptotic techniques gives the steady state solution [16]:

Reproduced with permission of the copyright owner. Further reproduction prohibited without permission.

$$A_z^o/D = (4(a_1 - a_4)/3a_2)^{1/2}/2\pi S \qquad (4.5.3)$$

The solution is stable $a_1 - a_4 > 0$ and $a_2 > 0$.

This solution can be used to determine the circulation of the shed vortices and the lift force on a stationary cylinder.

From Equation (4.4.23)

$$K = (a_0 + a_3)\, 2\pi S\, U/u_t$$

Equation (4.4.13) implies that the circulation of a shed vortex is

$$\Gamma = (a_0 + a_3)\, 2\pi S\, w_z^o A_z^o DU/u_t$$

but

$$w_z^o = 2\pi S\, U/D$$

so

$$\frac{\Gamma}{UD}\frac{u_t}{U} = (a_0 + a_3)(2\pi S)^2 \frac{A_z^o}{D} \qquad (4.5.4)$$

Equation (4.5.4) relates the circulation of a vortex shed from a stationary cylinder and the translational velocity of that vortex street to the model parameters.

The lift force on a stationary cylinder is found by evaluating the vortex force (Eqn. (4.4.18)) at y = 0. The amplitude of the vortex force can be expressed as an oscillating lift coefficient. The amplitude of the lift coefficient is:

$$C_{F_y}^o = \frac{2F_y(y=0)}{\rho U^2 D \cos(w_z^o t + \varphi)} = 4\pi S\left(a_3^2 (2\pi S)^2 + a_4^2\right)^{1/2} A_z^o/D \qquad (4.5.5)$$

Reproduced with permission of the copyright owner. Further reproduction prohibited without permission.

If the lift force on a stationary cylinder, the vorticity of a shed vortex and the translational velocity of the vortex street aft of a stationary cylinder are measured experimentally, Equations (4. 5. 4) and (4. 5. 5) can be used to provide two relationships between the model parameters.

4. 5. 2 Forced Cylinder Motion

One of the distinguishing characteristics of vortex shedding from a cylinder in a forced harmonic motion is a range of synchronization. As the frequency of imposed cylinder motion approaches the stationary shedding frequency, the fluid force on the cylinder changes from complex beats to simple harmonic oscillation as the vortex shedding locks onto the forcing frequency. The vortex shedding remains synchronized with the forcing frequency for a range of frequencies near the forcing frequency. The bandwidth of the synchronization range increases with increasing amplitude of forced vibration [4] [17]. The vortex forces on the cylinder also increase with increasing amplitude of vibration perhaps due to increased strength of the shed vortices [4] [5]. The vortex model predicts a range of synchronization for forced cylinder motion and the amplitude of the force on the cylinder increases with the amplitude of forced cylinder motion. These traits are used with experimental data to provide two additional relationships between the model parameters and experimental data.

If the cylinder is oscillated sinusoidally,

$$y = A_y \sin(\omega_y t + \varphi_y) \qquad (4.5.6)$$

The arbitrary phase angle φ_y is chosen as

Reproduced with permission of the copyright owner. Further reproduction prohibited without permission.

$$\varphi_y = \tan^{-1}(a_4 \omega_z^o / 2\pi S a_3 \omega_y) \qquad (4.5.7)$$

so that the fluid oscillation equation (4.4.19) becomes

$$\ddot{z} + \omega_z^{o2} z = (a_1' - a_4')U\dot{z}/D - a_2'\dot{z}^3/UD + d\omega_y^2 \cos \omega_y t \qquad (4.5.8)$$

where

$$d = \left(a_3'^2 + a_4'^2 \omega_z^{o2}/\omega_y^2 (2\pi S)^2\right)^{1/2} A_y$$

Equation (4.5.8) is in the form of the classic forced van der Pol oscillation [18]. The solution of Equation (4.5.8) is well known [18] and the solution will only be sketched here.

A solution of Equation (4.5.8) is assumed of the form

$$z = b_1(t) \cos \omega_y t + b_2(t) \sin \omega_y t \qquad (4.5.9)$$

where $b_1(t)$ and $b_2(t)$ are slowly varying parameters. Substituting Equation (4.5.9) into Equation (4.5.8) and retaining only first order terms such as $\dot{b}_1$ and $a_1 b_2$, and performing a harmonic balance produces the following variational equations:

$$2\dot{y} + x\frac{(\omega_z^{o2} - \omega_y^2)}{\omega_y} - \alpha y(1 - r^2) = \frac{d\,\omega_y^2}{A_z^o \omega_z^o} \qquad (4.5.10)$$

$$-2\dot{x} + y\frac{(\omega_z^{o2} - \omega_y^2)}{\omega_y} + \alpha x(1 - r^2) = 0 \qquad (4.5.11)$$

where

$$\alpha = (a_1' - a_4')U/D$$

Reproduced with permission of the copyright owner. Further reproduction prohibited without permission.

$$\left.\begin{aligned} x &= b_1 \omega_y / A_z^o \omega_z^o \\ y &= b_2 \omega_y / A_z^o \omega_z^o \\ r^2 &= x^2 + y^2 \end{aligned}\right\} \qquad (4.5.12)$$

The steady state solutions to Equations (4.5.10) and (4.5.11) $b_1(t) = b_1^o$ and $b_2(t) = b_2^o$, are found by setting $\dot{b}_1 = 0$ and $\dot{b}_2 = 0$. This gives

$$0 = x\sigma - y(1-r^2) - F \qquad (4.5.13)$$

$$0 = y\sigma + x(1-r^2) \qquad (4.5.14)$$

which are easily solved for x and y.

$$x = +\sigma r^2 / F \qquad (4.5.15)$$

$$y = -r^2(1-r^2)/F \qquad (4.5.16)$$

These equations can be combined to give

$$r^2\left(\sigma^2 + (1-r^2)^2\right) = F^2 \qquad (4.5.17)$$

where

$$F = \frac{2(d/D)\omega_y^2}{3\pi(A_z^o/D)^3 a_2 S \omega_z^{o2}} \qquad (4.5.18)$$

$$\sigma = \frac{(\omega_z^{o2} - \omega_y^2)2\pi S}{\omega_y \omega_z^o (a_1' - a_4')}$$

The amplitude of the solution is found by solving the cubic equation (4.5.17) numerically and substituting the result into Equations (4.5.15) and (4.5.16) which determine b_1^o and b_2^o. This simple harmonic solution

Reproduced with permission of the copyright owner. Further reproduction prohibited without permission.

becomes unstable if $r^2 < 1/2$ for $F > 8/27$ as shown in Figure 7 and complex wave forms result.

A relationship between the model parameters and experimental data is produced by matching the bandwidth of the range of synchronization with experimental data. If for a given amplitude of cylinder oscillation the frequencies of onset and termination of the synchronization range, ω_y^+ and ω_y^- respectively, are known, then the bandwidth can be defined by

$$\beta_w = (\omega_y^+ - \omega_y^-)/\omega_z^o \tag{4.5.19}$$

Since experimental data [16] show the synchronization range is nearly symmetric for small bandwidths,

$$\left.\begin{aligned} \omega_y^+/\omega_z^o &\approx 1+\beta_w/2 \\ \omega_y^-/\omega_z^o &\approx 1-\beta_w/2 \end{aligned}\right\} \tag{4.5.20}$$

The bandwidth of the model is defined by the stability boundaries for simple harmonic solution. If $F > 8/27$ the stability boundaries are defined by substituting $r^2 = 1/2$ into Equation (4.5.17).

$$\sigma^2 + 1/4 = 2F^2 \tag{4.5.21}$$

If F and σ in Equation (4.5.21) are evaluated at the frequency corresponding to either the onset or termination of the observed range of synchronization at a given amplitude of forced oscillation then the model bandwidth is matched with the experimentally observed bandwidth and a relationship is produced between the model parameters and experimental data. This relationship is produced by substituting

Reproduced with permission of the copyright owner. Further reproduction prohibited without permission.

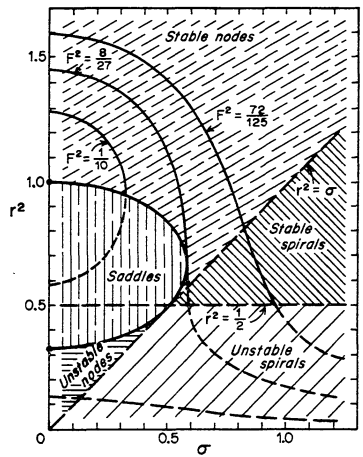

Fig. 7. Response of Forced Van der Pole Oscillator [18].

Reproduced with permission of the copyright owner. Further reproduction prohibited without permission.

Equations (4. 5. 18) and (4. 5. 20) into Equation (4. 5. 21).

$$\left[\frac{4\beta_w}{6\pi Sa_2(A_z^o/D)^2}\right]^2 + \frac{1}{4}$$

$$= 2\left[\frac{2(A_y/D)\left(a_3^2+a_4^2/(1+\beta_w/2)^2(2\pi S)^2\right)^{1/2}(1+\beta_w/2)^2}{3\pi Sa_2(A_z^o/D)^3 a_o}\right]^2 \quad (4.5.22)$$

The force on the oscillating cylinder of the model can be expressed in terms of an oscillating life coefficient given by the expression

$$C_{F_y} = \frac{2F_y}{\rho U^2 D \sin(\omega_y t+\bar{\varphi})}$$

$$= \frac{4\pi S\bar{A}\omega_y}{D\omega_z}\left(a_3^2(2\pi S)^2\omega_y^2/\omega_z^{o2}+a_4^2\right)^{1/2} \quad (4.5.23)$$

where

$$\bar{A}\sin(\omega_y t+\bar{\varphi}) = z-y$$

or from Equations (4. 5. 6), (4. 5. 12), (4. 5. 15) and (4. 5. 16)

$$\frac{\bar{A}}{D} = \left[\left(\frac{A_z^o r^2(1-r^2)\omega_z^o}{DF\omega_y} - \frac{a_4A_y}{2\pi SD\left(a_3^2+a_4^2/(2\pi S)^2\right)^{1/2}}\right)^2\right.$$

$$\left.+\left(\frac{A_z^o\sigma r^2\omega_z^o}{DF\omega_y}+\frac{a_3A_y}{D\left(a_3^2+a_4^2/(2\pi S)^2\right)^{1/2}}\right)^2\right]^{1/2} \quad (4.5.24)$$

The fourth relationship between the model parameters and experimental data is found by matching the rate of increase of lift force with

Reproduced with permission of the copyright owner. Further reproduction prohibited without permission.

increasing amplitude of forced vibration. The derivative $\partial C_{F_y}/\partial A_y$ is used to estimate the dependence of the lift force on the amplitude of forced vibration since this derivative can be evaluated in closed form as the amplitude of oscillation approaches zero at resonance with vortex shedding.

$$\lim_{\substack{A_y \to 0 \\ \sigma=0}} \frac{\partial C_{F_y}}{\partial A_y/D} = \frac{\partial C_{F_y}}{\partial \overline{A}} \lim_{\substack{A_y \to 0 \\ \sigma=0}} \frac{\partial \overline{A}}{\partial A_y/D} \tag{4.5.25}$$

As the amplitude of forced oscillation A_y approaches zero, for σ equal to zero, r^2 approaches 1 and b_1^o approaches zero while b_2^o approaches A_z^o so

$$\lim_{\substack{A_y \to 0 \\ \sigma=0}} \frac{\partial \overline{A}/D}{\partial A_y/D} = \frac{A_z^o}{2D} \lim_{\substack{a_y \to 0 \\ \sigma=0}} \frac{\partial r^2}{\partial A_y/D} - \frac{a_4}{2\pi S\left(a_3^2+a_4^2/(2\pi S)^2\right)^{1/2}} \tag{4.5.26}$$

$\partial r^2/\partial A_y/D$ is evaluated from Equation (4.5.17) and (4.5.18)

$$\frac{\partial r^2}{\partial A_y/D} = \frac{\partial r^2}{2F} \frac{\partial F}{\partial A_y/D} \tag{4.5.27}$$

From Equation (4.5.17)

$$\lim_{\substack{A_y \to 0 \\ \sigma=0}} \frac{\partial F}{\partial r^2} = \lim_{r^2 \to 1} \frac{(1-r^2)^2}{2F} - \frac{r^2(1-r^2)}{F} = 1 \tag{4.5.28}$$

From Equation (4.5.18)

$$\left.\frac{\partial F}{\partial A_y/D}\right|_{\sigma=0} = \frac{2\left(a_3^2+a_4^2/(2\pi S)^2\right)^{1/2}}{3\pi S(A_z^o/D)^3 a_2} \tag{4.5.29}$$

Reproduced with permission of the copyright owner. Further reproduction prohibited without permission.

$\partial C_{F_y}/\partial A_y/D$ is evaluated in the limit as the forced cylinder amplitude approaches zero at resonance with vortex shedding by substituting Equations (4.5.26) through (4.5.29) into Equation (4.5.25). This gives

$$\lim_{\substack{A_y \to 0 \\ \sigma=0}} \frac{\partial C_{F_y}}{\partial A_y/D} = 4\pi S \left[\frac{C_{F_y}^{o2}}{6(A_z^o/D)^4 (2\pi S)^4 a_2} - a_4 \right] \quad (4.5.30)$$

If the amplification in the vortex force with increasing cylinder amplitude at resonance with vortex shedding is known then Equation (4.5.30) provides a fourth relationship between the model parameters and experimental data. If one of the five model parameters a_o, a_1, a_2, a_3 and a_4 can be estimated then the remaining parameters can be found from these relationships.

4.5.3 Elastically Mounted Cylinder

The coupled oscillator equations for an elastically mounted cylinder are

$$\ddot{z}+\omega_z^{o2} z = (a_1'-a_4')\frac{U}{D}\dot{z} - a_2'\frac{\dot{z}^3}{UD} + a_3'\ddot{y} + a_4'\frac{U}{D}\dot{y} \quad (4.5.31)$$

$$\ddot{y}+2\xi_T+\omega_y\dot{y}+\omega_y^2 y = a_3''\ddot{z} + \frac{U}{D}a_4''\dot{z} \quad (4.5.32)$$

These equations are solved by first assuming a harmonic solution form:

$$\left.\begin{aligned} z &= A_z \cos\theta \\ \theta &= \omega_z(t-\varphi) \end{aligned}\right\} \quad (4.5.33)$$

Reproduced with permission of the copyright owner. Further reproduction prohibited without permission.

for the fluid oscillator equation. The linear differential equation describing the cylinder motion (4. 4. 19) is then solved for the cylinder displacement in terms of the harmonic fluid oscillations. The cylinder displacement as a function of the fluid oscillations can then be substituted back into the fluid oscillator equation to produce a single nonlinear autonomous differential equation which may be solved by asymptotic methods.

Equation (4. 5. 33) is substituted into Equation (4. 4. 21) to give:

$$\ddot{y}+2\xi_T\omega_y\dot{y}+\omega_y^2 y = -a_3''A_z\omega_z^2\cos\vartheta - a_4''\omega_z^o A_z\omega_z\sin\vartheta/2\pi S \qquad (4.5.34)$$

Solving for y and incorporating Equation (4. 5. 33) gives

$$y = \left[-a_3''(\omega_y^2-\omega_z^2)+2\omega_z^o\omega_y a_4''\xi_T/2\pi S\right] AF\omega_z^2 z$$

$$+\left[2a_3''\omega_z^2\omega_y\xi_T+a_4''\omega_z^o(\omega_y^2-\omega_z^2)/2\pi S\right] AF\dot{z} \qquad (4.5.35)$$

where the amplification factor is denoted by AF.

$$AF = 1\Big/\left(\left(\omega_y^2-\omega_z^2\right)^2+4\xi_T^2\omega_y^2\omega_z^2\right) \qquad (4.5.36)$$

The amplitude of the cylinder displacement is:

$$A_y = A_z AF^{1/2}\left[a_3''(\omega_z/\omega_y)^4+a_4''(\omega_z/\omega_y)^2(\omega_z/\omega_y)^2\Big/(2\pi S)^2\right]^{1/2}\omega_z^2 \qquad (4.5.37)$$

Equation (4. 5. 35) is substituted into the fluid oscillator Equation (4. 4. 19) to produce the single nonlinear equation.

Reproduced with permission of the copyright owner. Further reproduction prohibited without permission.

$$\ddot{z}+\omega_z^{o2} z = \Big[(a_1'-a_4')\omega_z^o/2\pi S+a_4'\Big\{-a_3''(\omega_y^2-\omega_z^2)$$

$$+2\xi_T\omega_z^o\omega_y a_4''/2\pi S\Big\}\omega_z^2\omega_z^o AF/2\pi S$$

$$-a_3\Big\{a_3''\omega_z^2 2\xi_T\omega_y+\omega_z^o a_4''(\omega_y^2-\omega_z^2)\omega_z^2 AF/2\pi S\Big\}\Big] z$$

$$-a_2'\dot{z}^3 2\pi S/\omega_z^o D^2$$

$$+\Big[a_3'\Big\{-a_3''(\omega_y^2-\omega_z^2)+2\omega_z^o\omega_y a_4''\xi_T/2\pi S\Big\}\omega_z^2$$

$$+a_4'\Big\{2\xi_T a_3''\omega_z^2\omega_y+\omega_z^o a_4''(\omega_y^2-\omega_z^2)/2\pi S\Big\}\omega_z^o/2\pi S\Big] AF\dot{z} \qquad (4.5.38)$$

This equation is of the form

$$\ddot{z}+\omega_z^{o2} z = \alpha_1\dot{z}-\alpha_2\dot{z}^3+\alpha_3\ddot{z} \qquad (4.5.39)$$

where the α_i are independent of the amplitude of the solution but are dependent on the frequency of solution. The solution is assumed to be oscillatory

$$z = A_z \cos \omega_z(t-\varphi) \qquad (4.5.33)$$

where $A_z(t)$ and $\varphi(t)$ are slowing varying in time and the α_i are assumed to be small parameters. The method of slowly varying parameters gives the following variational equations:

$$-2\dot{A}_z\omega_z = \alpha_1\omega_z A_z-3\alpha_2\omega_z^3 A_z^3/4 \qquad (4.5.40)$$

$$\dot{\varphi}\omega_z = -\alpha_3\omega_z/2 \qquad (4.5.41)$$

Reproduced with permission of the copyright owner. Further reproduction prohibited without permission.

$\dot{A}_z$ is set to zero for steady harmonic solutions, $A_z(t) = A_z^{(1)}$. Equation (4. 5. 40) therefore implies

$$A_z^{(1)} = (4\alpha_1/3\alpha_2)^{1/2}/\omega_z \tag{4. 5. 42}$$

If the full expressions for α_1 and α_2 are substituted into Equation (4. 5. 42) it may be shown that

$$\frac{3}{4}\left(\frac{A_z^{(1)}}{D}\right)^2 = \frac{(a_1 - a_4)\omega_z^{o2}}{a_2\omega_z^2(2\pi S)^2} - \frac{\omega_z^{o2}(\omega_y^2 - \omega_z^2)}{(2\pi S)^2 a_2'}\left[a_4' a_3'' + a_3' a_4''\right] AF$$

$$+ \frac{2\xi_T \omega_y \omega_z^o AF}{2\pi S a_2'}\left[a_4' a_4'' \omega_z^{o2}/(2\pi S)^2 - a_3'' a_3' \omega_z^2\right] \tag{4. 5. 43}$$

The order one estimate of the frequency of oscillation is ω_z^o, the stationary cylinder vortex shedding frequency. An order one estimate of the amplitude of fluid oscillation may be obtained from Equation (4. 5. 43) by setting $\omega_z = \omega_z^o$. A higher order estimate of the frequency of oscillation would be

$$\omega_z = \omega_z^o(1 - \dot{\varphi}) \tag{4. 5. 44}$$

where $\dot{\varphi}$ is assumed to be small. $\dot{\varphi}$ is evaluated at ω_z in order to achieve the maximum accuracy. If the full expression for α_3 from Equation (4. 5. 38) is substituted into Equation (4. 5. 41) to determine $\dot{\varphi}$ and the result substituted into Equation (4. 5. 44) then

$$\omega_z = \omega_z^o + \omega_z^o AF\left[(\omega_y^2 - \omega_z^2)\left(a_4'' a_4' \omega_z^{o2}/(2\pi S)^2 - a_3'' a_3' \omega_z^2\right)\right.$$

$$\left. -2\xi_T \omega_y \omega_z^2 \omega_z^o (a_4' a_3'' + a_4'' a_3')/2\pi S\right]/2 \tag{4. 5. 45}$$

Reproduced with permission of the copyright owner. Further reproduction prohibited without permission.

Equation (4. 5. 45) determines the frequency of the cylinder and fluid oscillation. This transcendental frequency equation is decoupled from Equation (4. 5. 43) which determines the amplitude of the fluid oscillator. If additional nonlinear terms in z were incorporated in the fluid oscillator model then these terms would couple the frequency and amplitude equations. The frequency equation can be solved numerically. The resultant frequency, ω_z, is substituted into Equation (4. 5. 43) to determine the amplitude of the fluid oscillations. A_z is then substituted into Equation (4. 5. 37) to determine the amplitude of the elastically mounted cylinder displacement due to vortex shedding.

4.6 DETERMINATION OF THE MODEL PARAMETERS FOR A CIRCULAR CYLINDER

Four relationships between the model parameters and experimental data have been formulated. These are:

1. Circulation and translational velocity of a vortex shed form a stationary cylinder, Equation (4. 5. 4).
2. Lift force on a stationary cylinder, Equation (4. 5. 5).
3. Bandwidth of synchronization of a forced cylinder, Equation (4. 5. 22).
4. Rate of increase of lift force with increasing amplitude of forced vibration, Equation (4. 5. 30).

There are five model parameters. If the value of one parameter can be estimated four of the parameters may be obtained in terms of the fifth. The parameter a_3 determines the magnitude of the fluid force on the cylinder due to acceleration of the near wake relative to the cylinder. It is felt this parameter can not exceed $\pi/4$ which is the

Reproduced with permission of the copyright owner. Further reproduction prohibited without permission.

theoretical value obtained by considering the total force on a cylinder in an accelerating inviscid fluid. Setting a_3 equal to zero does not imply that there is no added mass effect since the flow forward of the separation point remains attached to the cylinder effectively increasing the oscillating mass of the cylinder. Rather, a_3 equal to zero implies that the acceleration of the near wake does not greatly affect the fluid force on the cylinder.

The model parameters are determined by estimating a value for a_3 then solving Equation (4.5.4) for a_o and Equation (4.5.5) for a_4 and substitute these into Equation (4.5.22) and (4.5.30) to produce two equations in the variables a_2 and A_z^o which may be solved simultaneously numerically.

The input experimental data for vortex circulation and vortex translational velocity is taken from results reported by Chen [14] which are shown in Figure 8. ℓ is the lateral spacing between vortices. The measurements of the amplitude of the vortex lift force are either estimates made by pressure tip integration or direct measurements made on cylinder test sections and are shown in Figure 2. The relatively large scatter in the results is at least partly the result of spanwise correlation effects. The bandwidth data shown in Figure 9 is from Koopman [17]. The rate of increasing amplitude of vortex lift force with increasing amplitude of vibration as the amplitude of vibration approaches zero is extrapolated from data presented by Bishop and Hassan and is given in Table 1.

Unfortunately the various bits of data available are taken over a large range of Reynolds numbers. For example, Koopman's results

Reproduced with permission of the copyright owner. Further reproduction prohibited without permission.

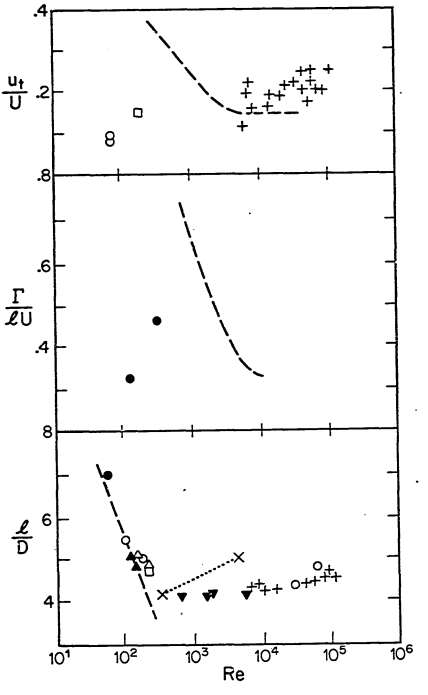

Fig. 8. Translational Velocity, Circulation, and Lateral spacing of Vortices Shed from a Stationary Cylinder [14].

Reproduced with permission of the copyright owner. Further reproduction prohibited without permission.

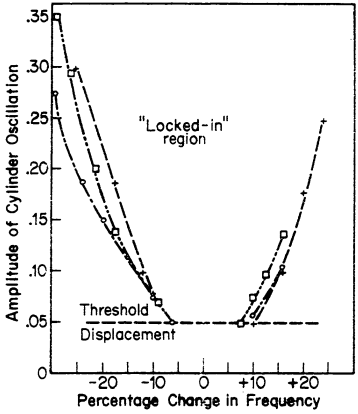

Fig. 9. Regions over which Cylinder Motion Controls Shedding Frequency, --, Re = 100, -••-, Re = 200, -•-, Re = 300 [16].

Reproduced with permission of the copyright owner. Further reproduction prohibited without permission.

were measured at a maximum Reynolds number of 500 while Bishop and Hassan's results are for a Reynolds number of 100,000. Although the data are within the subcritical Reynolds number range they are insufficient to establish any meaningful trends with Reynolds number. Any such variations are neglected until they can be specified more accurately.

The following approximate mean values of the experimental input data were chosen for the subcritical Reynolds number range.

$$\left.\begin{aligned} & C^{o}_{F_y} = .5 \\ & \frac{u_t}{U}\frac{\Gamma}{UD} = .4 \\ & \beta_w = .4 \quad \text{for } A_y/D = .2 \\ & \lim_{\substack{A_y \to 0 \\ \omega_y = \omega^{o}_z}} \frac{\partial C_{F_y}}{\partial A_y/D} = 1.68 \end{aligned}\right\} \qquad (4.6.1)$$

The following model parameters correspond to these data if a_3 is set to zero.

$$\left.\begin{aligned} & a_o = .48 \\ & a_1 = .44 \\ & a_2 = .20 \\ & a_3 = 0 \\ & a_4 = .38 \end{aligned}\right\} \qquad (4.6.2)$$

Reproduced with permission of the copyright owner. Further reproduction prohibited without permission.

These imply with Equation (4.5.3) and S = .2 that the amplitude of the fluid oscillator for a stationary cylinder is $A_z^o/D = .53$.

A_y/D	.2	.3	.4	.5
$(C_{F_y})_{max}/C^o_{F_y}$	1.45	1.72	1.99	2.46

Table 1. Relation between lift force and amplitude of forced oscillation, $C^o_{F_y} = .6$. (From [4]).

4.7 NATURE OF THE SOLUTION

The fluid and structural oscillators become internally resonant as the vortex shedding frequency approaches the natural frequency of the cylinder structure. Large amplitude cylinder vibrations are excited. The cylinder vibration is fedback into the fluid oscillator through the fluid force terms. This feedback effect produces frequency entrainment and affects the amplitude of cylinder vibration at resonance with vortex shedding.

4.7.1 Frequency Entrainment

The frequency equation (4.5.45) produces a frequency entrainment effect if $a''_4 a'_4/(2\pi S)^2 > a''_3 a'_3$. The effect is maximum for $a_3 = 0$ as is shown in Figure 10. For $a_3 = 0$, the frequency of the fluid and cylinder oscillation will be greater than the stationary cylinder shedding frequency if the natural frequency of the cylinder structure is greater than the stationary cylinder shedding frequency, and the frequency of cylinder and fluid oscillations will be less than the stationary cylinder shedding

Reproduced with permission of the copyright owner. Further reproduction prohibited without permission.

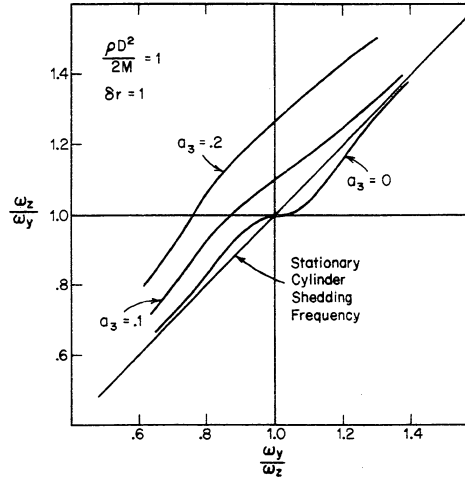

Fig. 10. Entrainment as a Function of a_3.

Reproduced with permission of the copyright owner. Further reproduction prohibited without permission.

frequency if the natural frequency of the cylinder structure is less than the stationary shedding frequency. The frequency entrainment is produced by feedback from the structural oscillator to the fluid oscillator. The entrainment effect is shown in Figures 11 and 12 in comparison with the experimental results of Feng. Both the model and the experimental results show a distinct frequency entrainment. However the model under predicts the frequency entrainment. This suggests the existence of an amplitude-frequency interaction term in the fluid oscillator such as a cubic term in z. Possibly the finite band of frequencies associated with the actual shedding process plays a large role in the entrainment effect with different frequency components being amplified as a range of detuning is transversed.

The frequency entrainment for an elastically mounted cylinder is a function of the structural damping, ξ_s, and the mass ratio, $\rho D^2/2m$, for fixed model parameters. A simple measure of the frequency entrainment can be defined in order to explore the relationship between frequency entrainment and these parameters. If ε and Δ are defined as

$$\frac{\omega_z}{\omega_y} = 1 - \varepsilon \tag{4.7.1}$$

$$\frac{\omega^o_z}{\omega_y} = 1 - \Delta \tag{4.7.2}$$

then the frequency of oscillation, ω_z, will be within a band of $\varepsilon\omega_y$ of the natural frequency of the cylinder structure for the entrainment band given by

Reproduced with permission of the copyright owner. Further reproduction prohibited without permission.

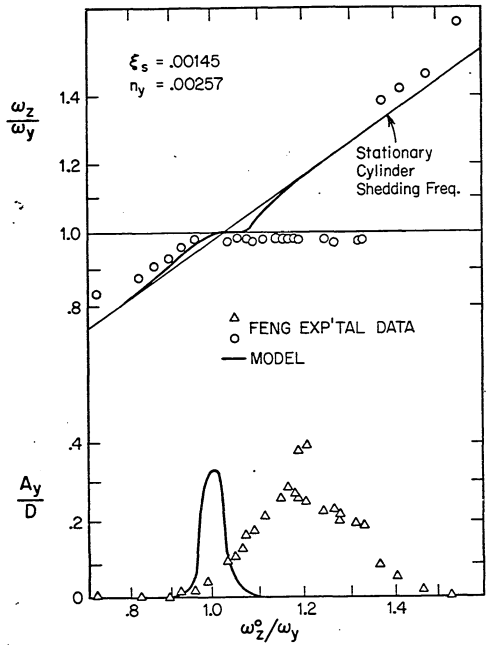

Fig. 11. Comparison of Model and Experimental Results.

Reproduced with permission of the copyright owner. Further reproduction prohibited without permission.

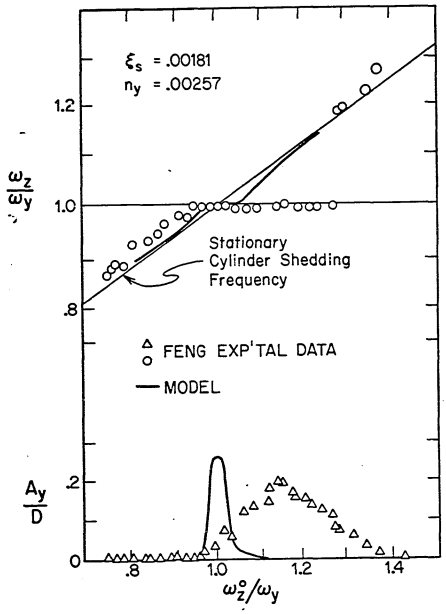

Fig. 12. Comparison of Model and Experimental Results.

Reproduced with permission of the copyright owner. Further reproduction prohibited without permission.

$$\beta_e = \Delta\left(\frac{\omega_z}{\omega_y} = 1+\epsilon\right) - \Delta\left(\frac{\omega_z}{\omega_y} = 1-\epsilon\right) \qquad (4.7.3)$$

β_e is termed the entrainment band and is shown in Figure 13. For a given ξ_s, $\frac{\rho D^2}{2m}$ and ϵ, it is a measure of the entrainment effect. If Equations (4.7.1) and (4.7.2) are substituted into the frequency equation (4.5.45) and only first order terms are retained in ϵ, Δ and ξ_s to produce a simple closed for expression for the entrainment band then

$$\beta_e(\epsilon) = 2(\gamma+\epsilon)/(1-4\gamma^2) \qquad (4.7.4)$$

where

$$\gamma = \frac{a_4}{4\pi S a_o} \frac{\rho D^2 a_4}{4m\pi S} \frac{\epsilon}{\left[\epsilon^2+(\xi+\rho D^2 a_4/4m\pi S)^2\right]} \qquad (4.7.5)$$

Equation (4.7.4) can be further simplified by noting the maximum value of γ is .2 with the model parameters defined by the set (4.6.2) so $4\gamma^2 \ll 1$ and a useful approximation is

$$\beta_e = 2\gamma+2\epsilon \qquad (4.7.6)$$

If there were no entrainment effect produced by the model then the entrainment band would be 2ϵ. The increase in entrainment band due to the model entrainment effect is 2γ.

The entrainment band is a function of both structural damping and the ratio of the displaced fluid mass to the cylinder mass. The change in the entrainment band with variations in these parameters is shown in Figure 14 where the entrainment band for $\epsilon = .01$ is plotted

Reproduced with permission of the copyright owner. Further reproduction prohibited without permission.

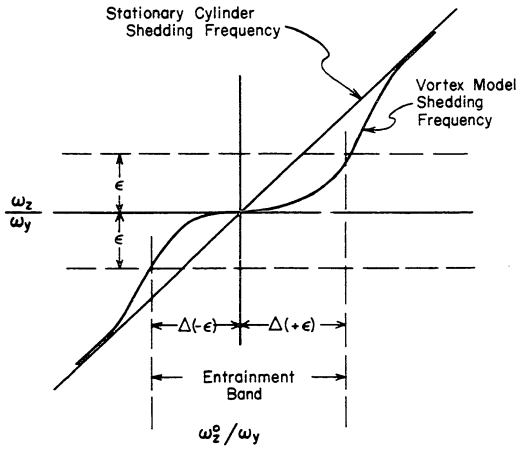

Fig. 13. Entrainment Band.

Reproduced with permission of the copyright owner. Further reproduction prohibited without permission.

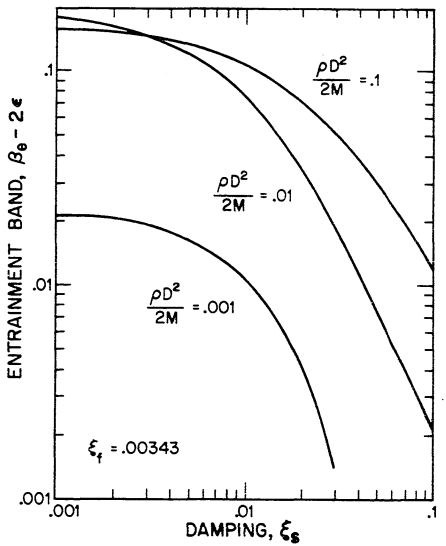

Fig. 14. Variation in the Entrainment Band with Damping and mass Ratio.

Reproduced with permission of the copyright owner. Further reproduction prohibited without permission.

as a function of structural damping and the mass ratio. If the structural damping is reduced then the entrainment band increases. This trend can be seen in the experimental results of Feng in Figures 11 and 12. Secondly if the structural damping factor is greater than the damping factor, ξ_f, due to viscous damping in the model fluid interaction, which is often the case since the damping due to the fluid forces is ordinarily small, then the entrainment band will increase with the ratio of displaced fluid mass to cylinder mass. This implies, for example, that the entrainment effect for a structure oscillating in water would be far greater than for the same structure oscillating in air.

4.7.2 Cylinder Amplitude at Resonance

For a given set of model parameters amplitude of cylinder vibration is a function of the structural damping factor, mass ratio and the ratio of vortex shedding frequency from a stationary cylinder to the natural frequency of the cylinder structure. The peak amplitude of cylinder oscillation for the resonant condition can be found in terms of a single variable called reduced damping by making the resonant condition approximation

$$\omega_y \approx \omega_z \approx \omega_z^o \tag{4.7.7}$$

Incorporating the approximation in Equations (4.5.37) and (4.5.43) makes it possible to express the approximate peak resonant cylinder amplitude in closed form as

Reproduced with permission of the copyright owner. Further reproduction prohibited without permission.

$$\frac{\tilde{A}_y}{D} = \frac{2\pi\left(a_3^2+a_4^2/(2\pi S)^2\right)^{1/2}}{\delta_r^T}\left[\left(\frac{A_z^o}{D}\right)^2+\frac{4\left(a_4^2/(2\pi S)^2-a_3^2\right)}{3Sa_2\,\delta_r^T}\right]^{1/2} \quad (4.7.8)$$

The total reduced damping, δ_r^T, is the sum of structural and fluid components:

$$\delta_r^T = \frac{2m(2\pi(\xi_s+\xi_f))}{\rho D^2} = \delta_r + a_4/S \quad (4.7.9)$$

where δ_r is the reduced viscous structural damping, $2m(2\pi\xi_s)/\rho D^2$.

If $a_4^2/(2\pi S)^2 > a_3^2$ as has been previously postulated then the terms in parenthesis on the right side of Equation (4.7.8) produce a reinforcement effect where the amplitude of vibration of the cylinder increases more rapidly with decreasing damping than would a resonant linear oscillator responding to a constant amplitude forcing function. This arises because of feedback from the structural oscillator to the fluid oscillator which increases the amplitude of the fluid forces on the cylinder and the amplitude of both oscillators. The reinforcement effect produces a rapid increase in the model amplitude with decreasing damping as shown in Figure 15. Also shown is the experimental evidence of Feng [11] at a Reynolds number of 10^4 and Scruton [12] at a Reynolds number of 10^5. The amplitude of vibration as predicted by Equation (4.7.8) with $a_3 = 0$ and $C_{F_y}^o = .5$ shows good agreement with experimental evidence except at low amplitudes where the lack of spanwise correlation may account for the fact that the correlated flow model over predicts the resonant cylinder amplitude.

Reproduced with permission of the copyright owner. Further reproduction prohibited without permission.

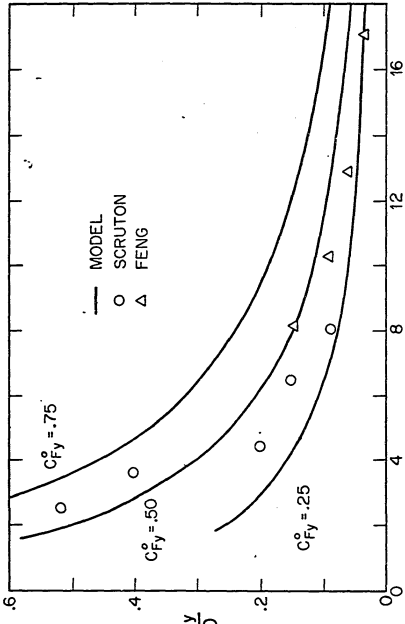

Fig. 15. Resonant Cylinder Amplitude as a Function of Damping, $\delta = 2\pi\xi_s$.

Reproduced with permission of the copyright owner. Further reproduction prohibited without permission.

4.8 EFFECT OF VARYING INPUT EXPERIMENTAL PARAMETERS ON MODEL RESPONSE

New experimental data can be used to generate a set of model parameters which may have a significantly different model response. Rather than construct large tables of parameters a set of approximate partial derivatives have been numerically constructed to illustrate the manner in which the model parameters change with the experimental input data. If one experimental input varies slightly then the change this produces in the model parameters may be approximated by:

$$\left.\frac{\partial a_i}{\partial e_j}\right|_{\underline{e}} \approx \frac{a_i(e_1, \cdots, e_j+\mu e_j, \cdots) - a_i(e_1, \cdots, e_j-\mu e_j, \cdots)}{2\mu} \quad (4.8.1)$$

where $\underline{e}$ is the fundamental set of input experimental data and μ is a small paramter. A set of derivatives is constructed using Equation (4.8.1) in Table 2 for $\mu = .025$ and in parenthesis for $\mu = .25$. The partial derivatives of A_z^o are included for convenience. The partial derivatives change only slightly with the ten fold increase in μ. This suggests that these derivatives should provide a good approximation for the change in the model parameters with a change in input parameters as large as 25%. These derivatives are therefore useful for estimating the change in response of the elastically mounted cylinder for new input data.

The effect of varying the experimental inputs on the entrainment band of the elastically mounted cylinder is estimated by taking the partial derivatives of the entrainment band, Equation (4.7.6), with respect to the model inputs and using the known changes in the model

Reproduced with permission of the copyright owner. Further reproduction prohibited without permission.

parameters with experimental inputs (Table 2). This gives:

$$\frac{1}{\beta_e - 2\varepsilon}\frac{\partial \beta_e}{\partial e_i} = \frac{2}{a_4} - \frac{1}{a_o}\frac{\partial a_o}{\partial e_i} - \frac{2\xi_f \xi_T}{a_4(\epsilon^2 + \xi_T^2)}\frac{\partial a_4}{\partial e_i} \qquad (4.8.2)$$

This set of partial derivatives is evaluated at the input experimental data given by the set (4.6.2) and is shown in Table 3.

	$\frac{\partial a_i}{\partial C^o_{F_y}}$	$\frac{\partial a_i}{\partial\left(\frac{\partial C_{F_y}}{\partial A_y/D}\right)}$	$\frac{\partial a_i}{\partial\left(\frac{u_t \Gamma}{U^2 D}\right)}$	$\frac{\partial a_i}{\partial \beta_w}$
$\frac{A^o_z}{D}$	.92 (.92)	0 (0)	-1.0 (-1.2)	.38 (.48)
a_0	-1.1 (-1.2)	0 (0)	2.8 (2.8)	-.46 (-.46)
a_1	0 (0)	-.016 (-.016)	1.3 (1.3)	-.44 (-.44)
a_2	-.96 (-1.1)	-.062 (-.064)	2.2 (2.3)	-.74 (-.58)
a_3	0	0	0	0
a_4	0 (0)	0 (0)	1.1 (1.1)	-.35 (-.36)

Table 2. Change in Model Parameters With Change in Experimental Input Data.

Reproduced with permission of the copyright owner. Further reproduction prohibited without permission.

e_i	$\frac{1}{\beta_e - 2\varepsilon} \frac{\partial \beta_e}{\partial e_i}$
$C^o_{F_y}$	2.0
$\frac{\partial C_{F_y}}{\partial A_y / D}$	0.
$\frac{u_t \Gamma}{U^2 D}$	$\frac{-5.1 \xi_f}{\xi_T \left(\left(\frac{\varepsilon}{\xi_T} \right)^2 + 1 \right)}$
β_w	$-.78 + \frac{1.6 \xi_f}{\xi_T \left(\left(\frac{\varepsilon}{\xi_T} \right)^2 + 1 \right)}$

Table 3. Change in Entrainment Band
With Change in Experimental Input Data.

Increasing the lift coefficient on a stationary cylinder increases the force exerted by the fluid oscillator on the structural oscillator and so the entrainment band increases. The rate of increase of the amplitude of the lift force on a cylinder in forced vibration with increasing amplitude has little effect on the bandwidth. Increasing either the circulation of the shed vortices from a stationary cylinder of the translational velocity of the vortex street decreases the entrainment band. Increasing the bandwidth of forced vibration increases the

Reproduced with permission of the copyright owner. Further reproduction prohibited without permission.

entrainment band of an elastically mounted cylinder only if the fluid damping is large compared to the structural damping.

The effect of varying experimental input data on the peak amplitudes of resonant vibration of an elastically mounted cylinder is estimated by taking the partial derivative of the peak resonant amplitude (Eqn. (4. 7. 8)) and using the known change in the model parameters with experimental inputs (Table 2). This gives

$$\frac{D}{\tilde{A}_y}\frac{\partial(\tilde{A}_y/D)}{\partial e_i} = \left(\frac{1}{a_4} - \frac{1}{\delta_r^T S}\right)\frac{\partial a_4}{\partial e_i} + \frac{\left(2\frac{A_z^o}{D}\frac{\partial A_z^c/D}{\partial e_i} + \frac{8\pi a_4^2}{3(2\pi S)^3 a_2 \delta_r^T}\right)\left(\left(\frac{2}{a_4} - \frac{1}{\delta_r^T S}\right)\frac{\partial a_4}{\partial e_i} - \frac{1}{a_2}\frac{\partial a_2}{\partial e_i}\right)}{2\left((A_z^o/D)^2 + 8\pi a_4^2/(2\pi S)^3 a_2 \delta_r^T\right)} \tag{4. 8. 3}$$

The set of partial derivatives generated from Equation 4. 8. 3) is listed in Table 4 where the derivatives are evaluated at the input experimental data given by the set (4. 6. 2).

The peak amplitude of the elastically mounted cylinder will increase if any of the experimental inputs are increased with the exception of the circulation and translational velocity of a vortex shed from a stationary cylinder.

Reproduced with permission of the copyright owner. Further reproduction prohibited without permission.

$\frac{D}{A_y}\frac{\partial \tilde{A}_y/D}{\partial e_i}$				
δ_r^T \ e_i	$C_{F_y}^o$	$\frac{\partial C_{F_y}}{\partial A_y/D}$	$\frac{u_t \Gamma}{U^2 D}$	β_w
2	2.0	.10	-1.4	.52
4	2.0	.092	-.73	.33
8	2.0	.077	-.24	.18
16	2.0	.059	.072	.088

Table 4. Change in Resonant Amplitude of Elastically Mounted Cylinder With Change in Input Experimental Data.

Reviewing Tables 2 through 4 it can be seen that while the model parameters and model response generally vary with changes in the input experimental data there are apparently no jump effects where a small change in the experimental data inputs could produce a large change in the model response.

4.9 PIVOTED ROD

The pivoted rod approximates the motion of a fixed free bending cantilever in the first mode. The present model is applied to this geometry using an assumed linear mode shape. The model response is then compared with experimental data.

The rod is spring supported and pivoted at the base and vibrates transverse to the free stream as shown in Figure 16. A viscous

Reproduced with permission of the copyright owner. Further reproduction prohibited without permission.

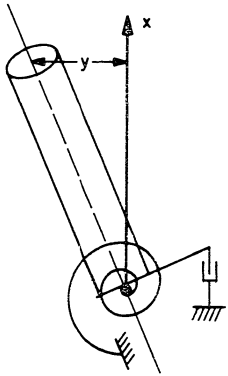

Fig. 16. Pivoted Rod.

Reproduced with permission of the copyright owner. Further reproduction prohibited without permission.

damping force is applied at the base. The following spatial distributions for the cylinder and fluid model are used.

$$Y(x,t) = y(t)x/L$$
$$Z(x,t) = z(t)x/L \qquad (4.9.1)$$

L is the length of the rod. x is the spanwise length measured from the pivot. y(t) is the displacement of the cantilever tip. These relations are substituted into the system equations. The Galerkin technique is applied by multiplying these equations by the assumed spatial distributions and integrating the equations over the span of the cylinder to produce two ordinary differential equations. This procedure neglects all spanwise flow effects. Applying the Galerkin technique to the oscillator equations (4.4.19) and (4.4.21) and incorporating the spatial distributions of Equation (4.9.1) produces the following integral equations:

$$\int_0^L \left[\rho D^2 \ddot{z}(x/L)^2 + K' u_t \omega_z^o (x/L)^2 z/D\right] dx$$
$$= \int_0^L \left[(a_1 - a_4)\rho DU(x/L)^2 \dot{z} - a_2 \rho D \dot{z}^3 (x/L)^4 + a_4 \rho DU(x/L)^2\right] dx \qquad (4.9.2)$$

$$\int_0^L \left[m\ddot{y}(x/L)^2 + 2\xi_T m(x/L)^2 \dot{y} + k(x/L)^2 y\right] dx$$
$$= \int_0^L a_4 \rho DU\dot{z}(x/L)^2 dx \qquad (4.9.3)$$

The system differential equations are then:

$$\ddot{z} + \omega_z^{o2} z = (a_1' - a_4')U\dot{z}/D - 3a_2'\dot{z}^3/5UD + a_4' U\dot{y}/D \qquad (4.9.4)$$

Reproduced with permission of the copyright owner. Further reproduction prohibited without permission.

$$\ddot{y}+2\xi_T\omega_y\dot{y}+\omega_y^2 y = a_4''\dot{z} \qquad (4.9.5)$$

where

$$a_i'' = \frac{\rho D^2}{M} \qquad a_i' = \frac{a_i}{a_o}$$

and M is the "equivalent" mass.

$$M = \int_o^L mx^2 dx \Big/ \int_o^L x^2 dx \qquad (4.9.6)$$

Equations (4.9.4) and (4.9.5) are identical to the basic fluid and structural oscillator equations (4.4.19) and (4.4.21) except for the factor of 3/5 which multiplies the cubic term in the fluid oscillator equation and the substitution of equivalent mass for mass per unit length. With these changes all the previous results for the elastically mounted cylinder apply. In particular the equation describing the peak resonant amplitude as a function of damping for $a_3 = 0$ is:

$$\frac{\tilde{A}_y}{D} = \frac{a_4}{2S\delta_r^T}\left[\frac{5(a_1-a_4)}{9\pi^2 S^2 a_2} + \frac{5a_4^2}{18\pi^2 S^3 a_2 \delta_r^T}\right]^{1/2} \qquad (4.9.7)$$

Equation (4.9.7) is plotted in Figure 17 in comparison with the experimental results of Vickery and Watkins [20] and Hartlen. The present model provides a good approximation to the experimental data for amplitudes between 10 and 60 percent of cylinder diameter. Note that the three sets of experimental data nearly fall on the same curve as is also the case for the 1 dimensional oscillation peak amplitudes shown in Figure 3. This tends to confirm

Reproduced with permission of the copyright owner. Further reproduction prohibited without permission.

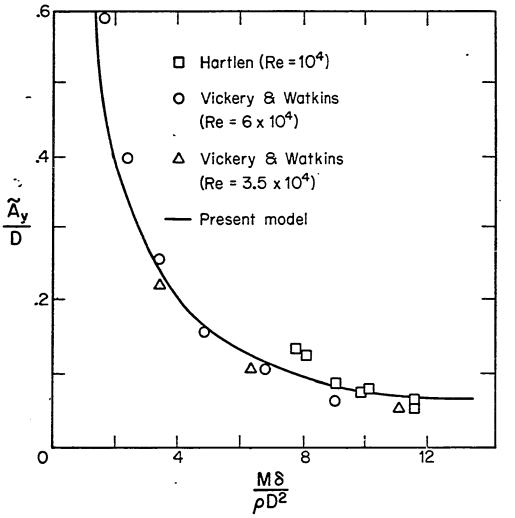

Fig. 17. Tip Amplitude of Pivoted Rod at Resonance with Vortex Shedding, $\delta = 2\pi\xi_s$.

Reproduced with permission of the copyright owner. Further reproduction prohibited without permission.

the model prediction that the peak resonant cylinder amplitude can be expressed as a function of reduced damping alone.

4.10 SUMMARY AND CONCLUSIONS

A model has been developed for vortex induced vibration of a circular cylinder. The model is based on a control volume approach to the vortex shedding process and the von Karman idealization of the vortex street. The two degree of freedom model is composed of fluid like and structural oscillators which interact through the force exerted between the fluid and the cylinder. The model parameters are determined from experimental data by matching the model response to experimental observation for the cases of a fixed cylinder and forced cylinder motion. The model provides a basis for predicting the response of untested structures.

If the cylinder is elastically mounted then the model predicts the cylinder resonates with vortex shedding as the shedding frequency approaches the natural frequency of the cylinder and large amplitude oscillations will result. The model predicts that the response of the cylinder is a function of the ratio of natural shedding frequency to the natural frequency of the cylinder structure, the structural viscous damping and the ratio of displaced fluid mass to the mass of the cylinder.

The model shows an entrainment effect, that is the frequency of vortex shedding from the elastically mounted cylinder is entrained by the natural frequency of structural oscillation. The model predicts that the entrainment effect will increase with decreasing structural

Reproduced with permission of the copyright owner. Further reproduction prohibited without permission.

damping and this is confirmed by experimental results. The model also predicts the entrainment effect will increase with the ratio of displaced fluid mass to cylinder mass except in the case of very small values of structural damping.

The peak resonant cylinder amplitude of the model due to resonance with vortex shedding can be expressed in terms of a single variable called reduced damping. The peak resonant cylinder amplitude increases sharply with decreasing damping due to a fluid feedback effect. The model predictions of peak resonant cylinder amplitude as a function of reduced damping are in good agreement with experimental data both for one dimensional cylinder motion and for the response of a pivoted rod.

4.11 REFERENCES

1. Strouhal, V., "Uber eine besondere Art dey Tonerregung," Wied. Ann. Physid Chem., Neue Folge, Band V, 1878.

2. Rayleigh, Lord, Philosophical Magazine, Vol. 7, 1879, p. 149.

3. Landweber, L., and Grimminger, G., "Progress Report on the Lateral Vibration of Circular Cylinders Caused by Motion Through a Fluid," DTMB Technical Note.

4. Bishop, R. E. D. and Hassan, A. Y., "The Lift and Drag Forces on a Circular Cylinder in a Flowing Fluid," Proceedings of the Royal Society of London, Vol. 277, Series A, 1964, pp. 51-75.

5. Hartlen, R. T., Baines, W. D., and Currie, I. G., "Vortex-Excited Oscillation of a Circular Cylinder," University of Toronto, Report UTME-TP 6809, Nov. 1968.

6. Skop, R. A. and Griffin, O. M., "A Model for the Vortex Excited Resonant Response of Cylinders," Offshore Technology Conference, 1973.

7. Tobes, G. H. and Ramamurthy, A. S., "Fluidelastic Forces on Circular Cylinders," Journal of Basic Engineering, Sept. 1969.

8. Chen, Y. N., "Fluctuating Lift Forces of the Karman Vortex Streets on Single Circular Cylinders and in Tube Bundles," Part 2, ASME J. Eng. for Industry, May 1972.

Reproduced with permission of the copyright owner. Further reproduction prohibited without permission.

9. Coder, D. W., "Hydrodynamic Forces on Oscillating and Nonoscillating Smooth Circular Cylinders in Crossflow," Naval Ship R. & D. Center, Report 3639, 1972.

10. El-Sherbiny, S. E., "Effect of Wall Confinement on the Aerodynamics of Bluff Bodies," Ph. D. Thesis, University of British Columbia, 1972.

11. Feng, C. C., "The Measurement of Vortex Induced Effects in Flow Past Stationary and Oscillating Circular and D-Section Cylinders," M. A. Sc. Thesis, The University of British Columbia, 1968.

12. Scruton, C., "On the Wind Excited Oscillation of Stacks, Towers, and Masts," Proceedings of the Wind Effects on Buildings and Structures Conference, NPL, Teddington, England, June 1963.

13. Jones, G. W., Cincotta, J. J., and Walker, R. W., "Aerodynamic Forces on a Stationary and Oscillating Circular Cylinders at High Reynolds Numbers," NASA TR R-300, Feb. 1969.

14. Chen, Y. N., "Fluctuating Lift Forces of the Karman Vortex Streets on Single Circular Cylinders and in Tube Bundles, Part 1," ASME J. Eng. for Industry, May 1972.

15. Weihs, D., "Semi-infinite Vortex Trails, and Their Relation to Oscillating Airfoils," J. Fluid Mech. (1972), Vol. 54, Part 4, pp. 679-690.

16. Bogoluibov, N. N. and Mitroplosky, Y. A., Asymptotic Methods in the Theory of Nonlinear Oscillations, Gordon & Breach, New York, 1961.

17. Koopman, G. H., "The Vortex Wakes of Vibrating Cylinders at Low Reynolds Numbers," J. Fluid Mech. (1967), Vol. 28, Part 3, pp. 501-512.

18. Van der Pol, B., "Forced Oscillations in a System with Nonlinear Resistance," Phil. Mag., 1927.

19. Stoker, J. J., Nonlinear Vibrations, Interscience, New York, 1966.

20. Vickery, B. J., and Watkins, R. D., "Flow Induced Vibrations of Cylindrical Structures," Research Report R34, Dept. of Civil Engineering, University of Sydney, 1955; see also Proceedings of the First Australian Conference on Hydraulics and Fluid Mechanics, 1962.

Reproduced with permission of the copyright owner. Further reproduction prohibited without permission.

V. GENERAL CONCLUSIONS

A bluff structure exposed to a fluid flow can be excited to large amplitude vibrations. Two mechanisms for the transfer of energy from the fluid to the structure are considered here. First the fluid force on the structure is modeled as dependent only on the relative velocity and angle of attack of the fluid to the structure. The resultant vibrations are called galloping. This galloping model is valid as long as the frequency of vortex shedding from the bluff structure is much greater than the natural frequency of the structure. If the frequency of vortex shedding is near the natural frequency of the structure then the vortex shedding can lock onto structural oscillation. The vortex shedding process is modeled as a single degree-of-freedom oscillator which interacts with the structure through fluid forces exerted between the structure and the fluid. Both models for the interaction between the structure and the fluid generate autonomous nonlinear differential equations with oscillatory solutions. These equations are analyzed by the asymptotic method discussed in Chapter II.

The asymptotic technique is based on the approximation of Bogoliubov and Mitropolsky as applied to internally resonant, autonomous systems. In Chapter II it is shown that:

(1) Internally resonant autonomous oscillators may be divided into two classes,

(i) Harmonic internal resonance. A necessary condition for harmonic internal resonance is that natural frequencies of the principal coordinate

Reproduced with permission of the copyright owner. Further reproduction prohibited without permission.

oscillators be nearly harmonics of some frequency. Harmonic resonance is characterized by the sensitivity of the solution to small changes in the detuning between oscillators.

(ii) Combined internal resonance. In this case the response of the oscillators is substantially independent of small changes in detuning. Combined internal resonance can only occur outside the band of frequencies that contain harmonic resonance.

A model for multi-dimensional galloping is developed in Chapter III. A simple approximate criteria for the stability of the zero solution and an estimate for the maximum amplitude of galloping are produced. Examples are made with a noninertially coupled structure having plunge and torsion degrees of freedom. A cubic approximation to the nonlinear aerodynamic coefficients is used. These examples have shown that:

(2) Simple harmonic solutions were found in every case.

(3) Outside the band of natural frequencies which produce harmonic resonance the response is either zero, dominated by plunge with no first order torsion, or dominated by torsion with no first order plunge.

(4) As the system approaches harmonic resonance both the torsion and plunge degrees of freedom achieve first order limit cycles.

(5) The bandwidth of frequencies containing harmonic resonance increases with free stream velocity and the

Reproduced with permission of the copyright owner. Further reproduction prohibited without permission.

ratio of fluid density to structural density.

(6) The response remains constant or increases with free stream velocity.

A model is developed in Chapter IV for vortex induced vibration of a circular cylinder. The model is based on a control volume approach to the vortex shedding process and the von Karman idealization of the vortex street. The model features both a fluid and structural oscillator. The model parameters are determined from experimental data by matching the model response to experimental observation for the cases of fixed and forced cylinder motion. The model predictions are then compared with experimental data for the elastically mounted cylinder case. The model provides a basis for predicting the response of untested structures. The model predicts:

(7) The response of an elastically mounted cylinder is a function of the ratio of the natural shedding frequency to the natural frequency of the cylinder structure, the viscous structural damping and the ratio of displaced fluid mass to the mass of the cylinder.

(8) The entrainment effect, where the vortex shedding frequency is entrained by the natural frequency of an elastically mounted cylinder, will increase with decreasing structural damping. This is confirmed by experimental results. The model also predicts the entrainment effect will increase with the ratio of displaced fluid mass to cylinder mass except for very small values of structural damping.

Reproduced with permission of the copyright owner. Further reproduction prohibited without permission.

(9) The peak resonant cylinder amplitude of an elastically mounted cylinder at resonance with vortex shedding is a function of a single variable called reduced damping. The peak resonant amplitude of the cylinder increases sharply with decreasing damping due to a fluid feedback effect. The model predictions of resonant cylinder amplitude as a function of reduced damping are in good agreement with experimental data both for one dimensional cylinder motion and for the response of a pivoted rod.

Reproduced with permission of the copyright owner. Further reproduction prohibited without permission.